Ph.D. Program in Civil, Chemical and Environmental Engineering

Curriculum in Structural and Geotechnical Engineering, Mechanics and Materials

Department of Civil, Chemical and Environmental Engineering

Polytechnic School, University of Genoa, Italy.

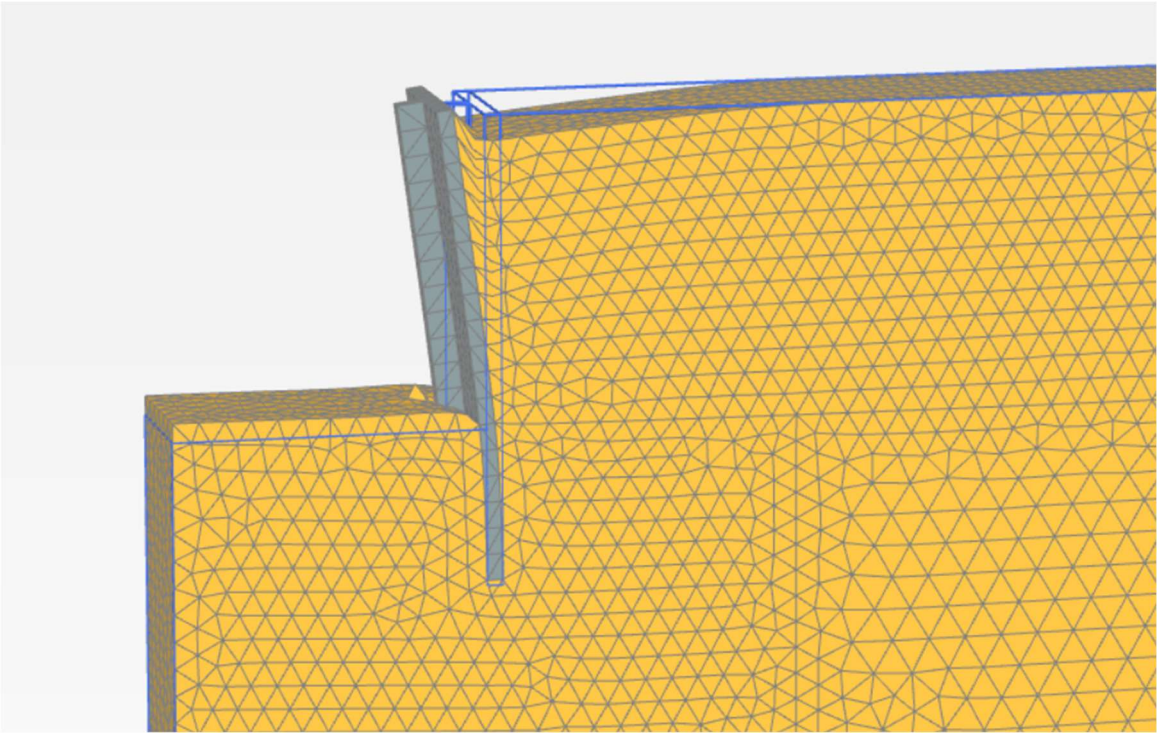

Mitigation of ground and retaining structure displacements due to excavations: analysis and modelling of soil structure interaction

Daniela Sauvageon

MITIGATION OF GROUND AND RETAINING STRUCTURE DISPLACEMENTS DUE TO EXCAVATIONS: ANALYSIS AND MODELLING OF SOIL STRUCTURE INTERACTION

BY

DANIELA SAUVAGEON

Dissertation discussed in partial fulfillment of
the requirements for the Degree of

DOCTOR OF PHILOSOPHY

Civil, Chemical and Environmental Engineering
curriculum in Structural and Geotechnical Engineering, Mechanics and Materials,
Department of Civil, Chemical and Environmental Engineering, University of Genoa, Italy

November, 2024

Adviser:
Prof. Riccardo Berardi – Department of Civil, Chemical and Environmental Engineering, University of Genoa

External Reviewers:
Prof. Vincenzo Fioravante – Department of Engineering, University of Ferrara
Prof. Manuel Antonio de Matos Fernandes – Department of Civil and Georesources Engineering, University of Porto

Examination Committee:
Prof. Monica Barbero – Department of Structural Engineering, Building and Geotechnics, Politecnico of Torino
Prof. Carlo Lai – Department of Civil Engineering and Architecture, University of Pavia
Prof. Marco Lepidi – Department of Civil, Chemical and Environmental Engineering, University of Genoa

Substitutes:
Prof. Riccardo Pietro Castellanza – Department of Environment and Earth Sciences, University of Milan – Bicocca
Prof. Andrea Bacigalupo – Department of Civil, Chemical and Environmental Engineering, University of Genoa

Ph.D. program in Civil, Chemical and Environmental Engineering

Curriculum in Structural and Geotechnical Engineering, Mechanics and Materials

Cycle XXXIV

INDEX

1. INTRODUCTION

The research is developed in the field of soil-structure interaction studies, focusing particularly on the retaining structures for deep excavations and on harbour berthing structures.

With regard to the first type of structures, the problem concerns the execution of deep excavations in urbanised areas, reducing induced displacements and adopting different support solutions from traditional techniques with anchors or struts.

As far as the second one is concerned, the problems arise from the requirement to conform the existing docks, an issue linked mainly to a deepening of the seabed (dredging) or to possible erosion phenomena occurring at the foundation level, caused by the action of ship propellers.

1.1. GENERAL REMARKS ON ANALYSIS OF DISPLACEMENTS INDUCED BY EXCAVATIONS

The construction of deep excavations is a highly topical issue, as the use of underground spaces for the performance of various human activities is increasingly being observed. Particularly in urban areas, the construction of infrastructures for transport, parking and commercial activities is experiencing considerable development (Callisto, 2011).

In general terms, the execution of deep excavations inevitably gives rise to more or less significant displacements in the ground behind and in front of the excavation.

In urban areas, the prediction and control of the ground displacements associated with the excavation is one of the crucial aspects of the project as the resulting settlements can cause damage to existing structures.

The execution of an excavation close to a building can in fact induce vertical and lateral movements and give rise to differential settlements and rigid rotations; it follows that the knowledge of the horizontal and vertical displacements and the zone of influence of the excavation is particularly important.

The assessment of the effects induced by the execution of excavations can be carried out by adopting simplified methods, that can be useful for preliminary estimation of the displacements induced under free-field conditions, or by resorting to more accurate approaches, based on numerical analyses.

In the literature, several simplified methods for deep excavations are currently available, from the pioneering contribution of Peck (1969) and Clough & O'Rourke (1990) until the recent work of Ou & Hsieh (2011) on the basis of which the settlement profile caused by an excavation can be estimated mainly in relation to the type of soil, the shallow or deep deformation mechanisms and the excavation geometry.

There are many factors influencing the movements induced by deep excavations including the dimensions of the excavation, the stiffness of the support system, the excavation phases, the type of soil and its mechanical properties: displacement typically increase when the depth of the bottom and its width increase and decrease increasing stiffness of the retaining structures.

In order to reduce the ground settlement (an issue of particular importance when existing buildings and structures are close to the excavation), it is therefore necessary to reduce the horizontal displacement of the walls and the basal heave, thus also increasing the overall stability.

Unfortunately, it has been demonstrated that this aspect can only be partially solved by increasing the stiffness of support system (embedded wall and support elements).

In fact, even in presence of strongly constrained systems or massive and stiff structures, the unloading condition due to the stress removal induces deep movements, which involve ground settlement and horizontal displacements toward the excavation.

Because of this reason, a solution could be the improvement of ground strength and stiffness, which, as demonstrated by Ou et al. (2006), is more effective if it is carried out in the excavation "passive zone" /passive side of the wall. To this end, some possible solutions can be identified either by improving the soil mechanical characteristics or by inserting "structural inclusions" under the excavation bottom, inclusions that exert their function during all the excavation phases.

In relation to harbour berthing structures, there is an increasing demand for interventions aimed at making the docks suitable to remain in operation even after the dredging of the seabed, which is necessary for the docking of larger ships.

In addition, the action of the propellers, frequently induces localized excavations at the foundation level, with the risk of both excessive displacement and dock collapse.

Since these are important existing infrastructures, whose functionality must be maintained, it is therefore necessary to learn more about the magnitude and extent of the displacements induced by dredging and erosion, as well as how to intervene to limit the effects of these possible events.

Again, accurate numerical analyses, which can reliably simulate the evolutionary mechanisms under consideration, can provide useful insights both in terms of prediction and in terms of interventions to be implemented.

1.2. RESEARCH OBJECTIVES

The purposes of this thesis are:

- The analysis of the state of the art concerning displacements due to deep excavations, reinforcement and stiffening interventions at the base of excavations and retaining structures and mechanical response for soil-retaining structure interaction problems.
- Modeling of deep excavation-induced effects by parametric numerical analysis with the aim of estimating the accuracy and reliability of the numerical models and identifying quantities influencing ground displacements.
- The study of the behavior of "conventional" and "unconventional" engineering solution of retaining structures for deep excavations.
- Modelling of "unconventional" embedded retaining structures by numerical analyses to assess buttress wall function and behavior by parameterizing the main geometric quantities.

- Modelling of the response of gravity docks subjected to excavation and erosion phenomena in analogy with deep excavations in order to obtaining displacement envelopes for the evaluation of effects on port infrastructure and to develop reinforcement and stabilization criteria.

The final objective is to analyze the response of the soil-structure system, in order to verify the applicability of 'unconventional' engineering solutions, providing general and specific design suggestions.

1.3. DISSERTATION OUTLINE

The first part is devoted to the framing of the subject matter of the thesis. The first chapter is divided into sections each devoted to a specific topic. Initially, a brief description of the types of retaining structures is reported and the design principles and related uncertainties are briefly explained.

The next section provides an examination of the state of the art in the literature regarding the displacement and deformation induced by deep excavation with a description of the main methods for estimating retaining structures displacements and ground settlements.

The last section gives a general overview about numerical analysis, in particular about the finite element methods on which the computer code used for these studies is based.

The second part of the thesis is devoted to the study of the behavior of deep excavations through the development of a series of parametric numerical analyses.

The work was developed through FEM numerical analyses that are illustrated in Chapter 2.

A first phase of this PhD study provides the bi-dimensional modelling of the effects of deep excavations: geometry, constitutive soil models and parametrization are here illustrated as well as the quantities influencing ground displacements are highlighted. The objective of this first stage is to assess the reliability of numerical modeling through comparison with literature results.

In order to have a reliable tool, the parameters for the constitutive models were chosen calibrated to real soil behavior so that the numerical model reproduces the experimental result of triaxial tests on a literature soil type. In this way, the results are not affected by the selection of model parameters.

The central part of the chapter is devoted to examining the operation and behavior of embedded retaining walls equipped with structural inclusions, referred to as cross walls and buttress walls. The study of the response of such retaining structures, carried out performing 2D and 3D numerical analysis is reported. A series of parametric models were developed using Plaxis 2D and Plaxis 3D, varying some geometric features to evaluate their influence on the response of the structure in terms of displacements and deformations. Interesting and useful original results are then provided.

The third part is devoted to an in-depth analysis of the response of gravity docks subjected to excavation at the foot, aimed at simulating localized erosion phenomena or a deepening of the seabed, in analogy with deep excavations. Some results carried out by numerical FEM analysis are reported, with the purpose of analyzing the deformation and displacement mechanisms of the sandy or silt-clay type fill and foundation soil, and an examination of the local and global response of the structure in relation to

geotechnical soil improvement interventions, to obtain results on the displacements to which the structure may be subjected as well as the definition of sizing and optimization criteria for the intervention.

Finally, in Chapter 4, some comments are reported. The results pointed out in the previous chapters are summarized and some specific topics, which need further research efforts, are discussed.

2. DEEP EXCAVATIONS: RETAINING STRUCTURES AND INDUCED DISPLACEMENTS

2.1. INTRODUCTION

Retaining structures should be built for many reasons, as for example to support permanent or temporary excavations, to provide a quay in a dock, to provide abutments for a bridge deck.

Whatever the reason of construction, a retaining wall is typically needed to provide support for natural and made ground, supporting vertical face of soil or rock.

In fact, retaining structures may be built in natural ground or before a backfill is placed. In this regard, it is possible, in general terms, to distinguish between "walls" and "embedded walls". Because of the many situations and soil conditions in which they are used, these particular geotechnical structures are constructed from a variety of materials and used different methods to support the ground.

In this chapter some examples of wall types are described, after a general part about earth pressure related to retaining structures.

Thereafter it is reported an examination of the state of the art in the literature regarding the displacement and deformation induced by deep excavations with a description of the main methods for estimating retaining structure displacements and ground settlements.

Finally, a general overview about numerical analysis, in particular concerning the finite element method, is mentioned.

2.2. EARTH PRESSURE AND RETAINING STRUCTURES

2.2.1. Introduction

Retaining structures, defined in agreement with Italian and European technical codes, have the purpose of safely supporting a volume of soil and consist of elements that receive actions imposed by the supported soil.

Generally, the following types are considered to be retaining structures (EC7, 2004):

- gravity walls: walls of stone or plain or reinforced concrete having a base footing with or without a heel, ledge or buttress. The weight of the wall itself, sometimes including stabilizing masses of soil, rock or backfill, plays a significant role in the support of the retained material. Examples of such walls include concrete gravity walls having constant or variable thickness, spread footing reinforced concrete walls and buttress walls.
- embedded walls: relatively thin walls of steel, reinforced concrete or timber, supported by anchorages, struts and/or passive earth pressure. The bending capacity of such walls plays a significant role in the support of the retained material while the role of the weight of the wall

is insignificant. Examples of such walls include cantilever steel sheet pile walls, anchored or strutted steel or concrete sheet pile walls and diaphragm walls.

- composite retaining structures: walls composed of elements from the above two types of wall. A large variety of such walls exists, and examples include double sheet pile wall cofferdams, earth structures reinforced by tendons, geotextiles or grouting and structures with multiple rows of ground anchorages or soil nails.

Main requirement of a retaining wall is stability against translation phenomena along the foundation plane and overturning, as well as loss of stability in the foundation due to exceeding the limit load, as shown in Figure 2.1 taken from EC7.

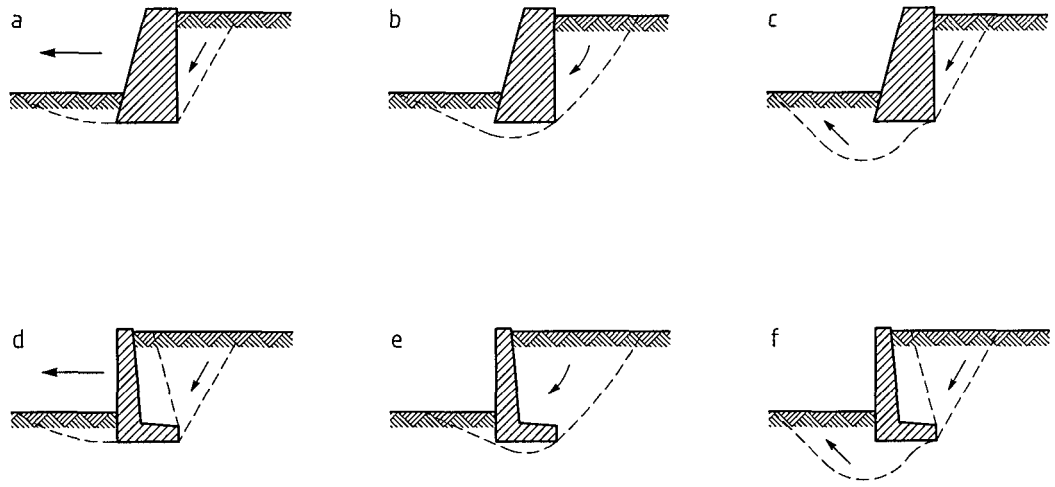

Figure 2.1 — Examples of limit modes for foundation failures of gravity walls (from Eurocode 7)

Walls are essentially subject to rigid motions of translation and rotation. Actions come from the ground to the rear, and resistances, in the absence of externally applied forces, are derived from self-weight and friction in the foundation along the sliding plane. In addition, at the base of the wall, due to the partial deepening of the foundation relative to the ground plane, translation resistance may arise, which is related to passive resistance. The sizing of these retaining structures is carried out by referring to active boundary equilibrium conditions.

Embedded walls are slender retaining structures constituted by reinforced concrete panels (diaphragms), rows of piles, sheet piles, they are built to support excavations of relevant height and they are constructed before starting excavation operations as it is not capable of self-supporting.

Important aspects for such structures are the structural and geotechnical stability of the system and the deformation phenomena of the soil to be supported.

Embedded walls are frequently constrained along their height by structures such as struts and anchors that have the function of counteracting forces and limiting displacements, during the excavation phases and when the work has been completed. Regarding anchorages, particularly the type of ties used in numerical analyses, they will be described in more detail in a later section.

Embedded walls are considered deformable retaining structures because they can deform by rotating rigidly around a point or by inflections along the height, depending on the degree of interlocking at the footing and the presence and position of external constraints and the stiffness of the wall.

Therefore, from a structural point of view, an embedded wall can be considered as a beam with different degrees of restraint depending on its depth below the bottom of the excavation and the presence or absence of auxiliary support structures.

Actions come from soil and water pressures and any external surcharge while resistances are provided by mobilizing passive resistance in the area below the excavated bottom plus any external forces related to the constraint systems (multi-constrained walls).

The mobilization of active forces and passive resistances is related to the displacements of the embedded wall with respect to the ground, which are in themselves related to the shape of the deformation, and for this reason it is not possible to know a priori their magnitude and distribution and the resulting force diagrams.

There are solutions in the literature referring to simple diagrams such as those shown in Figures 2.2 and 2.3, respectively, for the simple case of a cantilever wall subject to rotation with respect to a point and for embedded wall fitted at the footing with a constraint level at the top; however, numerical methods must often be used for calculation.

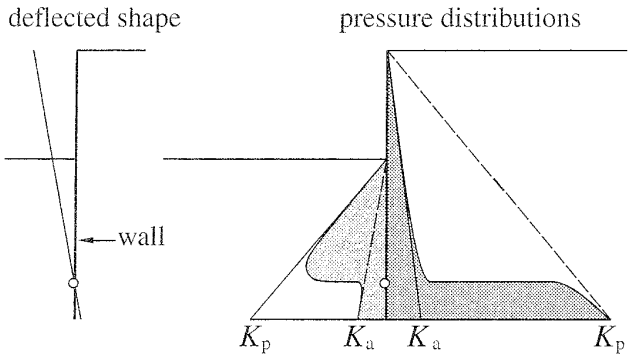

a) cantilever wall

Figure 2.2 Deflected shape and pressure distribution schemes of a cantilever wall.

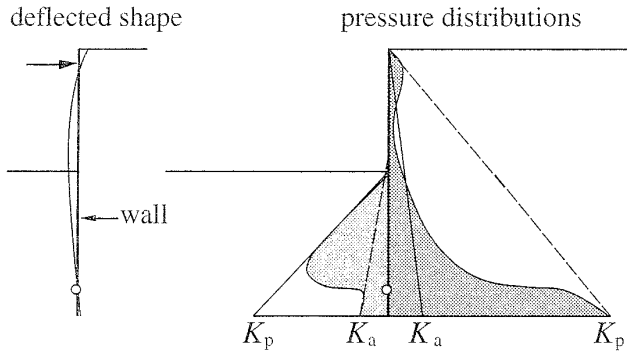

b) propped wall

Figure 2.3 Deflected shape and pressure distribution schemes of a top constrained wall

The stability of the embedded wall should be verified in relation to the phenomena of rigid rotation, bottom excavation instability and collapse of restraint systems as well as structural collapses of the structure or some of its parts.

Figure 2.4 adapted from EC7 illustrates some possible instability phenomena in gravity walls and embedded walls.

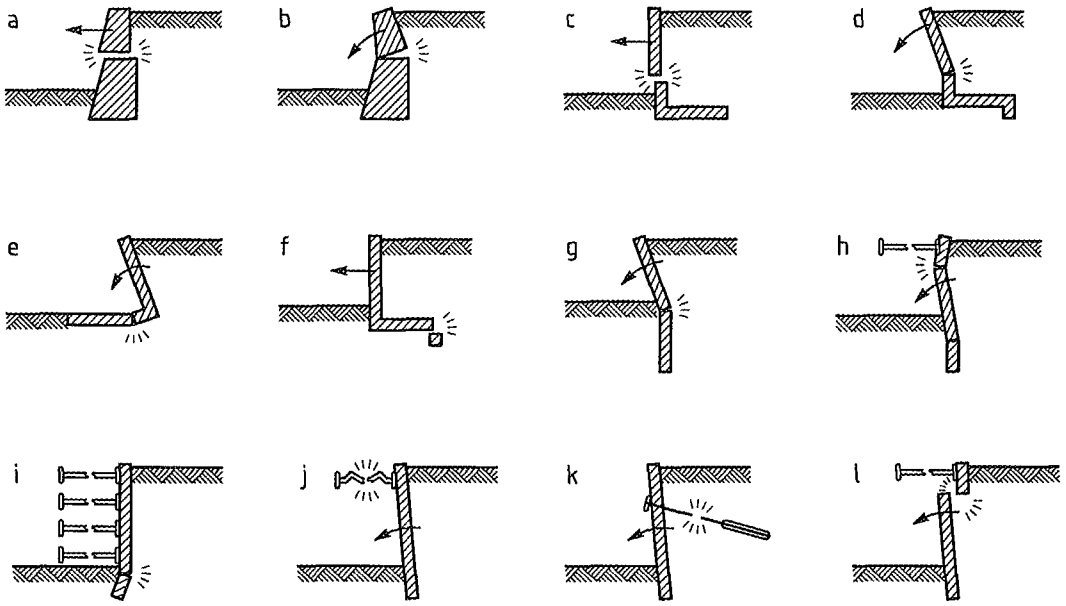

Figure 2.4 Examples of limit modes for structural failure of retaining structures (from Eurocode 7)

Moreover, it should be remembered that both retaining walls and embedded walls should also be verified against the overall stability of the supported soil.

In all retaining structures, the stress state regimes that depend on soil displacements are activated. The ratio of horizontal effective stresses to the initial vertical ones is the pressure coefficient K .

Without going into detail, as is well known, in the case of soil displacements toward the structure, associated with a reduction in horizontal effective stresses, active limit equilibrium conditions can be reached ($K=K_A=1/N_\phi$), while in the case where the displacements are zero, the initial at rest conditions remain ($K=K_0$). If, on the other hand, the soil is compressed laterally, passive resistance ($K=K_P=N_\phi$) can be mobilized (Figure 2.5).

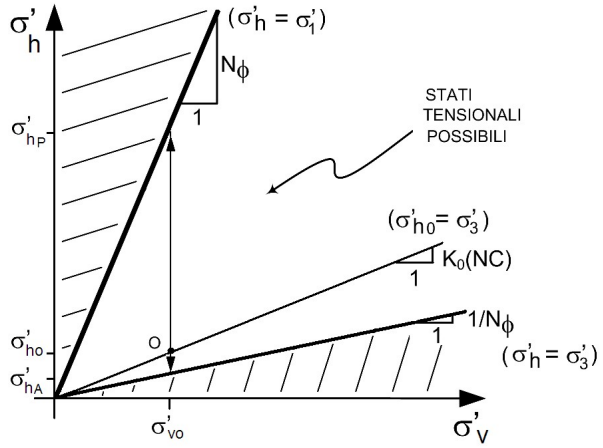

Figure 2.5 Failure conditions; conditions at rest; active and passive limit states (from Berardi 2021)

It is noted that many studies have shown that active limit equilibrium conditions can occur with small soil displacements, compatible with those resulting from the execution of an unsupported excavation of moderate height and with those supportable by a retaining structure. In the other hand, much larger displacements are required for a full mobilization of the passive resistance. Figure 2.6 taken from Clough, Duncan (1991) shows some values of the coefficients of K_A, K_0 and K_P as a function of relative displacement, i.e., the ratio of displacement to wall height.

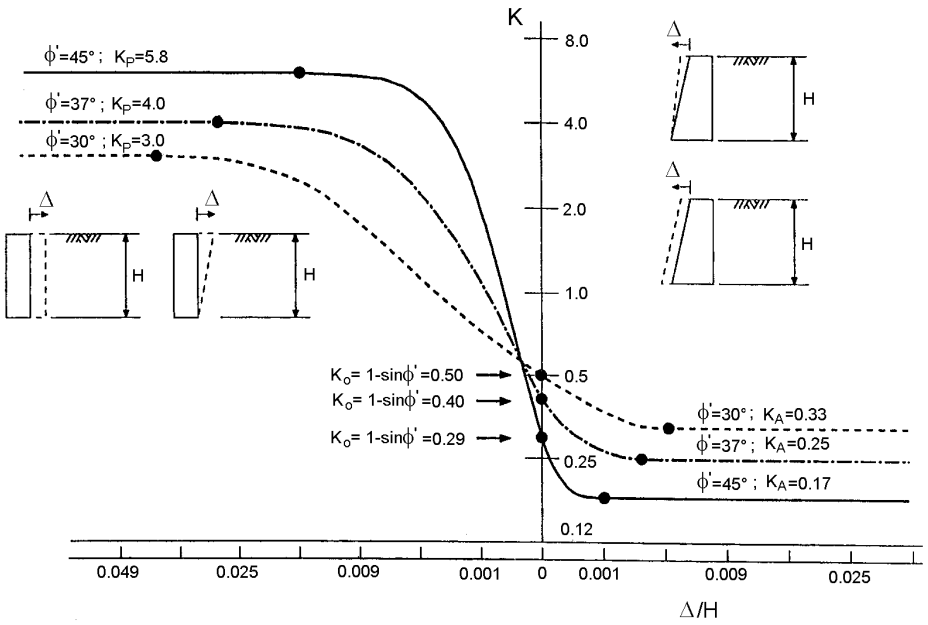

Figure 2.6 Relationship between retaining wall displacements and soil stresses (from Clough, Duncan, 1991)

The definition of the load conditions also influences the structural analyses of the retaining structures since both actions and resistances depend on the values of the pressure coefficients.

Therefore, considering that embedded walls support high excavations and one of the requirements is to limit displacements to the back, especially in presence of existing constructions, the adoption of many and rigid restraint levels, which limit displacements during the excavation phases, may result in at-rest load conditions being maintained instead of active ones. The actions on structures under such conditions are greater being $K_0 > K_A$.

Finally, it is noted that in unloading problems associated with the reduction of horizontal effective stresses with nearly constant vertical stresses, the most dangerous condition for the structure is the long-term condition, so stability calculations must be performed in the effective stresses.

2.2.2. Retaining structures: general remarks

In the design process, the first stage is to assess the appropriateness of a structure for the given application. There are actually many different types of earth retaining structures. Preliminary design should consider different types of retaining structures and the possible ways in which they might fail to perform satisfactorily. For doing this, it is necessary to have an approximate idea of the subsoil types and their distribution in the site of interest.

The principal different types of retaining structures are briefly described in the following paragraphs.

GRAVITY WALLS

According to Eurocode 7, the defining characteristics of a gravity wall is that “The weight of the wall itself…plays a significant role in the support of the retained material”.

For this type of wall, the supporting function is provided by the wall's own weight and the weight of the soil directly acting on it.

Gravity walls can be made of stone, blockwork, plain or reinforced concrete and may include a base footing, ledge or buttress (Figure 2.7). They have a rugged construction, but they are not economical for large retained heights.

Mass concrete gravity wall: the dimensions of the wall are such that the resultant earth pressures on it produce not tensile stress in any part of the wall, since it cannot be assumed that joints between concrete or masonry blocks have any tensile strength.

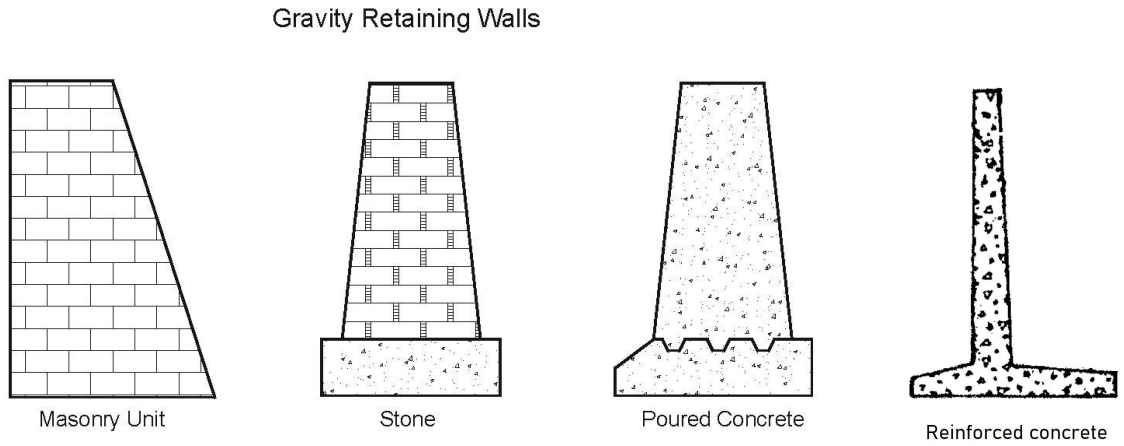

Figure 2.7 Examples of gravity walls

EMBEDDED WALLS

According to Eurocode 7, the defining characteristic of an embedded wall is that "the bending capacity of the wall plays a significant role in the support of the retained material while the role of the weight of the wall is insignificant". Embedded walls are relatively thin walls made of steel, reinforced concrete, or timber, which are supported by anchorages, struts, and passive earth pressure. Examples include cantilever steel-pile walls, anchored or strutted steel or concrete sheet-pile walls, and diaphragm walls.

Sheet-pile walls

Sheet pile walls are widely used to construct flexible support systems, often for both large and small waterfront structures, or in a temporary works (Figure 2.8).

It is often used in unfavourable soil conditions (e.g. soft clays) because no foundations are needed. Although sheet piles are easily driven from ground level, construction is straightforward even where water is present, when other types of structure are difficult to build.

Figure 2.8 Example of steel sheet-pile wall

Sheet-pile walls are able to follow complex plan shapes and cause minimal soil displacement during driving. In fact, they can be constructed in low headroom conditions, with a variety of modern installation methods that cause low environmental impact; in addition, their speed of installation and extraction leads to a high degree of sustainability. On the negative side they can be expensive if used to provide a permanent solution, traditional installation methods can be very noisy, wall depth is limited by section size, loads and standard stock lengths. Moreover, in certain ground conditions, installation may need to be preceded by water jetting.

These structures can be made by different materials: steel, timber and reinforced concrete.

Steel is the most commonly used material in construction because it is characterized by a number of advantages like a large variety of cross section, low cost, relatively light weight. Reusability for temporary works and others.

Wood is usually used for temporary works, short spans, up to 2-m high cantilevered walls, or braced sheetings.

Reinforced concrete can be used for permanent structures, with a variety of cross sections.

Although more durable than steel, concrete sheet-piles need a thicker section, which increases the displacement of the soil during driving, and hence the driving resistance. In addition, the high weight pf each concrete element may make the use of this type of elements uncompetitive with steel piles.

Bored pile walls

Bored pile wall instead can be constructed in almost any ground conditions. They have the advantage that their construction noise and vibration are relatively low, allowing the installation also close to existing buildings. Bored piles can support both high vertical load and lateral heart pressures and they may be of three configurations, as it is illustrated in Figure 2.9:

- Intermittent: large gaps between adjacent piles (spacing s > diameter d) allow the use in overconsolidated soils or soils with natural cementing, and with groundwater below excavation level.
- Contiguous: piles are in contact along their length or have a small gap between adjacent piles. Watertightness cannot be ensured but in very low permeability soils, seepage will be negligible.
- Secant: piles interlocking (spacing s < diameter d). Primary concrete piles typically have no reinforcement, and secondary piles are installed whilst primary pile concrete is still not hardened. In this casa seepage will be negligible and the overall bending stiffness of the wall will be considerably increased.

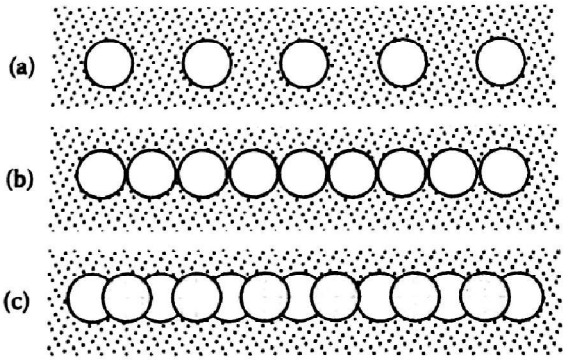

Figure 2.9 Plan view through typical wall configurations: (a) intermittent (b) contiguous (c) secant (from Clayton et al. 2013)

The top of the piles is usually capped by a reinforced concrete beam to distribute loads, and bored pile walls are typically covered. Plant requirements for bored pile walls construction can range from relatively modest to very substantial and they should be of low maintenance unless the workmanship is of low quality.

Bored pile walls, of which it can be seen an example in Figure 2.10, can be realised in a wide range of diameters and to almost any geometric layout.

Horizontal deformation moreover can be restricted to 1%-2% of the retained height when tied back with anchors.

Bored pile walls are more expensive than sheet-pile or soldier pile walls but tend to be cheaper to construct than diaphragm walls.

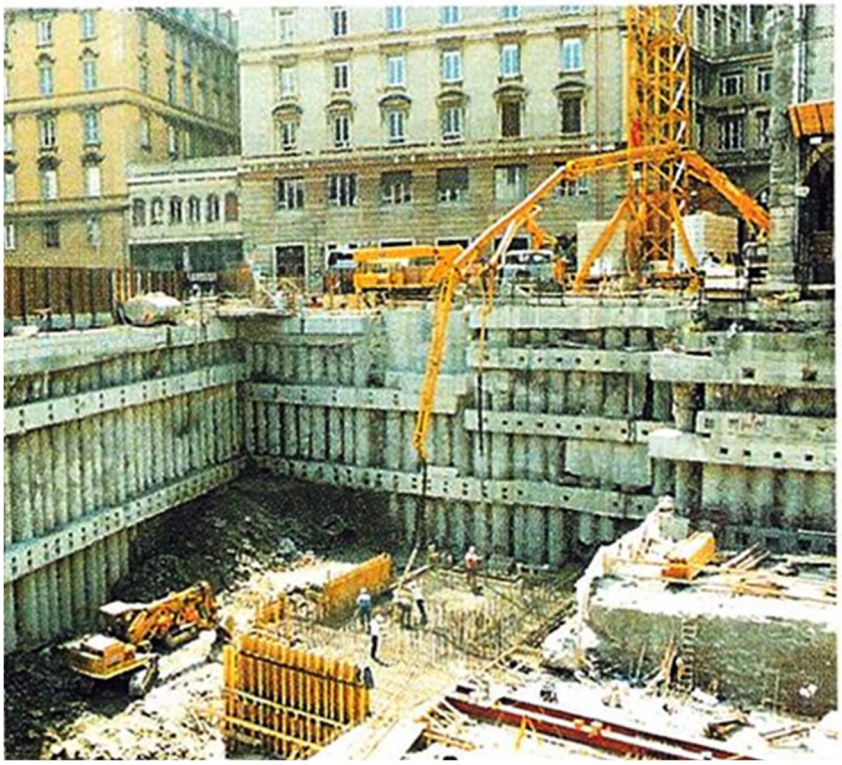

Figure 2.10 Example of excavation sustained by bored-pile walls

Diaphragm walls

A diaphragm wall is a reinforced concrete structure constructed in situ panel by panel and is often used on congested sites, close to existing structures where the excavation depth and ground conditions would prove problematic for piled walls.

The expansion in the use of this type of construction is due to the commercial availability of bentonite as a trench supporting slurry, the experience of construction in urban areas and the resolution of practical problems such as improvement in excavation techniques.

Diaphragm wall construction provides maximum economy either where it can provide both temporary and permanent ground support, or where the diaphragm walling can help to avoid underpinning of adjacent structures, or the need of groundwater control.

The cost of installation depends on different factors such as the configuration and dimensions of the wall and it may be influenced by:

- The required embedment below excavation level, either for stability or seepage control
- The nature of the ground to be excavated.
- Stability requirements such as the need of anchorages
- Site construction factors (slurry treatment, available services, restriction on time and working space

By way of illustration the construction sequence for a continuous slurry trench diaphragm wall is shown in Figure 2.11, while an example of diaphragm wall construction is shown in Figure 2.12.

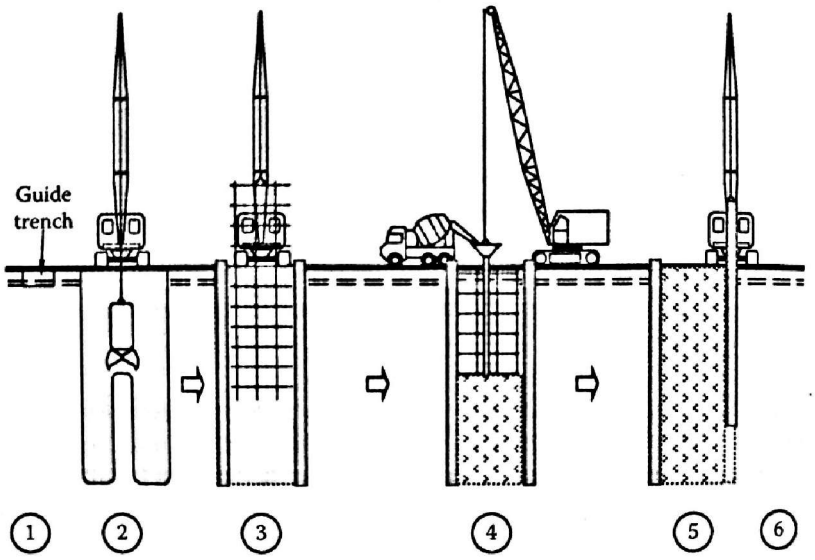

Figure 2.11 Diaphragm wall construction phases (from Clayton et al. 2013)

Diaphragm walls offer high lateral load and moment capacity, are potentially watertight and carry significant vertical loads (leading to their use as deep foundation elements).

In addition, with tieback anchors horizontal displacements can be restricted to 1%-2% of the retained height.

They can be constructed in conditions of low headroom, have a high tolerance potential and cause relatively low noise and vibration. However, they are uneconomic in small developments, are associated with large plant and labour demands and the length of panel excavation makes it difficult to follow irregular plan shapes.

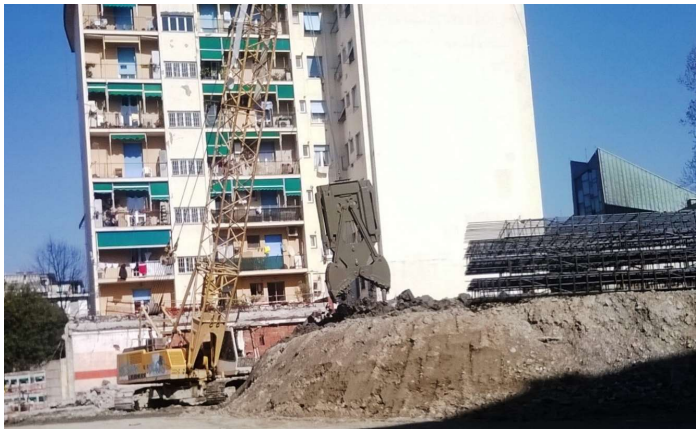

Figure 2.12 Diaphragm wall construction.

King post ("soldier pile") walls

King post walls are structures typically constructed using vertical stell H-piles, installed at regular spacings, with either precast or in situ concrete panels placed horizontally between them (see Figure 2.13).

The concrete panels transfer the earth pressure horizontally to the king posts which transmit the load vertically and through bending moment support the retained. The king posts may be supported by props, ground anchors and soil beneath the retained soil (where they are driven below the base of the supported soil).

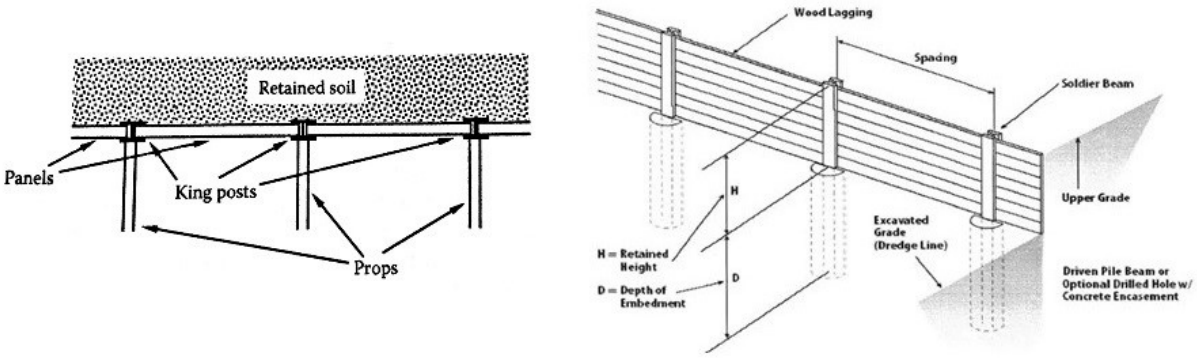

Figure 2.13 Plan of King post wall showing steel H-piles and concrete or wood panels

Figure 2.14 Example of King post wall

In many cases the construction methods require that H-piles are driven from the surface to the wanted level in a soil and these can be stiffened across an excavation as it is dug. As excavation proceeds the soil is cut back between the H-piles and either timber or precast or in situ reinforced concrete panel is placed between the piles. If the soil is too hard to allow the H-piles to be driven, then their locations can be prebored. An example of King post wall is reported in Figure 2.14.

Jet-grouted walls

Jet-grouting creates a column of soil-cement by rotating a horizontal jet of grout in the ground over a specified depth of treatment, mixing grout with the in-situ soil. Creation of columns at relatively close centres will produce a sort of wall which is similar to a secant pile wall, although less resistant and thus with lesser ability to counteract lateral earth pressure.

The process is illustrated in Figure 2.15.

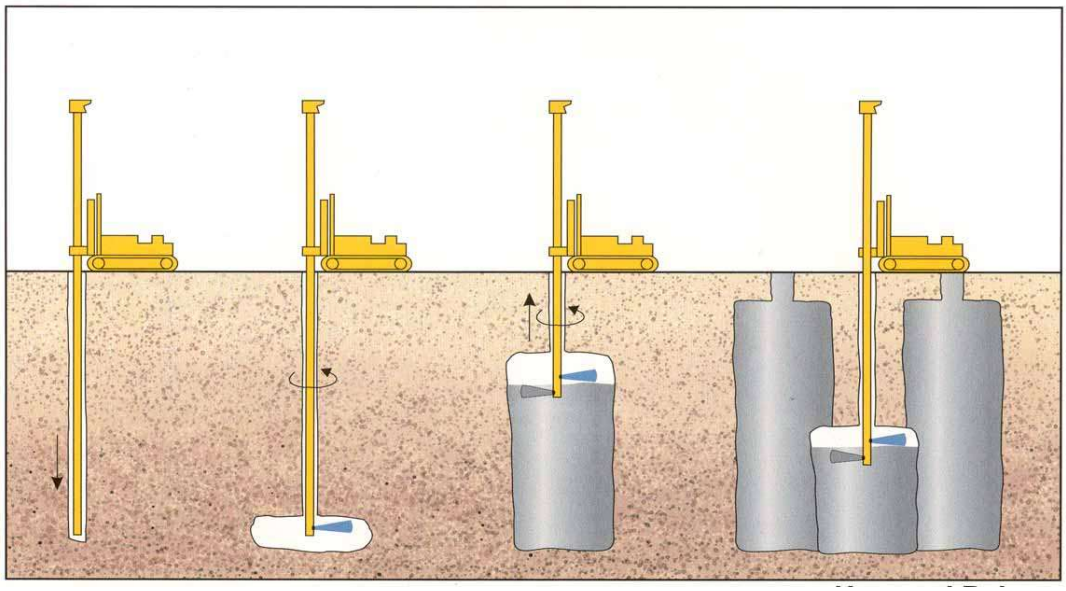

Figure 2.15 Creating phases of jet-grouted wall.

At first an open hole is drilled to the required wall depth and then the columns are constructed from the bottom upward, with alternate columns being formed before the infill columns.

In favourable ground conditions this process is cheaper and faster than bored piling, but the final product has poorer aesthetic, and it is a less sustainable work because of the large mass of soil cement created in the ground and the need to remove cement-contaminated material displaced by the grout and ejected at the ground surface.

2.2.3.Structural supports of the retaining wall.

ANCHORS AND STRUTS

Anchors are geotechnical structures used to transfer tensile stresses to the soil by activating resistant contributions at some distance from the structure under consideration or otherwise in areas that offer the possibility of absorbing the stresses involved. Such structures commonly find application in stabilizing excavation cuts, unstable slopes, retaining structures; reinforcing tunnel vaults, absorbing hydraulic uplift forces, and constraining foundations subject to tensile stresses.

The 2012 AGI-AICAP recommendations define anchors as "structural elements working under tensile stress, consisting of steel or other suitable materials, even of considerable length, which, being bonded to the ground, are capable of transmitting coercive forces to soils and rocks".

The main elements of injected-bulb anchor (Figure 2.16) are:

- anchor head
- free length;
- bond length.

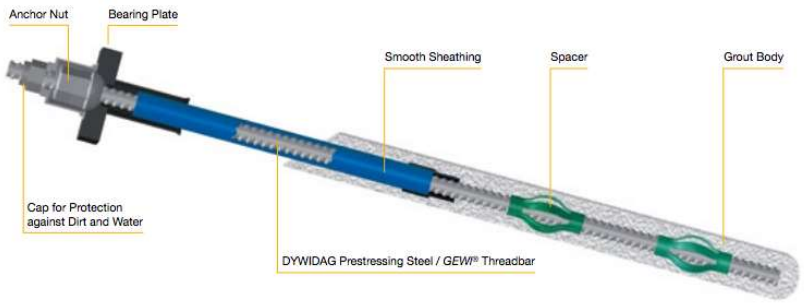

Figure 2.16 Elements of injected-bulb anchor

The anchor head consists of the elements that transmit the tensile force applied to the anchorage to the anchored structure; it includes the locking device and the bearing plate.

The free length of the anchor has the function of transferring the tensile force from the header to the foundation and must remain free from the soil for the entire design life and be protected from corrosive

phenomena. The length of the free part must allow the foundation to be anchored in soils with suitable geotechnical characteristics.

The foundation part of the anchor (bond length) is bonded directly to the ground through a grout body, capable of transmitting the applied tensile load to the soil in which it is located; the reinforcement must be protected against possible corrosion phenomena.

There are mainly three modes of failure affecting the anchorage, and these are:

a) failure of the anchorage at the bulb-soil interface (geotechnical ULS)
b) failure due to global instability (stability ULS)
c) structural failure of the anchor (structural ULS).

In Figure 2.17 are reported these three modes of failure.

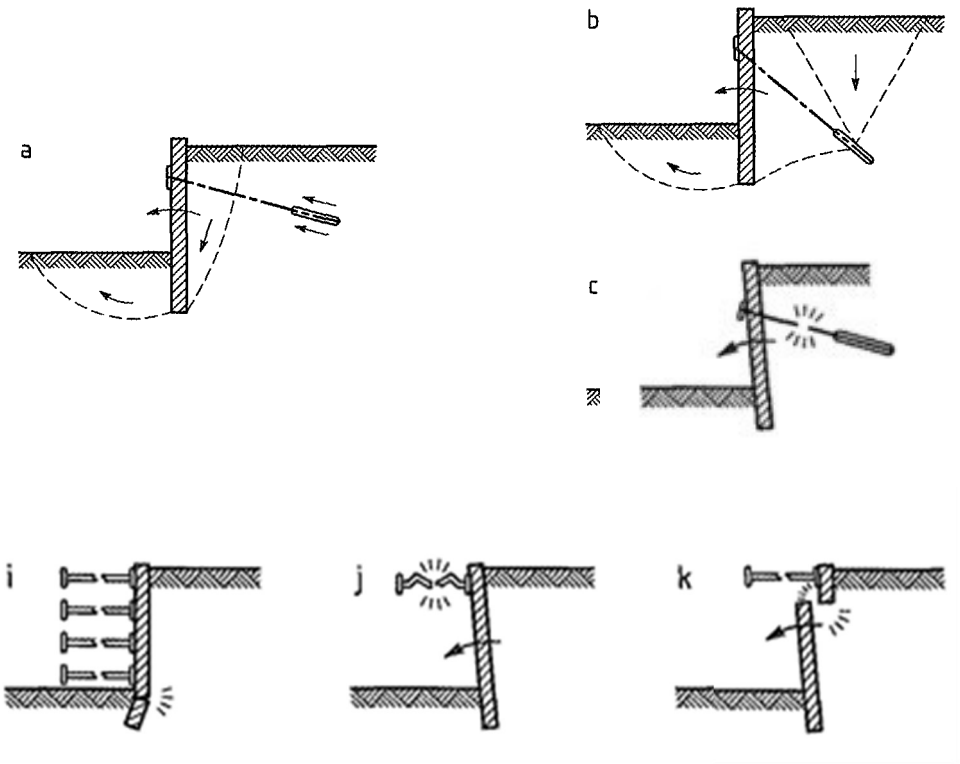

Figure 2.17 Examples of failures conditions for anchorage systems (anchors and struts - from Eurocodes 7)

Anchorages can be divided into:

- pre-stressed anchorages;
- non pre-stressed anchorages.

In addition, there is also the classification according to the reinforcement type (Figure 2.18):

- strand anchors;
- bar anchors.

Stranded tie rods have the advantage of being flexible systems through shortening and lengthening of the strands, easy transportation and installation.

Bar ties, on the other hand, consist of bars formed by modular steel elements connected by joints.

In pre-stressed anchors, the design force is applied and then it is kept constant, ensuring stability and limiting the displacement of the structure to which the anchor has been connected (e.g. an embedded wall for a deep excavation). Often, the most common pre-stressed anchorage are strand anchors because pre-tightening is easily applied to the strands.

On the contrary, in non-pre-stressed anchors, the force is activated when the anchor reacts to displacements of the connected structure

Finally, anchors can also be classified according to the duration of their design life:

- temporary anchorage: the design life is less than two years
- permanent anchorage: the design life is more than two years

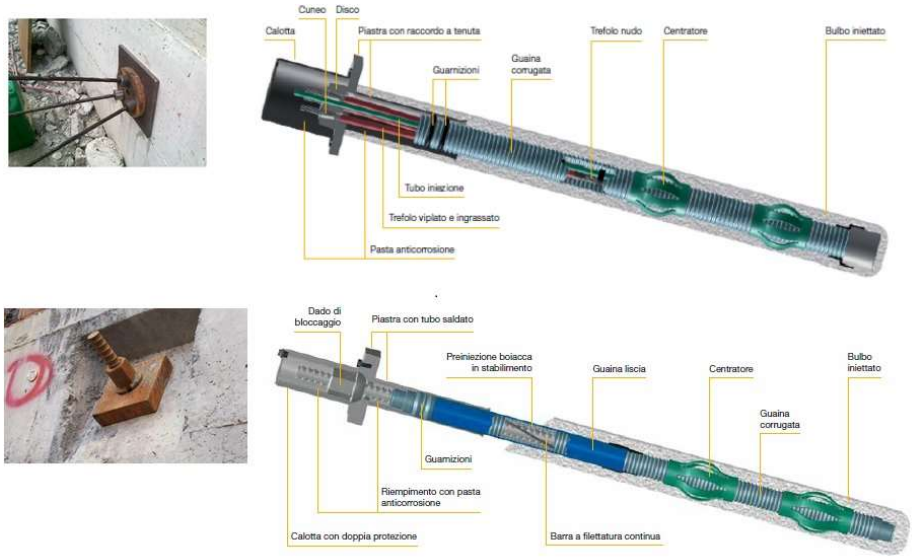

Figure 2.18 Example of strand and bar anchors

Struts are supports, generally made of steel or concrete but sometimes also of timber, which are used to retain the walls of a vertical excavation. They are installed within the excavation as the trenching work progresses and generally support each side of the excavation.

They can be very effective for retaining deep excavations, providing high rigidity and structural strength; installation problems can arise, affecting displacements of the walls to which they are connected; construction site management can be problematic because of the size and bulkiness of the elements that make up the system (Figure 2.19).

Figure 2.19 Example of excavation with struts

2.2.4. Failure design of retaining structures

Retaining structures must be designed constructed and maintained in such a way that they are fit for use throughout their entire working life.

Design is carried out to ensure that the reliability of a structure is appropriate for the consequence of failure, which might include risks to life, economic performance, society, and the environment.

According to Eurocodes, structures must be designed built and maintained so that they meet the following requirements:

- Serviceability. Over it intended design life, the structure should meet specified service requirements, with sufficient reliability and a reasonable maintenance cost
- Safety. The structure should survive all events likely to occur during its construction and use.
- Fire. Structural performance should remain satisfactory for a required period of time.
- Robustness. The structure must not be damaged by extreme events to an amount disproportionate to the severity of the event.

Limit state design separates desired states of the structure from undesired states. Serviceability limit states are states that correspond to conditions beyond which specified service requirements for a structure or structural member are no longer met. Ultimate limit state are instead states associated with collapse or with other similar forms of structural failure.

Eurocode 7 lists five ultimate limit state (Figure 2.20) to consider:

- Verification of static equilibrium (EQU): loss or EQU is avoided when, for cases where soil strength does not have much impact on stability, the sum of the destabilising forces is less than the sum of the stabilising forces.
- Verification of resistance to uplift (UPL): it can occur as when the mass of the new structure is less than the weight of the ground and groundwater that it displaces.

- Verification of resistance to hydraulic failure due to large hydraulic gradients (HYD): piping and hydraulic heave can occur especially in fine grained granular soils when pore pressure exceeds the total stress at or near the bottom of the retaining structure.
- Verification of ground strength (GEO): it includes situations where failure can occur in the soil without involvement of the structural strength like overall instability, sliding and bearing capacity failure.
- Verification of structural strength (STR): it regards the ability of the structure to support imposed ground loads. This includes not only the strength of the retaining structure but also structural elements (anchorages, wale, struts).

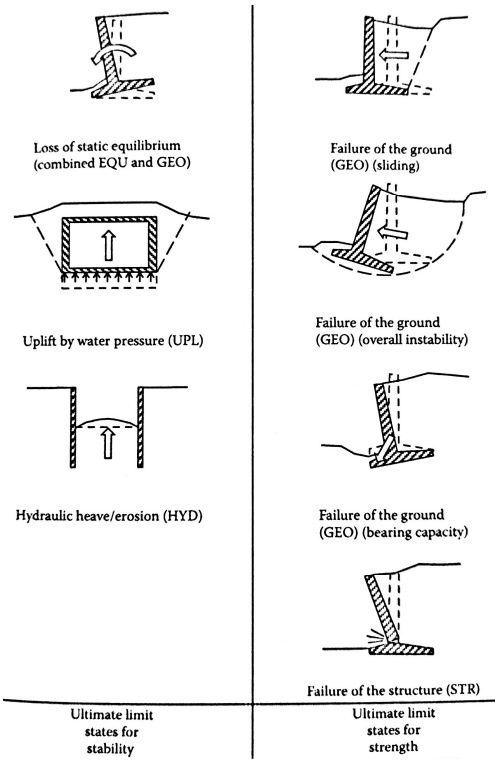

Figure 2.20 Example ultimate limit state for retaining structures, for stability and strength (from Clayton et al. 2013)

Summarizing, for any retaining wall/soil system, the engineer must identify all possible failure mechanisms for serviceability and ultimate limit states and design to prevent them.

2.2.5. Uncertainties in design

An engineer typically has to deal with a number of uncertainties: for example, the extent of different type of ground are usually not be completely defined due to limited site investigations.

In addition there is often uncertainty about the real value of geotechnical parameters and different calculation methods can lead to different results.

The uncertainties in the ground model regards aspects related to different factors such as soil boundaries, soil properties, groundwater, site investigation and presence of services.

A good design has to recognise and take account of uncertainties and unknowns in these aspects. The ground model developed is the result of the knowledge of local geology in combination with the results of field observation and testing, and boreholes in order to elaborate sections which show the expected composition of different types of ground, the groundwater regimes and man-made deposits.

However, given the geological setting of a site, certain features can be suspected but the exact three-dimensional geometry of the ground is always difficult to determine with a high level of certainty. Estimating ground geometry from borehole data is subjected to a limited number of investigation points, the gradational boundaries between some materials and the necessity to idealise the ground as a series of zones constituted by material with similar geotechnical properties. In addition design is made more uncertain by the difficulty to determine the groundwater regime.

According to EC7, serviceability and ultimate limit states can be checked in different ways: by adopting "prescriptive methods", using calculations (from simple hand calculations to sophisticated numerical models like finite element or finite difference), on the basis of the results of physical modelling and load tests or using an observation method.

In the field of earth retaining structures, calculations are most commonly used to compare available resistance with the expected loads that needs to be designed for. Some loads (e.g. vertical dead weight loads) can be expected to be more-or-less constant during the life of the structure. Others, such as wind loads, snow load, earthquake loads and accidental impacts are temporary.

EC7 identifies four design situations that have to be satisfied:

- Permanent loads resulting from the normal use.
- Transient loads from temporary conditions
- Accidental loads from exceptional conditions
- Seismic loads from earthquakes.

Calculations are typically carried out by adopting commercial computer software, that is a sort of "black box" which the user cannot easily check for performance. Hopefully the user manual gives the results of benchmark testing to give some confidence with the product, but calculation methods involve simplifications anyway.

For example, hand calculation methods based on close-form equations can generally be derived by simplifying the problem, so that mathematical solutions can be obtained, and methods based on different simplifications will give different solutions. Moreover, benchmarking exercises carried out by various finite element programs have demonstrated that differences in boundary locations and conditions, and mesh discretization can have a significant influence on the displacements predicted around deep basement retaining structures.

The geotechnical model of the soil provides a geometric simplification adopted in calculating the displacements or the stability of the retaining structure. As mentioned above, the ground is divided into

geometric zones thought to contain material with similar geotechnical properties. Groundwater regimes are estimated from site investigation data and parameters are required for each soil, or rock zone that significantly affect stability and displacement of the structure. Parameters adopted in calculations cannot be known with exactness for a number of reasons such as

- Geometric simplification errors due to limited investigation holes and in-situ tests.
- Variability of material properties within each zone.
- Measured properties determined from in situ or laboratory tests are affected by a range of factors (properties from in situ test could be affected by borehole disturbance for example)
- Directly measured soil properties depend upon the method used to determine them.
- Indirectly deduced properties depend upon the method of in situ testing and on the correlation used to determine the required parameter from test results.
- Parameters required for the different constitutive models available in numerical modelling are not all measurable, but some must be estimated.

Summarizing, geotechnical calculations always involve uncertainty and empiricism to some extent. Therefore, a margin of safety is required to allow for the above unknowns, that can be broadly classified in geometric, calculation and properties uncertainties.

2.3. DISPLACEMENTS AND DEFORMATION INDUCED BY DEEP EXCAVATION

2.3.1. Introduction

The prediction of displacements induced by the execution of excavations in urban areas can be preliminarily performed by simplified methods based on empirical relationship and field data. They are calibrated on free field conditions measurement, under the hypothesis that adjacent buildings are not be able, because of their stiffness, to change the displacement field.

This neglects the soil-structure interaction and generally results in an overestimation of differential settlement and deformation of the structures.

Simplified methods allow an easy comparison between different design approaches, and they are very useful in the infrastructure planning and development phase.

Another benefit of their application is the possibility to distinguish cases in which the effects induced by the excavation on buildings are of low magnitude and do not require further investigation from those in which a more accurate assessment of the effects has to be carried out by numerical analysis of soil-structure interaction.

In general, a preliminary assessment of displacements induced by a deep excavation can be made using simplified procedures based on displacement measurements performed on true size excavations (e.g. Peck 1969; Clough & O' Rourke, 1990; Ou, 2006).

Displacements induced by a deep excavation depend on many factors including the size of the excavation, the type and stiffness of the support system, the mechanical characteristics of the soils affected by the excavation: they increase as excavation depth and width increase, decrease as the stiffness of the

support structures increases and are strongly influenced by the initial effective stress and by the mechanical behaviour of the soils (Rampello, 2017).

Other factors are related to construction procedures and their quality of execution: significant increases in displacement can be caused, for example, by an initial phase of cantilever excavation, method of excavation, execution of retaining structure, delays in installation of the constraint levels, deep drainage, presence of overloading on the back of the excavation, etc.

Despite the multiplicity of the factors mentioned, empirical procedures based on the experimental observations allow to estimate the maximum displacements induced by excavations and to identify the typical settlement profiles.

Therefore, if the maximum settlement induced by the excavation is known, the profile of the ground subsidence can be estimated using a non-dimensional shape of the subsidence profile, defined according to the soil interacting with the excavation, the main deformation mechanisms and the excavation geometry.

Matos Fernandes (2015) proposed a comprehensive study on the aspects related to the control and prediction of displacements induced by deep excavations. Starting on the observation of real case studies, consolidated literature knowledge and numerical analyses performed *ad-hoc*, and also considering the considerable technological advances in the execution of excavations and retaining structures, as well as innovations in monitoring, an interesting contribution aimed at controlling and limiting displacements based is proposed (Matos Fernandes 2007). This contribution suggests eight “golden rules” (defined as 'RELIABLE' approach, from the first letters of those golden rules) referred to the construction and proper characteristics of the retaining structures, to the support systems adopted, as well as to the construction phases and timing, that influence the response of the excavation-retaining structure system.

2.3.2. Displacement of retaining structures

An early semi-empirical method to determine the maximum horizontal displacement of multi-anchored walls in cohesive soils has been proposed by Mana and Clough (1981). The authors propose, limited to the case of excavations in soft clays, to evaluate the maximum horizontal displacement δ_{max}, normalized to the retaining height H of the wall, according only to the value of the safety factors FS related to the excavation bottom heave.

Figure 2.21 shows the correlation between the maximum normalized horizontal displacement (δ_{max}/H) and the safety factors FS, for a specific support structure.

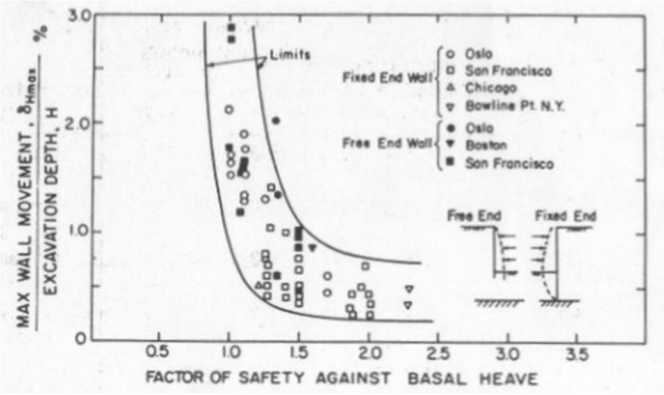

Figure 2.21 Relationship between safety factors and the non-dimensional horizontal maximum displacement of the wall (by Mana and Clough 1981)

Later on in 1989, Clough, Smith and Sweeney proposed a similar but simpler semi-empirical method, in which the maximum horizontal displacement δmax, normalized to the wall height H, is expressed as a function not only of the value of safety factor FS related to the excavation bottom heave, but also in dependence of the value of the support structure stiffness $EI/\gamma_w s^4$ where EI is flexural stiffness of the bulkheads, s is spacing between support levels and γ_w is specific weight of water.

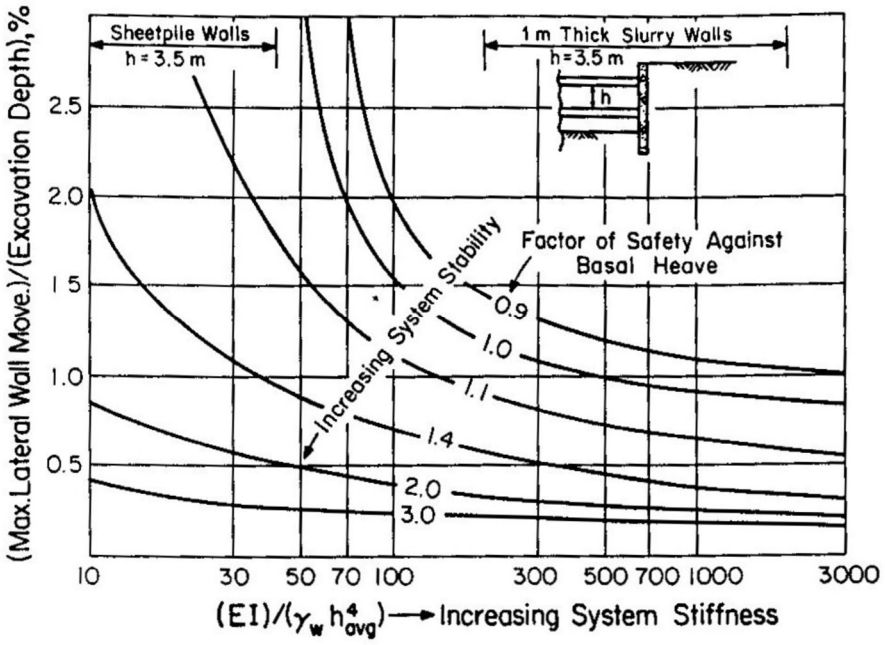

Figure 2.22 Relationship between maximum normalized displacement, support structure' stiffness and safety coefficient (by Clough, Smith and Sweeney 1989)

Figure 2.22 illustrates the influence that wall stiffness and support spacing can have on movements. These factors are most important when FS is low although there are many other factors that affect movements beyond those considered in this chart. It can be note that as FS falls below 1,5, movements increase rapidly.

This chart can be used to assist in predicting maximum horizontal wall displacement when movements are mainly due to the excavation and support process. It is shown how as FS value becomes over 2, and base stability is guaranteed, the maximum movement decrease below 0,5%, and how if FS value is close to 1, movements can exceed 2% H even with good construction.

Therefore, with typical values of stiffness and FS these graphs would indicate displacements on the order of 0.5 to 1% of excavation depth.

Later on, Clough and O'Rourke (1990) first define qualitatively the types of embedded walls deformations, represented in Figure 2.23.

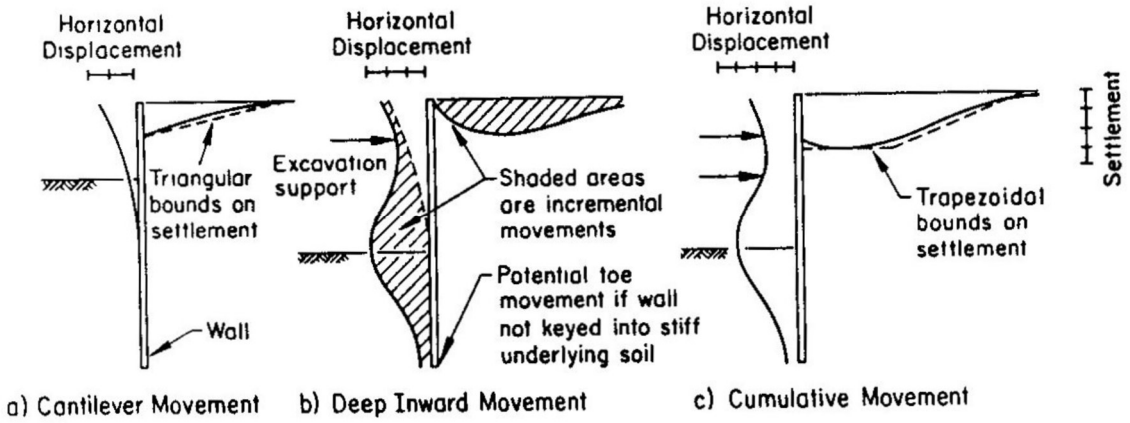

Figure 2.23 Typical profiles of movements for braced and tied-back walls (from Clough and O'Rourke 1990)

At the initial stages of construction of the retaining structure, soil may be excavated before the installation of a support system, the wall deforms as a cantilever (Fig. 2.23 a) and the adjacent soil settles such that vertical surface movements increase in inverse proportion to distance from the edge of excavation with a triangular distribution of displacement. These displacement profiles are characteristic of flexible walls where the supports are installed after considerable excavation has been made and cantilever walls.

When the excavation advances to deeper elevations, upper wall movement is restrained by installation or stiffening of support system and deep movement of the wall occurs (Fig. 2.23 b).

The combination of cantilever and deep inward movement results in the cumulative wall and ground displacement profiles shown in Figure 2.23 (c). If deep inward movement is the predominant form of wall deformation, settlements tend to be bounded by a trapezoidal displacement, if on the other hand cantilever movement is predominant, settlements tend to follow a triangular pattern.

The Authors therefore present some diagrams that collect measures of horizontal displacement of retaining walls and ground settlement, taking care to represent data according to the type of soils, and to exclude measures from cases not well documented. Clough and O'Rourke collect in a chart reported in Figure 2.24 the values of the maximum horizontal displacement δ_{max} and in Figure 2.25 the values of the maximum soil settlement of several different retaining structures depending on excavation height H.

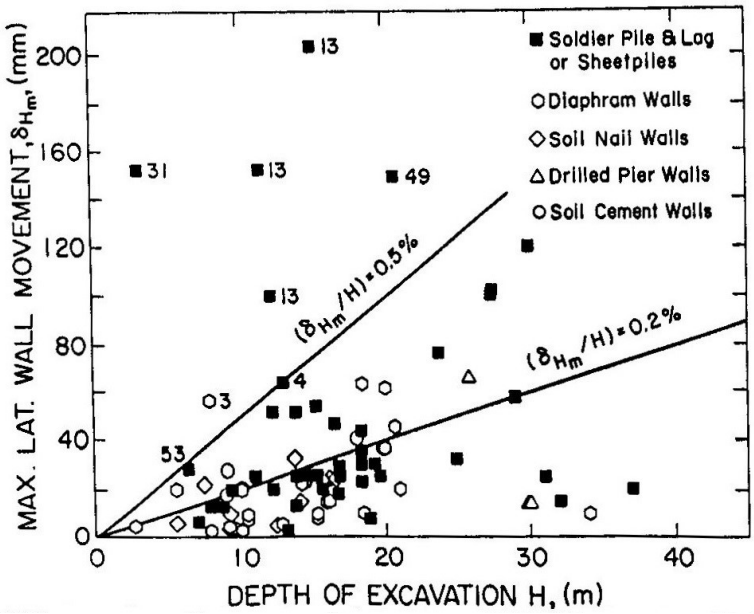

Figure 2.24 Maximum horizontal displacement values in sand and hard clays (by Clough and O'Rourke, 1990)

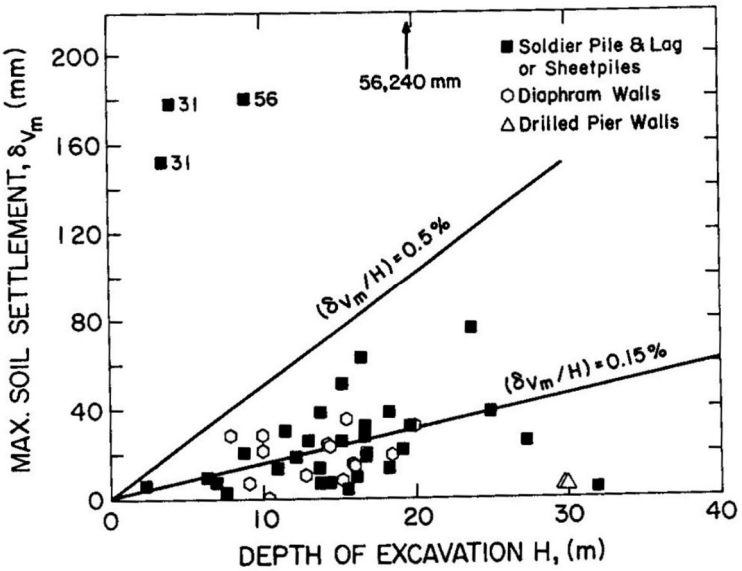

Figure 2.25 Maximum soil settlement values in the soil retained by insitu walls (by Clough and O'Rourke, 1990)

As can be seen, on average the value of the maximum horizontal displacement shall be 0.2% of the excavation depth and almost all the values are less than 0.5%, moreover the typology of the support structures does not seem to play any role.

The vertical settlement instead tends to average about 0.15% (Figure 2.24).

Additionally it is shown in Figure 2.26 a table, taken from Rampello (2017), summarizing the values of the maximum horizontal displacement of embedded walls $\delta_{h,max}$ and the values of the maximum ground settlement $\delta_{v,max}$ obtained from monitoring of several excavations, both normalized in relation to the excavation depth H.

	terreno	$\delta_{h\,max}/H$ (%)	$\delta_{v\,max}/H$ (%)
Clough e O'Rourke (1990)	arg. consistenti sabbie e ghiaie	0,2	0,15
	argille tenere ($F_s > 2,0$)	< 0,5	--
	argille tenere ($F_s < 1,2$)	> 2,0	--
Ou et al. (1993)	argille tenere (F_s elevato)	0,2-0,5	0,5-0,7
Carder (1995)	argille molto consistenti	0,125 (rig. alta) 0,2 (rig. media) 0,4 (rig. bassa)	0,1-0,2
Fernie e Suckling (1996)	argille molto consistenti	0,15 ÷ 0,2	0,15
Wong et al. (1997)	$h < 0,6H$	< 0,20	< 0,35
	$h > 0,6\,H$	< 0,35	< 0,50

Figure 2.26 Measurements of $\delta_{h,max}$/H and $\delta_{v,max}$/H (from Rampello, 2017)

In another work, Long (2001) analyzed data from monitoring of induced displacement of about 300 excavation real cases, and summarized them in a table reported in Figure 2.27.

	sistema di contrasto	$\delta_{h\,max}/H$ (%)	$\delta_{v\,max}/H$ (%)
$h < 0,6H$ terreni consistenti	puntoni	0.17 (96)	0.12 (37)
	ancoraggi	0.19 (57)	0.15 (19)
	top down	0.16 (16)	0.20 (12)
$h > 0,6H$ (terreno consistente a fondo scavo)	puntoni	0.39 (25)	0.50 (15)
	ancoraggi	0.15 (3)	0.14 (1)
	top down	--	--
$h > 0,6H$ (terreno tenero a fondo scavo)	puntoni	0.84 (35)	0.80 (13)
	ancoraggi	0.91 (3)	--
	top down	0.60 (4)	0.79 (4)

Figure 2.27 Average values of $\delta_{h,max}$/H and $\delta_{v,max}$/H (from Rampello, 2017 adapted from Long, 2001)

Data are collected in three groups based on the type of soil in which excavation is executed and the support systems.

However, the relationship between maximum displacement and excavation depth is generally characterized by large scattering, since the depth of excavation is not the only geometric parameter on which displacement depends.

On the other hand, it seems more appropriate to correlate the maximum settlement on the back of the excavation with the maximum horizontal displacement of the retaining wall, since the displacement profiles of the wall and the ground are governed by the same factors.

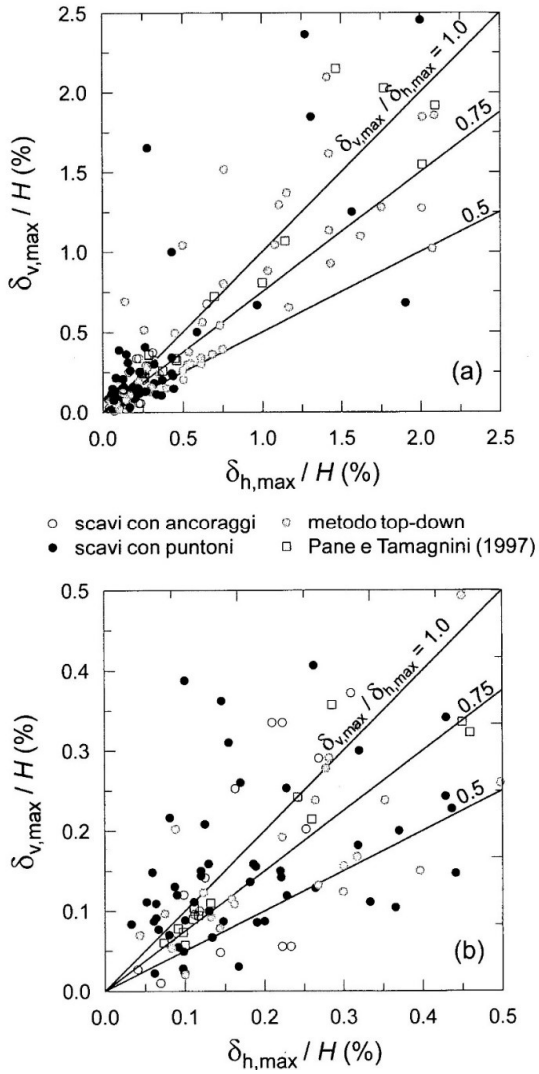

Figure 2.28 Maximum displacement on the back of excavation as a function of maximum horizontal displacement of embedded walls (Rampello, 2017)

The graphs in Figure 2.28 by Rampello (2017), report values of the maximum normalized settlement on the back of excavation $\delta_{v,max}/H$ obtained by Long (2001) as a function of maximum normalized horizontal displacement of the embedded wall $\delta_{h,max}/H$, including the database of Pane & Tamagnini (1997) and the lines of inclination 0.5 0.75 and 1 proposed by Ou et al. (1993) to indicate prevalent trends observed for deep excavation in Taipei, Chicago, San Francisco and Oslo (Mana & Clough, 1981; Ou et al. 1993). Most of the data are plotted in the range $\delta_{v,max} = 0.5 – 1\ \delta_{h,max}$ with the lower limit corresponding to excavations in sandy soils and the upper limit from excavations in soft soils.

Once the maximum settlement $\delta_{v,max}$ is known, the profile of the subsidence can be evaluated by assuming a known shape of the subsidence profile, obtained from measurements on true size excavation.

2.3.3.Ground settlement

Method of Peck (1969)

The first practical approach for estimating ground movements adjacent to excavations was proposed by Peck (1969) which presented his work at VII ICSMFE in Mexico City. He collected ground surface settlement data measured adjacent to temporary braced sheet-pile and soldier pile walls and summarized the data in a chart (Figures 2.29 and 2.30).

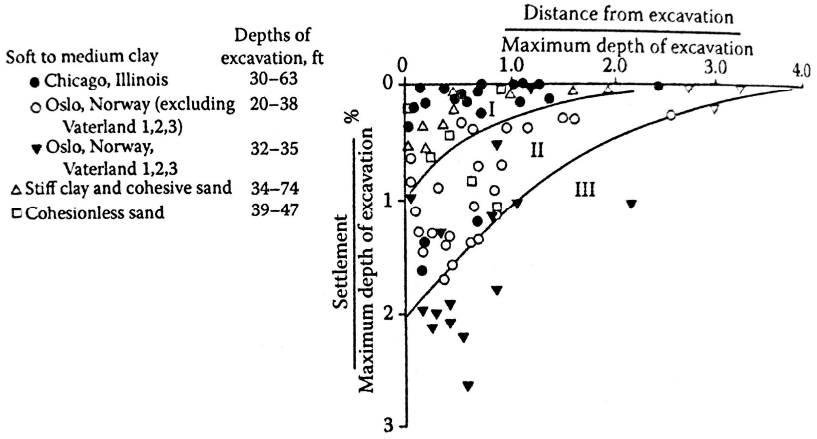

Figure 2.29 Summary of settlement adjacent to braced excavations in various soils as a function of distance from the edge of excavation (from Peck 1969)

This graph, drawn for the prediction of soil settlement adjacent to an excavation, takes into account-soil type, depth of excavation and distance from the excavation.

In particular this chart presents the settlement divided by final excavation depth H plotted against the distance from the insitu wall also divided by H.

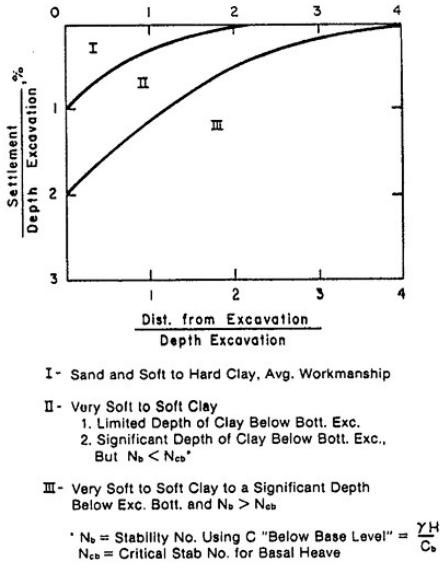

Figure 2.30 Summary of ground settlement adjacent to an excavation (Peck, 1969)

In the figure, γ is the unit weight of the soil above the excavation, H is the final depth of the excavation, and C_b is the undrained shear strength of the soil beneath the excavation.

Peck (1969) grouped the data of the chart into three categories. The categories were developed on the basis of the soil conditions and the level of workmanship employed during the construction of the wall. Author also identified that portions of the ground surface deformation patterns might be due to the bottom instability in the soft and medium clays.

Category I includes excavations in sands, stiff clays, and soft clays of small thickness. Category II includes excavations in very soft to soft clays that extend to a small distance below the bottom of the excavation or with a stability number, N_b, less than 6 or 7. Category III includes excavations in very soft to soft clays that extend to a significant depth below the bottom of the excavation, and with N_b greater than the critical stability number for basal heave.

As it can be seen in the figure, for the soils of Category I, the maximum surface settlement is limited to 1% of the final excavation depth H; for Category II the maximum surface settlement reached 2% of the final excavation depth. However, the extent of the influence at the ground extends 2 to 4 times the depth of the excavation.

The early work of Peck was subsequently developed by Mana and Clough (1981) using finite element analysis and later by Clough and O'Rourke (1990).

Method of Clough and O'Rourke (1990)

Clough and O'Rourke observed that a relatively well-defined grouping of excavation-induced settlement data was evident when the settlements were plotted as fractions of maximum settlement. So the Authors presented dimensionless settlement profiles as a basis for estimating vertical movement patterns adjacent to excavations in different soils.

Separate profiles were developed for sand, stiff to very hard clays, and soft to medium clays, as it is shown in Figures 2.31, 2.32, 2.33.

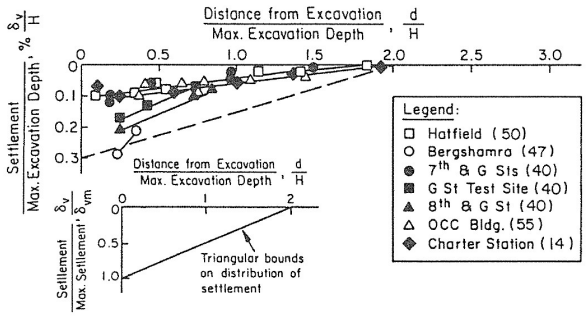

Figure 2.31 Summary of measured settlement adjacent to excavation in sand (Clough & O' Rourke 1990)

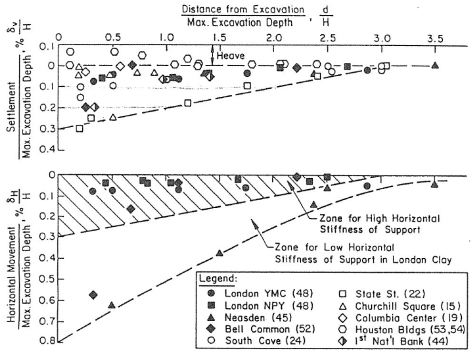

Figure 2.32 Summary of measured settlement and horizontal displacements adjacent to excavation in stiff to very hard clay (Clough & O' Rourke 1990)

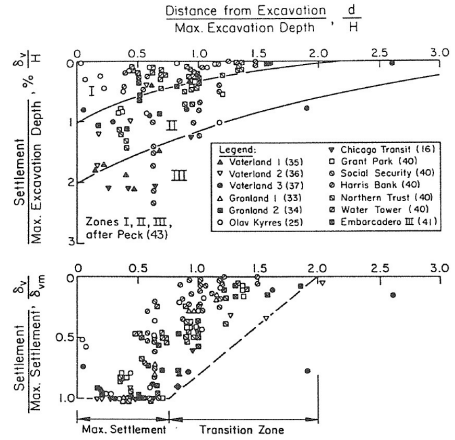

Figure 2.33 Summary of measured settlement adjacent to excavation in soft to medium clay (Clough & O' Rourke 1990)

Figure 2.34 presents dimensionless settlement profiles recommended as a basis for estimating vertical movement patterns adjacent to excavations in sand, stiff to very hard clays and soft to medium clays.

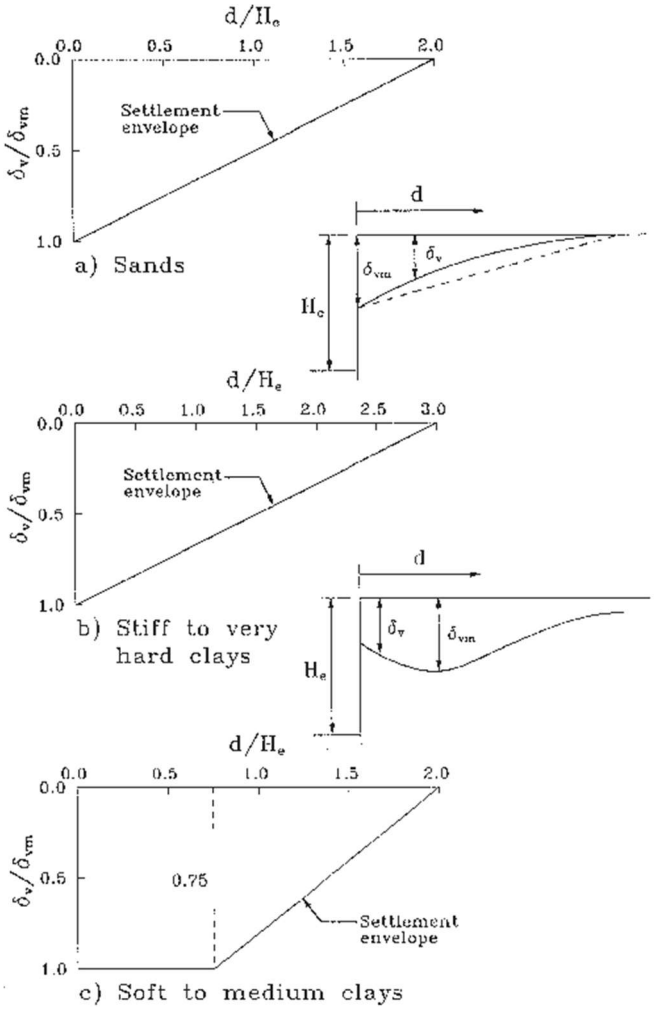

Figure 2.34 Dimensionless settlement profiles recommended for estimating the settlement adjacent to excavations in different soil types (Clough & O' Rourke 1990)

With the knowledge of the maximum settlement, the dimensionless diagrams can be used to obtain an estimate of the actual surface settlement. The figure shows that the settlement influence zone is 3H for excavations in stiff to very hard clays and 2H for excavations in sands and soft to medium clays. In soft clayey soils the settlement distribution in bounded by a trapezoidal envelope in which two zones of movement could be identified.

The zone in which the maximum settlement occurred was at $0 \leq d/H \leq 0.75$ where d is the distance from the excavation and H is the final depth of the excavation. Instead at $0.75 < d/H = 2.0$, there was a transition zone in which settlements decreased from maximum to negligible values.

In using the diagrams presented by Clough and O'Rourke (1990), it should be recognized that they pertain to settlements caused during the excavation and bracing stages of construction. Movements associated with other activities, such as dewatering, deep foundation removal or construction, and wall installation, must be estimated separately. Excavations in stiff to very hard clays show variable behavior, with heave possible in some conditions.

For stiff to very hard clays, the dimensionless diagram should be used as a conservative estimate, provided that the wall is stable and not affected by poor construction techniques, so in making judgements in these cases it is often valuable to refer to local construction experience.

Method of Hsieh and Ou (1998)

Hsieh and Ou (1998) suggest that there are two types of settlement profiles caused by excavations: (i) spandrel type, in which maximum settlement occurs very close to the wall; and (ii) concave type, in which maximum settlement occurs at a distance away from the supported wall as it is shown in Figure 2.35.

The spandrel type of settlement profile occurs if a large amount of wall deflection occurs at the first stage of excavation when cantilever conditions exist, and the wall deflection is relatively small at the subsequent excavation. After the initial stages of excavation, additional cantilever wall deflection is restrained by installation of support as the excavation proceeds to deeper elevations.

The concave settlement profile reflects the ground settlement profile that develops when the movements are more deepseated.

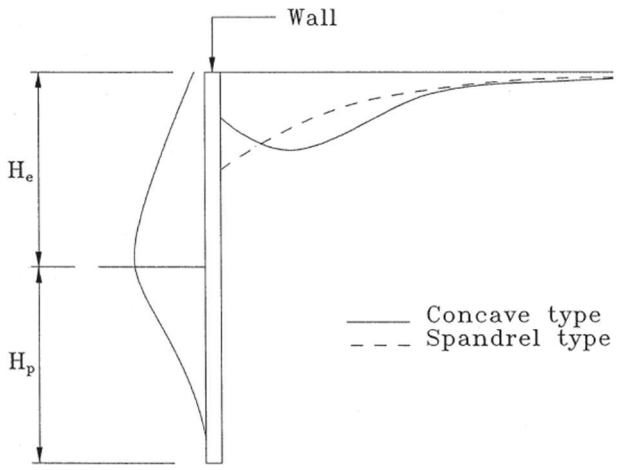

Figure 2.35 Types of settlement profile

The authors presented a relationship for a spandrel-type condition shown in Figure 2.36.

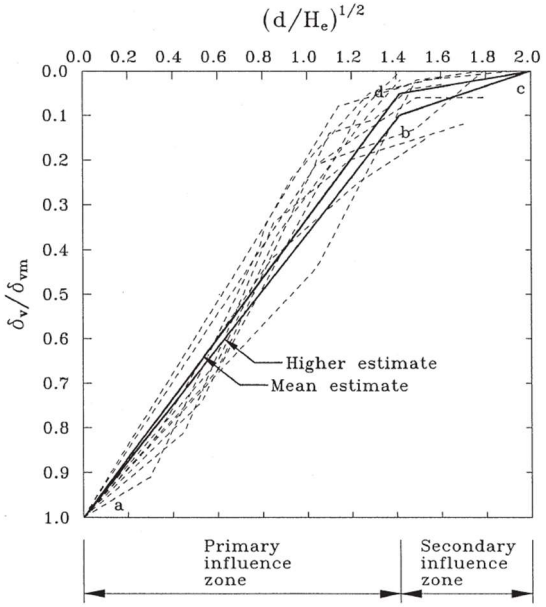

Figure 2.36 Proposed Method for Predicting Spandrel Settlement (Hsieh and Ou, 1998)

The data are presented as normalized settlement, $\delta_v/\ \delta_{vm}$, where δ_{vm} is the maximum ground surface settlement, versus the square root of the distance-from-the edge-of-the-excavation divided by the-excavation-depth (d/He). This relationship was based on 10 case histories from Taipei, Taiwan.

Hsieh and Ou (1998) also developed the curve in Figure 2.37 for the concaved settlement profile from case histories compiled by Clough and O'Rourke (1990) and obtained from additional sites in Taipei.

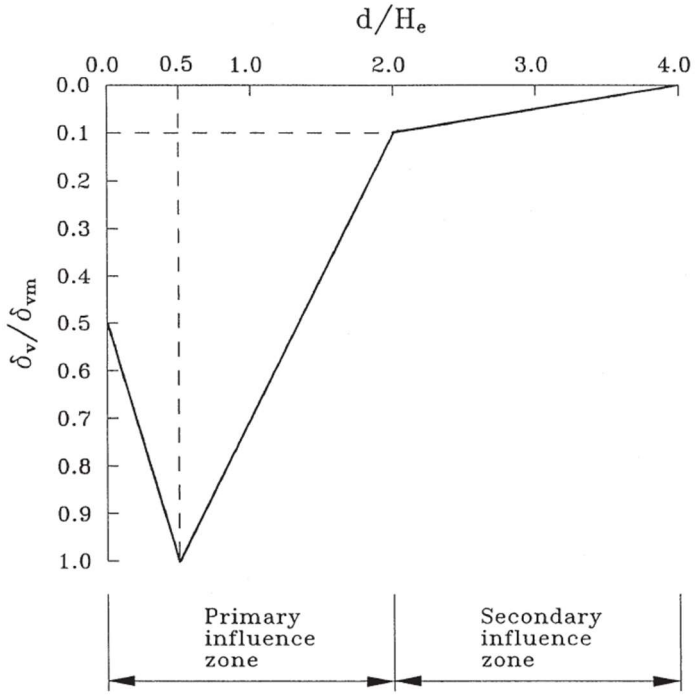

Figure 2.37 Proposed Method for Predicting Concave Settlement Profile (Hsieh and Ou,1998)

The Authors concluded that the distance from the wall to the point where the maximum ground surface settlement occurred was approximately equal to half the excavated depth. Assuming the maximum lateral wall deflection occurs near the excavation bottom, the distance where the maximum ground surface settlement occurs can be taken as half the final excavation depth (He/2). Evaluating case histories, the settlement at the wall was established as 0.5 δ_{vm} and the point d/He=2 corresponds to the extent of the primary influence zone, which was defined by Hsieh and Ou (1998) as being equaled to approximately two excavation depths (2He).

The case histories also showed that settlement was practically negligible at a distance from the wall corresponded to four excavation depths (4He) and was thus used as the farthest most point on the curve. For simplicity, a linear relationship was assumed between each turning point.

Methods of Ou (2006) and Ou and Hisieh (2011)

In 2006 Ou proposes a new method that changes the previous one, while maintaining the difference between primary and secondary influence zone.

The technique is based on typical shapes of the subsidence profile, observed on true size excavation, on the extension of the area of influence behind the excavation and on the distance at which the maximum settlement occurs.

In the procedure surface deformation mechanisms, typical of cantilever walls or retaining walls with maximum horizontal head displacements are distinguished from deep mechanisms in which the maximum displacement of the bulkhead occurs close to the excavation.

In the first case the subsidence profile is characterized by a maximum settlement nearby the retaining structure, and by a triangular shape with concavity downwards; in the second one the maximum displacement occurs at a distance from the wall little influenced by excavation depth and the profile is characterized by a change of curvature (Figure 2.38).

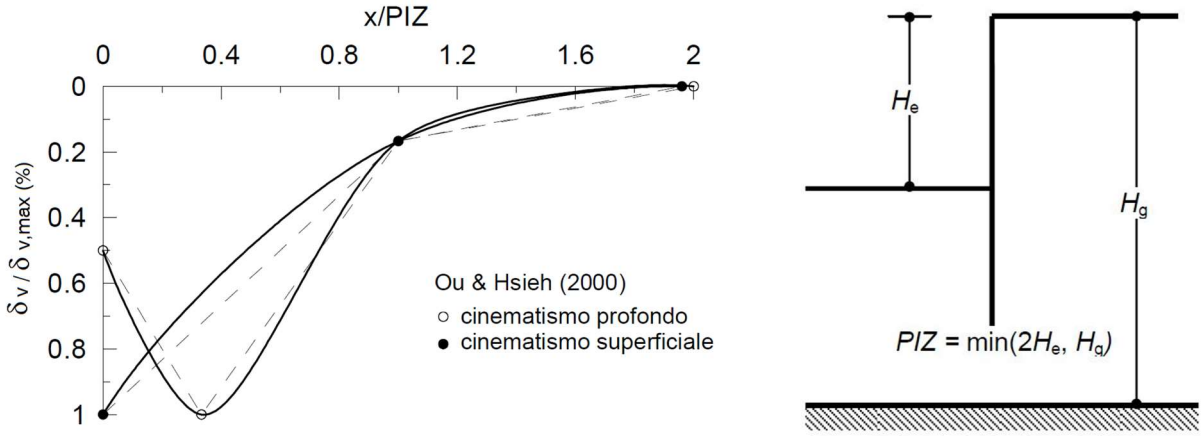

Figure 2.38 Normalized settlement profiles on the back of excavation (adapted from Ou, 2006)

Based on this Ou distinguishes a primary influence zone (PIZ) of the excavation in which the greatest subsidence variations occur, resulting in increased effects on adjacent buildings and a secondary zone (SIZ) where the sagging profile is characterized by lower gradients and less effect on buildings (Figure 2.39).

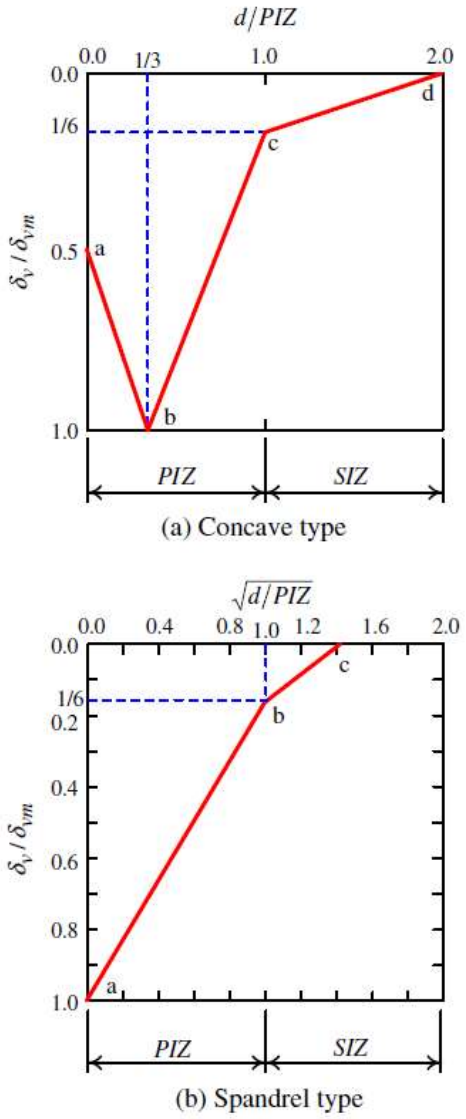

Figure 2.39 Proposed profile for predicting the ground surface settlement (from Ou and Hisieh, 2011).

For excavations in soils of medium to high soil composition, the extent of the zone of primary influence is defined as:

$$PIZ = \min\left(2H_e, H_g\right)$$

where H_e is the excavation depth and H_g is the depth of the layer of consistent soils below the bottom of the excavation (see Figure 2.38).

The ratio $\delta_v/\delta_{v,max}$ is plotted as a function of the distance x from the wall, normalized with respect to the primary influence zone; the line segments shown in the figure can be interpolated by splines to obtain an estimation of subsidence profile induced by an excavation once $\delta_{v,max}$ and PIZ are known.

Since Peck's pioneering work, much information and data have been gathered that allow better estimation of failure profiles. Equally, interventions aimed more at stabilising excavation face than at limiting the possible displacements with the traditional techniques of tie rods, struts, ground improvent shall be taken, and solutions involving structural inclusions, which will be studied below, are introduced.

2.4. NUMERICAL MODELS: GENERAL REMARKS

2.4.1. Introduction

In the following, the main aspects of numerical modelling using the FEM method are explained very briefly since numerical analysis was used for the subsequent analyses. For the purpose of synthesis, only the fundamentals are introduced.

Numerical models simplify the geometry of soil-structure interaction problems by dividing the soil and any structural members into elements. Within each element, the properties of the soil or structure are taken to be constant, simplifying geometry and properties variations and allowing a solution to be computed for each zone. These methods are increasingly used for retaining wall design thanks to the rapid growth of computing power.

For retaining wall analysis, the finite element and the finite difference methods are widely used, offering an invaluable tool for the assessment of serviceability and ultimate limit states, in particular when a highly hyper-static problem is to be faced, as occurs in multi-constrained embedded walls, interacting with ground and other structures (Matos Fernandes, 2015).

Besides, strongly non-linear problems cannot be solved accurately without reliable numerical analyses, allowing to use advanced constitutive models for structures and, above all, for the soil.

In this thesis the studies were carried out using the FEM computer code Plaxis2D and 3D.

2.4.2. Finite element method

The finite element method (FEM) is a numerical technique for solving the differential equations governing a boundary value problem. The zone of interest is divided into discrete areas called elements (usually triangular or rectangular) defined by node points located at the vertices and sometimes along the element edges.

Within each element, the behavior is idealized, and the quantity of interest (such as the displacement) is constrained to vary in a prescribed way (e.g. linear or quadratic). The value of this quantity at any element interior point is related to its values at the nodes, through interpolation or shape functions N based on the element geometry

$$\theta = \sum_{i=1}^{i=n} N_i \theta_i$$

where θ is the quantity and n is the number of nodes. In retaining wall analysis, the displacement is the usually the quantity of interest and differentiation of the shape functions gives expressions for the strain vector ε in term of nodal displacement a:

$$\varepsilon = Ba$$

where B depends on the element geometry. Then an appropriate constitutive relationship can be used to relate stresses σ and strains ε within the element:

$$\sigma = D\varepsilon = DBa$$

where D depends on the material properties. Applying virtual works theorems, element stiffness relationship can be established between applied loads F and resulting displacement at the nodes

$$F = Ka = \int (B^T DBd(vol))a$$

Finally a global stiffness matrix is obtained by assembling the contributions from each single element.

After applying boundary conditions (such as known forces and fixities displacement) the global system of equations is solved to give the unknown nodal displacements.

Internal strains in any element may be calculated from these displacements followed by stresses applying the constitutive relationships.

2.4.3. Geometric representation

The choice of mesh is very important and while there is no single correct mesh some perform better than others and certain meshes may be totally incorrect (too few elements/zones) or highly inefficient (boundaries excessively remote). However, some element/zine boundaries are fixed by division between material types, physical limits of the problem domain, changes in geometry etc., other boundaries are somewhere arbitrary. Smaller elements/zones must be used in areas where quantities of interest are likely to change rapidly, and larger elements/zones should be used further away (Figure 2.40). In addition, the mesh must be graded between such areas.

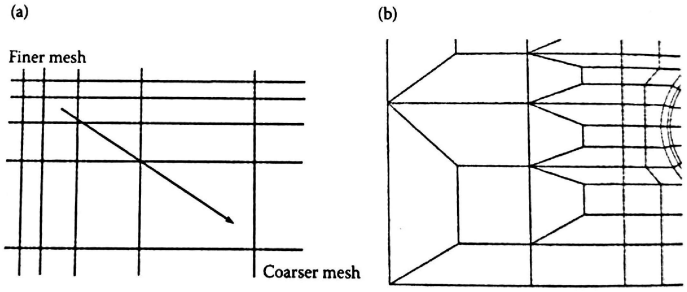

Figure 2.40 Mesh grading. (a) Simple (b) More advanced (from Clayton et al. 2013)

As regard the boundary conditions, near boundary are usually defined (e.g. retaining wall face or base of excavation). Far boundaries instead must be positioned sufficiently remotely from the structure so as not to restrict or constrain the solution in the area of interest. A simple method to investigate the adequacy of a mesh is to change the boundary conditions and observe the effect on key outputs.

For two-dimensional problems, the elements most widely used are quadrilateral and triangular elements (see Figure 2.41), and they may be augmented by one-dimensional line elements for relatively thin material zones that have particular tensile, flexural or interfacial properties. For three-dimensional models bricks and tetrahedra elements are employed together with two-dimensional elements for thin zones. The order of an element is defined by the interpolation functions it employs and is usually identified by the number of nodes it possesses. The 3-noded triangles and 4-noded quadrilaterals are capable of describing a linear variation in the principal quantities, whereas 6-noded triangles and 8-noded quadrilaterals can describe a quadratic variation.

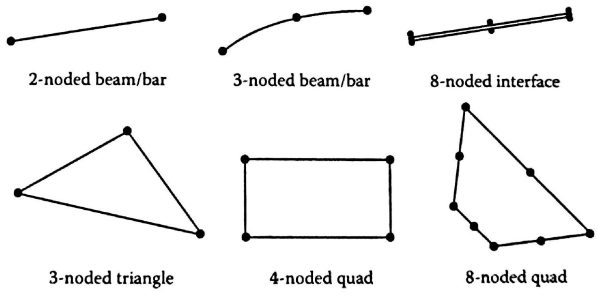

Figure 2.41 Examples of two-dimensional finite elements (from Clayton et al. 2013)

In addition, there is the degrees of freedom (d.o.f.) which describes the number of independent values of the principal quantity of interest associated with it. For example, a 6-noded triangle has 12 d.o.f. because there are two components of displacement (in x and y direction) at each node.

2.4.4. Constitutive models

FEM packages usually offer different constitutive models which can range from simple elastic models to highly sophisticated elasto-plastic strain-hardening/softening models. The choice is closely linked to the selection of appropriate soil parameters whose estimation is not always possible with sufficient accuracy.

As an example, the most basic form of constitutive behavior is the homogeneous isotropic linear elastic that requires only Young's modulus E and Poisson ratio ν, or alternatively shear and bulk modulus G and K. Although incapable for representing real soil behavior, it is quite common for structural members to be modelled as linear elastic in an earth-retaining system. Indeed, the extent and magnitude of ground movements are often overestimated using simple elastic models, not only because stiffness parameters are overestimated in conventional laboratory tests, but also because strain level in the field are frequently very small. For most soils mean effective stress and hence stiffness increases with the depth, so a non-homogeneous behavior occurs.

Moreover, many natural soils present anisotropy, so a different stiffness and strength properties in the horizontal and vertical directions of loading, because of the distribution of soil layers or of stress history. In these cases, cross anisotropic elastic models require five independent parameters (e.g. E_v, E_h, ν_{vh}, ν_{hh} and G_{vh}).

On account of the non-linear nature of most natural soils, the overall pattern of displacements predicted using a simple linear model may be incorrect; it is therefore often necessary to use non-linear constitutive models.

All soils present plastic behavior above certain levels of stress or strain. For effective stress analysis, the Mohr-Coulomb yield criterion in terms of c' and φ' is well established and widely offered in FEM programs. For total stress formulations indeed the equivalent Tresca yield criterion in terms of c_u can be used and if the soil is non-homogeneous, c' or c_u can vary with the depth.

Either perfect plasticity may occur, or the yielding may exhibit hardening or softening. The first is most frequently in FEM codes (for Mohr-Coulomb and Tresca criteria), but reduction of strength and stiffness after yield occurs in many natural soils. For this reason, there are some models (e.g. the Cam-Clay family models) that provide for strain softening as well as hardening.

3. ANALYSYS OF DEEP EXCAVATIONS SUPPORTED BY EMBEDDED WALLS WITH STRUCTURAL INCLUSIONS

3.1. INTRODUCTION

In general, the execution of an excavation induces displacements in the subsurface and in the structures interacting with it due to the change in total horizontal and vertical stresses associated with soil removal and the change in hydraulic conditions. Experience shows that the ground displacements are closely related to the horizontal displacements of the excavation support system, as described in the works of Mana and Clough (1981) and Rampello (2017) where it is shown that the maximum ground level displacements are between 50 and 100 percent of the corresponding horizontal displacements of the support structures. Therefore, a reduction of these displacements is necessary.

Traditional solutions (such as struts and anchors) can only partially reduce these displacements since these are systems that can only be implemented after excavation, when part of displacement has already occurred. It is possible, however, to use reinforcement solutions that can be installed before the excavation is carried out and can reach greater depths than the bottom. These types of solutions include structural inclusions that connect face walls (cross walls) and local stiffening and strengthening interventions in the portion of the ground that is to be excavated, including below the excavated surface (buttress walls).

In this chapter, the study of the response of such retaining structures by numerical analysis under bi- and tri-dimensional conditions is reported. A series of parametric models were developed using Plaxis 2D and Plaxis 3D FEM software, varying some geometric features to evaluate their influence on the response of the structure in terms of displacements and deformations.

3.2. MODELLING OF THE EFFECTS OF DEEP EXCAVATIONS

The objective of this first phase is to assess the reliability of numerical modelling by comparison with literature abacuses. An extensive series of parametric two-dimensional FEM analyses were planned: starting from a reference geometric scheme and certain types of support structures of usual application, a series of different scenarios were modelled with the aim of going to investigate quantities influencing ground displacements.

3.2.1. Geometric parametric model of excavation

As above mentioned, the first step of the work was to perform many analyses on different parametric models, in order to create a suitable database where to develop the next studies.

The parametric analyses refer to the geometric model in Figure 3.1.

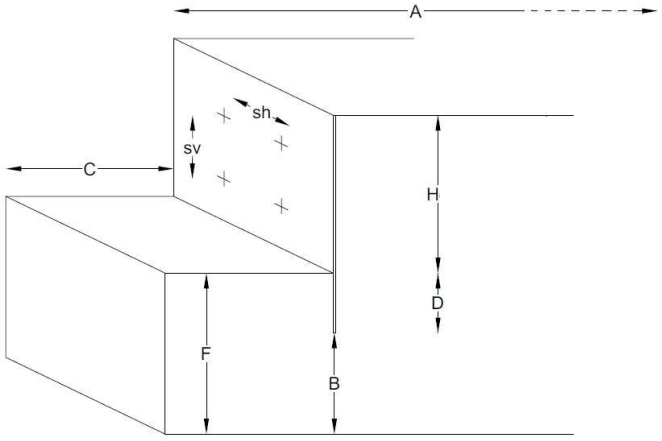

Figure 3.1 Geometric parametric model of excavation

A is linked to the extension of the mesh, and its value has been selected after suitable merging analyses; B is the thickness of the soil under the bottom of the retaining structure, C is the semi-width of the excavation, D is the embedded depth of the structure, H is the excavation depth, H_t is the total height of the structure, s_h and s_v are the horizontal and vertical centre-to-centre distance of the anchors and F is the depth of a rigid soil layer.

All these quantities were varied parametrically as shown in Table 3.1.

Table 3.1

Parameter	Values
A	6H
B	≥ 2D
C	24,12 m
D	2, 3, 4, 6 m
F	9, 18, 30 m
H	6, 9, 12 m

For every model three different displacement profiles have been extracted, as it is shown in Figure 3.2: the ground settlement u_y, the horizontal displacement of the retaining structure u_x and the bottom heave u_b.

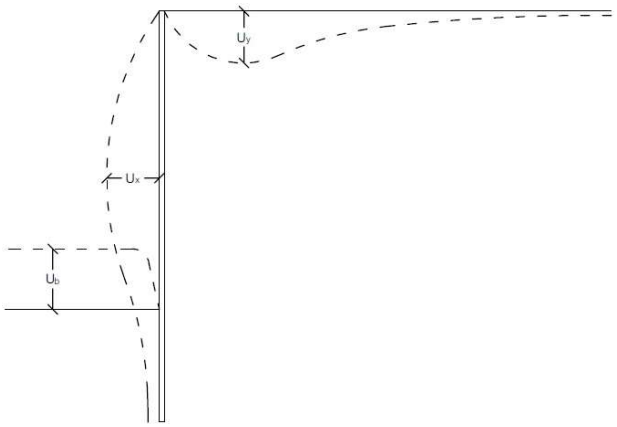

Figure 3.2 Displacement profile of excavation

3.2.2. Retaining structures

For these preliminary analyses, three types of retaining structures have been adopted: a 0,6 m thick concrete diaphragm, two embedded walls of 0,6 m diameter piles with a spacing i_p of 1,2 m and a wall of micropiles as it is shown in the figure. The axial and bending stiffnesses EA and EJ and the Posson ratio ν values, are reported in the table below (Table 3.2).

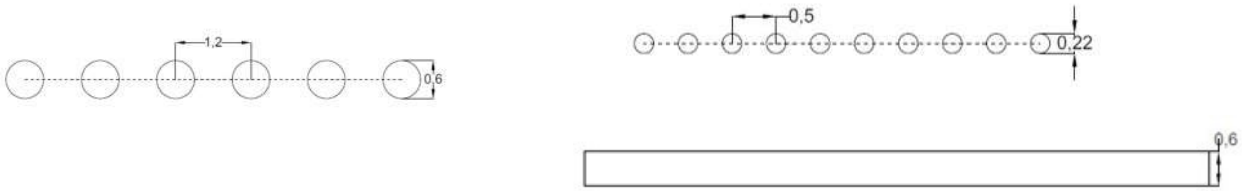

Table 3.2

	EA [kN/m]	EJ [kN/m²/m]	ν [-]	i_p [m]
Concrete diaphragm wall	1,89	$5,67\ 10^5$	0,2	-
Bored pile wall_1	7,35	$1,67\ 10^5$	0,2	1,2
Micropile wall	4,074	$1,27\ 10^4$	0,2	0,5

With these schemes, many parametric analyses have been performed; for the purposes of this study, in relation to what is analyzed in Sections 3.4, 3.5 and 3.6 below, the focus in the following is on the cases referred to the bored pile wall and diaphragm wall.

The choice of wall structures and support systems was determined by the need to have a representative case study corresponding to geometric and stiffness characteristics typical of real applications in engineering practice.

The support system in the numerical models is provided by structural constraints simulating anchorages made with tendon anchors, with horizontal spacing 2.4 m and appropriate anchor bond length. In the model, these constraints, represented by elastic elements, are characterized by their axial stiffness and by the horizontal spacing. The adopted geometrical schematization is similar the one illustrated in Figure 3.17.

The average value of the axial stiffness attributed to the constraints in the FEM model was estimated under the assumption that the deformation response remains almost in the elastic range. The constraints simulate multistrand anchors arranged in three/four rows along the height of the embedded walls, with number of strands (5 strands for each anchor – max axial force T≅750 kN), free and bond lengths, and other geometric parameters defined to result in a restraint system characterized by an average elastic stiffness EA of about 150 MN.

The design, from a static point of view, of the bond length (L_b) has been performed by assuming a limit average shear resistance along the bond length in the range $\tau_{s,u}$=200-250 kPa and the grout bulb diameter d= (1.2·16)=19 cm (Bustamante and Doix, 1985), with safety factor FS=2. These assumptions lead to:

$$L_b = \frac{T}{\pi \cdot (\alpha \cdot d) \cdot \left(\frac{\tau_{,su}}{FS}\right)} = \frac{5 \cdot 150}{\pi \cdot (1.2 \cdot 0.16) \cdot \left(\frac{200 \div 250}{2}\right)} \frac{[kN]}{\left[\frac{kN}{m}\right]} = 10 \div 12\ [m]$$

As for the definition of the value of the free length L_l, the position of the active wedge was defined by assuming an angle value α=(45°+ϕ'/2)=64° , derived as average value between those for T1 (ϕ'=41°) and T2 (ϕ'=34°) soils. Thus, starting from the position of the anchor heads along the wall and with inclination =10°, a minimum free length to install the anchor bulb outside the active wedge was defined.

Finally, an equivalent length L_{eq}=(L_l+0.5 L_b) was considered for calculating the axial stiffness of the "virtual"anchors.

According to the assumptions made, the axial displacement of the constraint δL, when subjected to an axial force T, may be assessed as:

$$\frac{\delta L}{T} = \frac{L_{eq}}{EA}$$

The following tables (Table 3.3 and 3.4) summarize the main quantities involved: the assumed value of the average axial stiffness 150 MN can be considered as representative of actual anchorage/constraint systems for the two types of embedded walls modelled in the numerical analyses.

Table 3.3

Piled embedded wall – H=12 m	Diaphragm wall – H=12 m						
Anchor level	No. of strands	Ll [m]	L_b [m]	L_{eq} [MN]	EA [MN]	L_{eq}/EA [m/MN]	L_{eq}/EA [m/MN] (with EA=150
1st row	5	≥8	10	13	136	0.0954	0.0867
2nd row	5	≥5	12	11	136	0.0808	0.0733
3rd row	5	≥5	13	11.5	136	0.0844	0.0767

Table 3.4

Piled embedded wall – H=12 m	Diaphragm wall – H=12 m						
Anchor level	No. of strands	Ll [m]	L_b [m]	L_{eq} [MN]	EA [MN]	L_{eq}/EA [m/MN]	L_{eq}/EA [m/MN] (with EA=150
1st row	5	≥7.5	10	12.5	136	0.0918	0.0833
2nd row	5	≥6	12	12	136	0.0881	0.0800
3rd row	5	≥5	13	11.5	136	0.0844	0.0767
4th row	5	≥4	12	10	136	0.0734	0.0667

3.2.3. Soil modelling

With regard to ground modelling, three simple stratigraphies have been defined with the aim of understanding at this stage the behavior and the response of the different constitutive models adopted. The first two schemes have homogeneous soil, respectively loose sand (T1) and dense sand (T2), while the third assumes a soil of better properties at the excavation depth (T1T2), as it is shown in Figure 3.3.

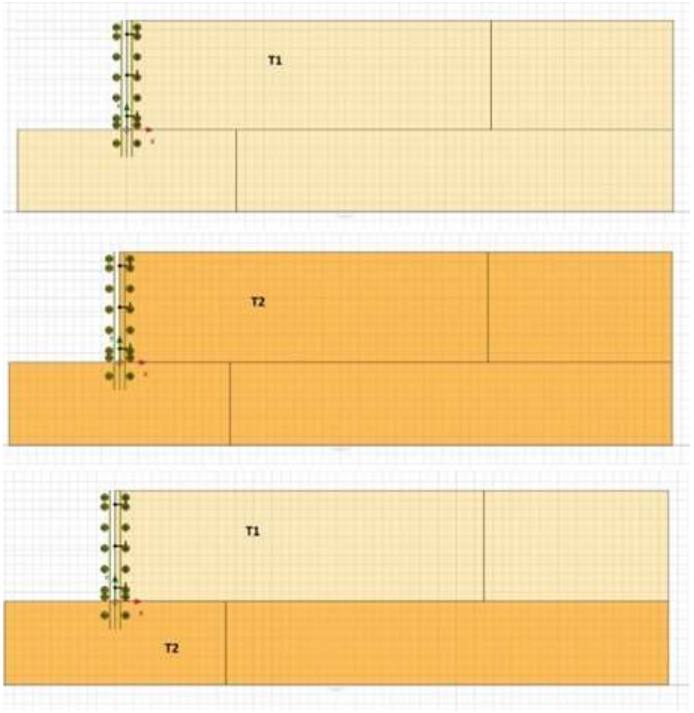

Figure 3.3 Soil stratigraphy schemes

Concerning soil modelling, several Fem analyses were carried out employing three different constitutive models, the Mohr-Coulomb model, the Hardening Soil model and the Hardening Soil Small model.

Starting from the simplest one, that is the linear elastic model of Mohr Coulomb, it was found that it is a model that turns out to be inaccurate and unsatisfactory, particularly in the specific case of excavations modelling. For this reason, the subsequent analyses were performed using the Hardening Soil Small model as constitutive model. The description of this last is reported in a subsequent paragraph.

For instance, Figures 3.4, 3.5, 3.6 show the results of a pile bulkhead 12 m height, pile diameter of 0,6 m, constrained by three levels of anchors in terms of horizontal displacement of the retaining structure, ground settlement and bottom heave.

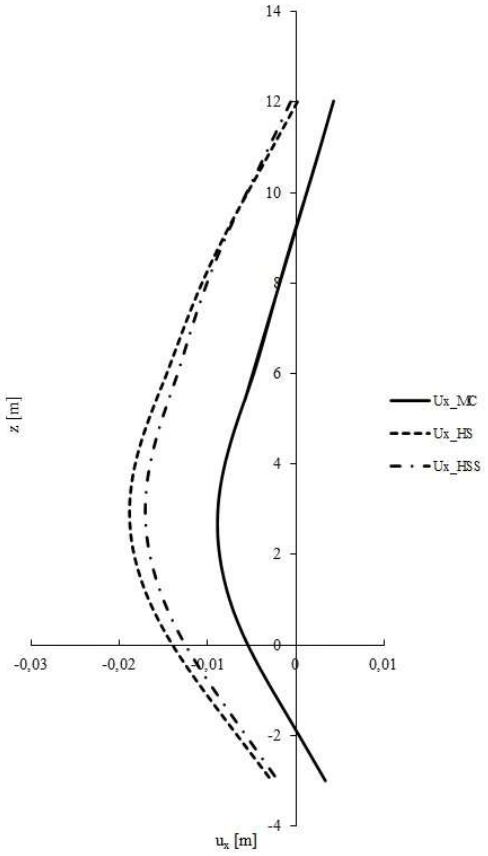

Figure 3.4 Horizontal displacement profile of M-C, HS and HSS finite element models

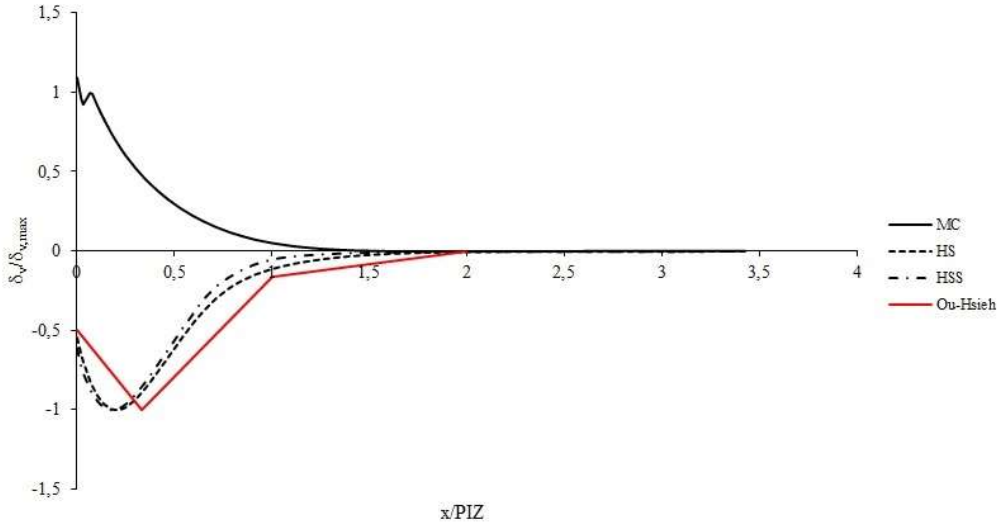

Figure 3.5 Settlement profile of M-C, HS and HSS finite element models

As can be seen from the figures, the perfectly plastic elastic model of Mohr Coulomb underestimates the horizontal displacements of the bulkhead and overestimates three times the bottom heave value of the excavation (as expected, because the same elastic module is adopted in loading and unloading).

The criticality on the elastic module is also reflected in the result of the ground settlement that even presents a sort of bulge that goes against the experimental evidence. (see comparison with Ou-Hsieh profile in Figure 3.5).

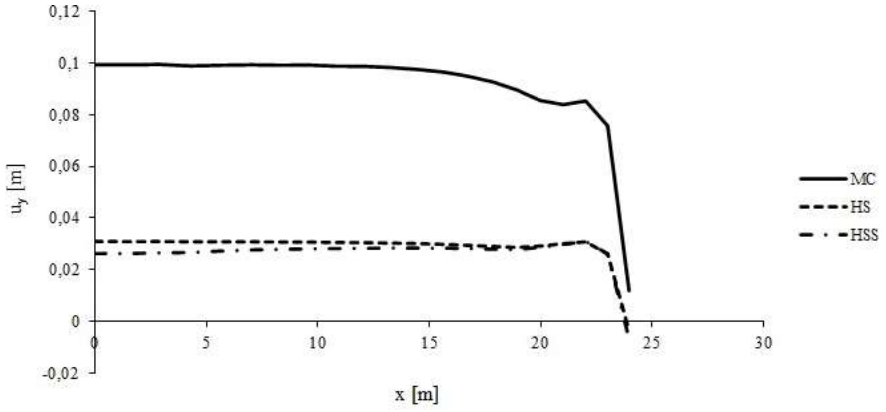

Figure 3.6 Bottom heave profile of M-C, HS and HSS finite element models

Table 3.5 shows the relationship between the maximum horizontal displacement of the embedded wall and the maximum ground settlement. It can be notice that for HS and HSS models $u_{x,max}/u_{y,max}$ falls in the range suggested by Rampello 2017 (see Figure 2.27) whereas for M-C model it has a value totally incoherent.

Table 3.5 Horizontal displacement and ground settlement of MC, HS and HSS models

	$u_{x,max}$ [m]	$u_{y,max}$ [m]	$u_{x,max}/u_{y,max}$ [-]
Mohr-Coulomb model	-0,009	0,006	-1,5
Hardening Soil model	-0,019	-0,015	1,27
Hardening Soil Small model	-0,017	-0,015	1,13

The following analyses were carried out employing more elaborate constitutive models that are better able to catch the soil behavior both to small and medium deformations and especially in relation to the phenomena of discharge.

With the purpose of having a reliable instrument, the parameters have been chosen calibrated on a real soil behavior in such a way that the numerical model reproduces the experimental result of triaxial tests on a literature soil type.

In this way results are not affected by the selection of model parameters.

The choice of the soils for the modelling fell on the Huston sand, whose parameters were calibrated comparing PLAXIS calculation results with those obtained from laboratory tests provided by Prof. J. Desrues (University Joseph Fourier, Grenoble, France). Based on these tests the model parameters for the Hardening Soil model were determined and they are presented in the table from the Plaxis Manual illustrated in Figure 3.7.

Parameter	Loose sand	Dense sand	Unit
Unit weight γ	17	17.5	kN/m^3
E_{50}^{ref} (p_{ref} = 100 kPa)	20000	37000	kN/m^2
E_{ur}^{ref} (p_{ref} = 100 kPa)	60000	90000	kN/m^2
E_{oed}^{ref} (p_{ref} = 100 kPa)	16000	29600	kN/m^2
Cohesion c'	0.0	0.0	kN/m^2
Friction angle φ'	34.0	41.0	°
Dilatancy angle ψ	0.0	14.0	°
Poisson's ratio ν_{ur}	0.2	0.2	-
Power m	0.65	0.5	-
K_0^{nc}	0.44	0.34	-
Tensile strength	0.00	0.00	kN/m^2
Failure ratio	0.9	0.9	-

Figure 3.7 Hardening Soil parameters for loose and dense Huston sand (Plaxis Manual)

Standard drained triaxial tests were performed on loose and dense sand specimens. In the first phase the sample is isotropically compressed up to a confining pressure of p' = -300 kN/m^2. In the second phase the sample is vertically loaded up to failure while the horizontal stress (confining pressure) is kept constant.

The computational results and measured data are presented in figures in the Material Manuals of the Plaxis software (Figures 3.8-3.11).

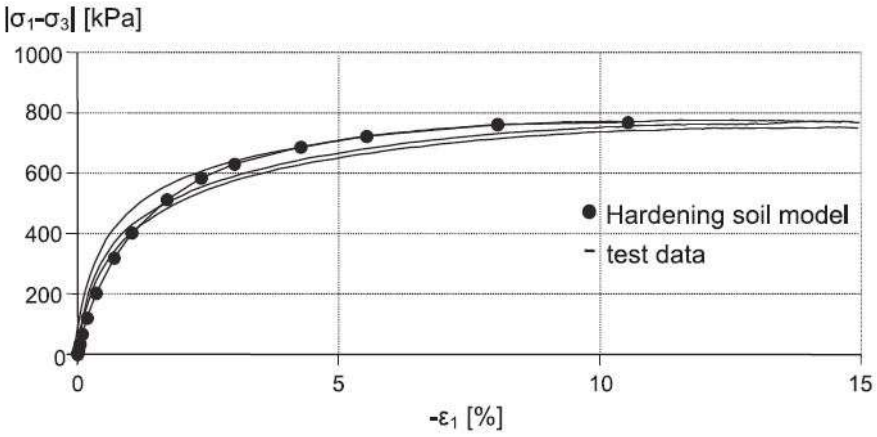

Figure 3.8 Results of drained triaxial tests on loose Hostun sand, deviatoric stress versus axial strain (Plaxis Manual)

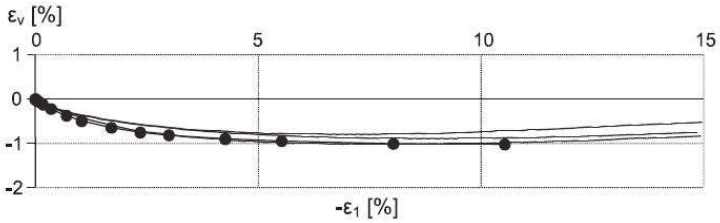

Figure 3.9 Results of drained triaxial tests on loose Hostun sand, volumetric strain versus axial strain (Plaxis Manual)

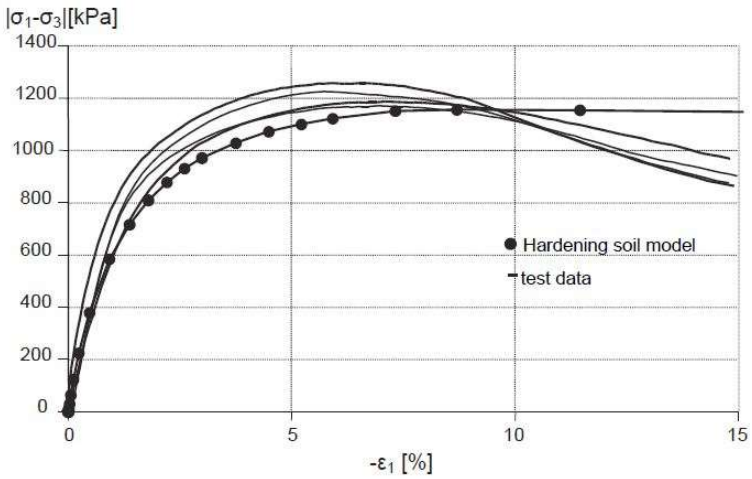

Figure 3.10 Results of drained triaxial tests on dense Hostun sand, deviatoric stress versus axial strain (Plaxis Manual)

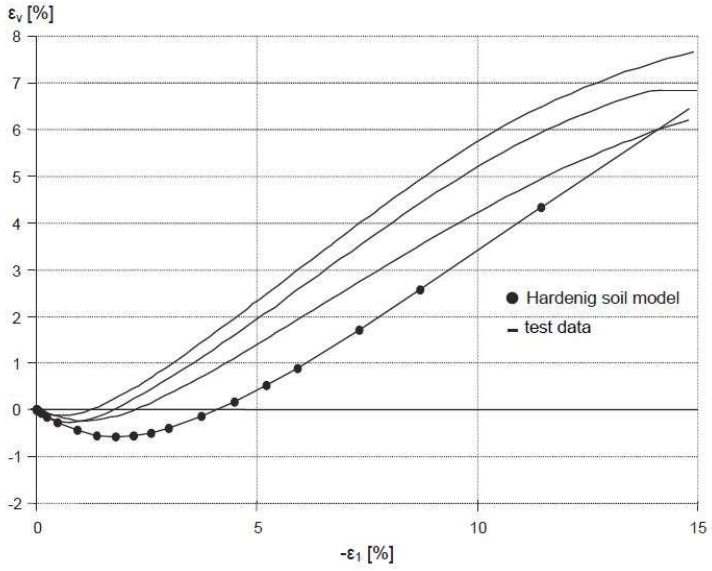

Figure 3.11 Figure 84: Results of drained triaxial tests on dense Hostun sand, volumetric strain versus axial strain

The figures show that the computational results match reasonably with the test data. It can be seen that the material response (measured and computed) shows gradual transition from elastic to plastic behaviour. As such the relation between the deviatoric stress and the axial strain can be approximated by a hyperbola.

The failure level is fully controlled by the friction angle (the cohesion is zero). The test results on dense sand show softening behavior after the peak load has been reached. Modelling of the softening behavior, however, is not incorporated in the Hardening Soil model, and thus, the deviatoric stress remains constant. It can also be seen from the test data that the dilatancy reduces during softening. However, in the Hardening Soil model the dilatancy continues to infinity, unless the dilatancy cut-off option has been used.

As will be explained in more detail below, The Hardening Soil Small model requires only two additional parameters to the Hardening Soil model.

The laboratory test data and the basic HS parameters are identical to those presented previously. The two additional small strain parameters used in the Hardening Soil model are reported in the table from the Plaxis Manual illustrated in Figure 3.12.

Parameter	Loose sand	Dense sand	Unit
G_0^{ref} (p_{ref} = 100 kPa)	70000	112500	[kN/m^2]
$\gamma_{0.7}$	0.0001	0.0002	[-]

Figure 3.12 Additional HSSmall model parameter for loose and dense Hostun sand

3.3. HARDENING SOIL SMALL MODEL

The original Hardening Soil (HS) model assumes elastic material behaviour during unloading and reloading. However, the strain range in which soils can be considered truly elastic, i.e. where they recover from applied straining almost completely, is very small. With increasing strain amplitude, soil stiffness decays nonlinearly (Herold and von Wolffersdoff, 2009).

Figure 3.13 gives an example of such a stiffness reduction curve. It shows the characteristic stiffness-strain behavior of soil with typical strain ranges for laboratory tests and structures.

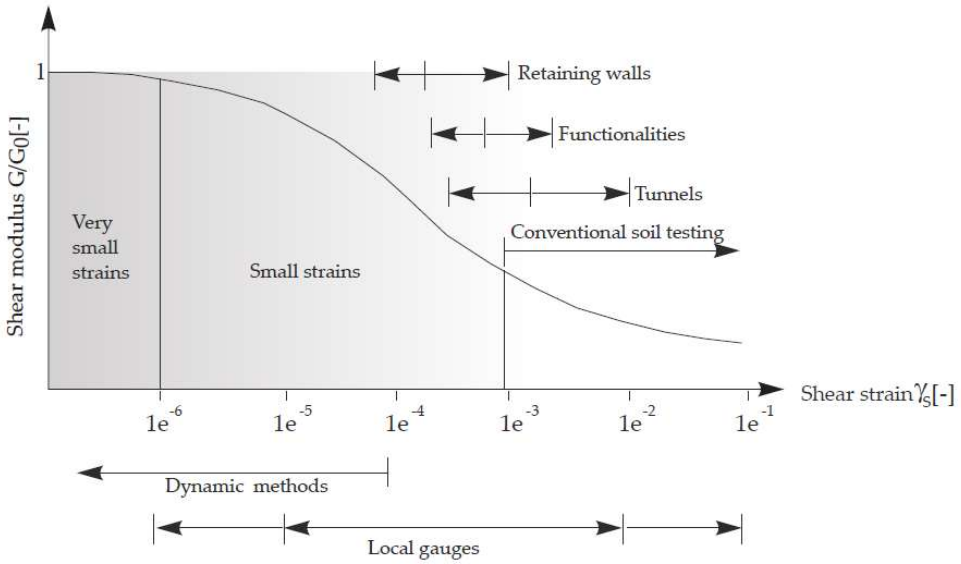

Figure 3.13 Characteristic stiffness-strain behaviour of soil with typical strain ranges for laboratory tests and structures, adapted from Atkinson (2000)

One feature of soil behavior that was still missing from the HS model is high stiffness at small strain levels ($< 10^{-5}$). Even in applications dominated by "engineering strain levels" ($> 10^{-4}$), stiffness at small strains can play an important role. It is commonly known that conventional models over-predict heave in excavation problems. In addition, these models overestimate the width and underestimate the gradient of the settlement trough behind excavations and above tunnels.

Small-stress stiffness can improve this aspect. In addition, small-strain stiffness can be used to model the effect of hysteresis and hysteretic damping in applications involving cyclic loading and dynamic behavior.

The HSSmall model is based on the Hardening Soil (HS) model and uses almost entirely the same parameters. Only two additional parameters are required to describe the stiffness behavior at small strains. These parameters are the initial or very small-strain shear modulus G_{0ref}, and the shear strain level $\gamma_{0,7}$ at which the secant shear modulus G is reduced to 70 % of G_{0ref}.

The following equation shows the corresponding relationship between G_{0ref} und $\gamma_{0,7}$:

$$\frac{G_s}{G_0} = \frac{1}{1 + \frac{3}{7} \cdot \left| \frac{\gamma}{\gamma_{0.7}} \right|}$$

The advanced features of the HSSmall model are most evident under workload conditions.

In this case, the model provides more reliable displacements than the HS model. When used in dynamic applications, the HSSmall model also introduces hysteretic damping of the material. Therefore, this advanced constitutive model is particularly suitable for the analysis of ductile structures for both static and dynamic applications. Material parameters of the HSSmall model can be obtained by conducting classical laboratory tests, like triaxial tests and resonant column tests without special instrumentation.

3.3.1. Model parameters

As above mentioned, compared to the standard Hardening Soil model, the Hardening Soil model with small-strain stiffness requires two additional stiffness parameters as input: G_{0ref} and $\gamma_{0.7}$. All other parameters, persist the same as in the standard Hardening Soil model.

G_{0ref} defines the shear modulus at very small strains ($\varepsilon < 10^{-6}$) at a reference minor principal stress of $-\sigma'3 = p_{ref}$.

The Poisson's ratio ν_{ur} is assumed a constant, so that the shear modulus G_{0ref} can also be calculated from the very small strain Young's modulus as:

$$G_0^{ref} = \frac{E_0^{ref}}{\left(2(1+\nu_{ur})\right)}$$

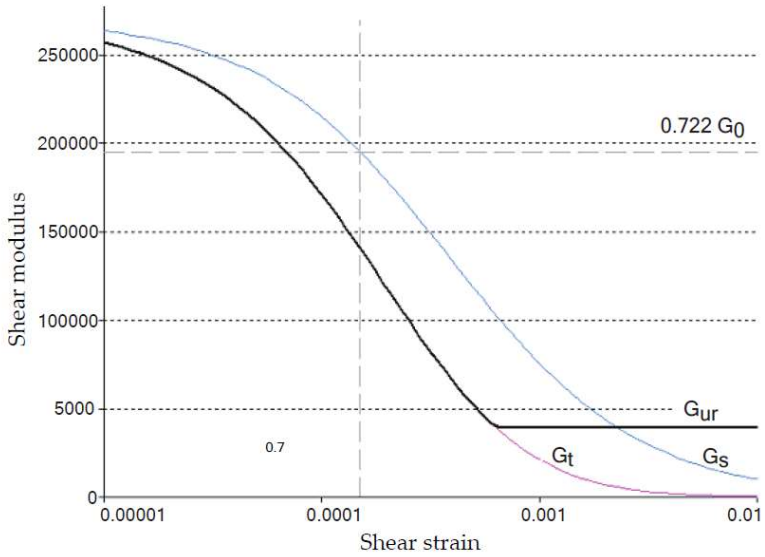

Figure 3.14 Secant and tangent shear modulus reduction curve (from Plaxis Manuals)

The threshold shear strain $\gamma_{0.7}$ is the shear strain at which the secant shear modulus G_{sref} is decayed to $0.722G_{0ref}$ (see Figure 3.14). The threshold shear strain $\gamma_{0.7}$ is to be supplied for virgin loading.

The input stiffness parameters of the Hardening Soil model with small-strain stiffness are summarized and listed below:

Table 3.6 Hardening Soil Small model parameters.

Power for stress-level dependency of stiffness	m	[-]
Secant stiffness in standard drained triaxial test	E^{ref}_{50}	[kN/m^2]
Tangent stiffness for primary oedometer loading	E^{ref}_{oed}	[kN/m^2]
Unloading/reloading stiffness from drained triaxial test	E^{ref}_{ur}	[kN/m^2]
Poisson's ratio for unloading-reloading	$\nu_{0.7}$	[-]
Reference shear modulus at very small strains	G^{ref}_0	[kN/m^2]
Threshold shear strain at which G_s=0.0722G_0	$\gamma_{0.7}$	[-]

Finally, Figure 3.15 illustrates the model's stiffness parameters in a drained triaxial test: E_{50}, E_{ur}, and $E_0 = 2G_0(1 + \nu_{ur})$.

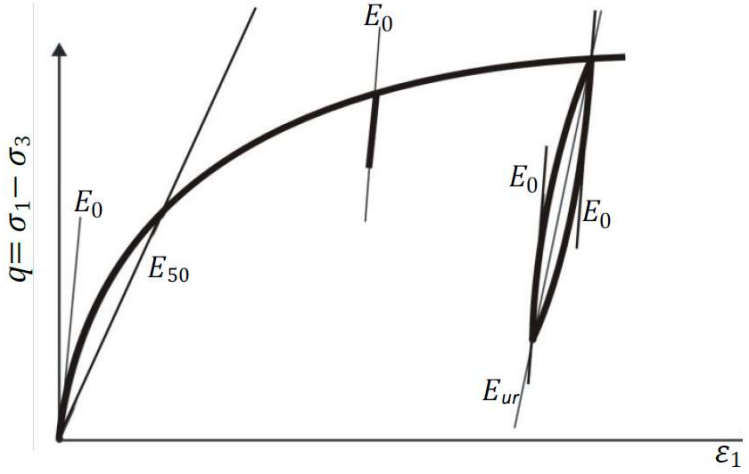

Figure 3.15 Stiffness parameters E_{50}, E_{ur}, and $E_0 = 2G_0 (1 + \nu_{ur})$ of the Hardening Soil model with small-strain (from Plaxis Manuals)

After a whole series of modeling, it was chosen to carry out parametric analyses by applying the Hardening Soil Small model as soil constitutive model, for the Huston loose sand (T1) and the Huston dense sand (T2) whose parameters are summarized in the following table:

Table 3.7 Soil parameters for Hardening Soil Small Model

	γ [kN/m^3]	E_{50}^{ref} [kN/m^2]	E_{ur}^{ref} [kN/m^2]	E_{oed}^{ref} [kN/m^2]	c' [kN/m^2]	φ' [°]	ψ [°]	ν [-]	G_0^{ref} [kN/m^2]	$\gamma_{0.7}$ [-]
Loose sand (T1)	17	20000	60000	16000	1	34	0	0.20	70000	0.0001
Dense sand (T2)	17.5	37000	90000	29600	1	41	14	0.20	112500	0.0002

3.4. 2D PARAMETRICAL FEM ANALYSES

As briefly mentioned above, a series of parametric numerical analyses were carried out that could replicate what is known in the literature, with the aim of having a starting framework on which to develop subsequent studies, with the objective of evaluating the behavior of the support structures and the soil interacting with them, carrying out a comparison of the results with experimental data from the literature.

The parameterization involved the quantities shown in Figure 3.1 and the type of support structure.

The cases studied involved usual situations, diaphragms and piles with spacing and dimensions usual for this type of work, creating a representative and useful case history to obtain results that are indicative but correspond to the real ones.

Two main geometries studied were the concrete diaphragm and the pile bulkhead, some results of which are given in the following in terms of displacement profiles. A summary of the various diaphragm models analyzed is given in Table 3.8.

Table 3.8

Name	Excavation depth [m]	horizontal spacing between struts [m]	vertical spacing between struts [m]	embedded depth [m]	soil type
DH9_b0.6_3T_HSS_D3_sh3_F18_T1	9	3	3	3	Loose sand
DH9_b0.6_3T_HSS_D6_sh3_F18_T1	9	3	3	6	Loose sand
DH12_b0.6_4T_HSS_D3_sh3_F18_T1	12	3	3	3	Loose sand
DH12_b0.6_4T_HSS_D6_sh3_F18_T1	12	3	3	6	Loose sand
DH9_b0.6_3T_HSS_D3_sh3_F18_T2	9	3	3	3	Dense sand
DH9_b0.6_3T_HSS_D6_sh3_F18_T2	9	3	3	6	Dense sand
DH12_b0.6_4T_HSS_D3_sh3_F18_T2	12	3	3	3	Dense sand
DH12_b0.6_4T_HSS_D6_sh3_F18_T2	12	3	3	6	Dense sand
DH9_b0.6_3T_HSS_D3_sh3_F18_T1T2	9	3	3	3	Loose and
DH9_b0.6_3T_HSS_D6_sh3_F18_T1T2	9	3	3	6	Loose and
DH12_b0.6_4T_HSS_D3_sh3_F18_T1T2	12	3	3	3	Loose and
DH12_b0.6_4T_HSS_D6_sh3_F18_T1T2	12	3	3	6	Loose and
DH12_b0.6_HSS_D6_T1	12	-	-	6	Loose sand
DH12_b0.6_HSS_D6_T2	12	-	-	6	Dense sand
DH12_b0.6_4T_HSS_D6_sh6_T1	12	6	3	6	Loose sand
DH12_b0.6_4T_HSS_D6_sh6_T2	12	6	3	6	Dense sand

Regarding the geometry of constraint placement, shown in Figures 3.16 and 3.17 the steps through which they are arranged are as follows:

- Excavation of 1.5 meters from ground level;
- Constraint placement 1 meter from ground level;
- Excavation 3 meters;
- Placement of the constraint 4 meters from the ground level;
- Progressive excavation of another 3 meters;

- Placement of the constraint at 7 meters from the ground level;
- Progressive excavation of another 3 meters (in case DH12);
- Placement of the constraint at 10 meters from ground level (in the DH12 case);
- Final excavation of 2 meters.

Interfaces with R_{inter}=1 between the retaining structure and the ground were also modeled.

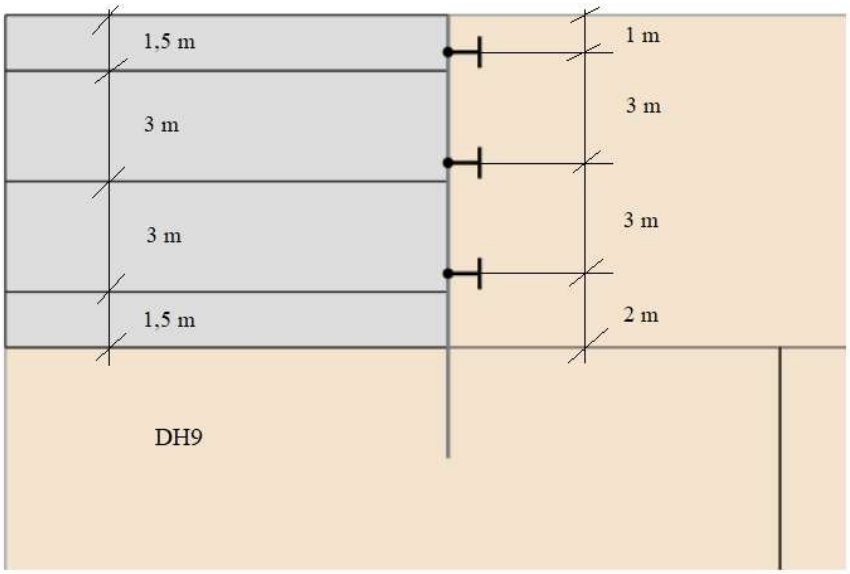

Figure 3.16 Geometry of constraint placement and excavation phases for concrete diaphragm and excavation depth of 9 m.

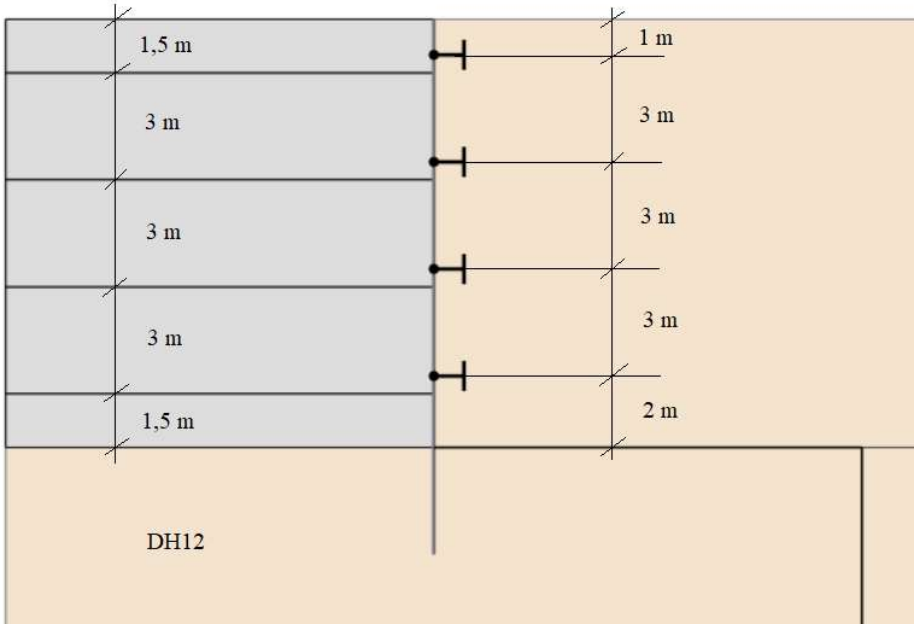

Figure 3.17 Geometry of constraint placement and excavation phases for concrete diaphragm and excavation depth of 12 m.

By way of example, some of the results of this parametric analysis are shown in Figure 3.18 a, b, c, in terms of horizontal displacement, vertical settlement and bottom heave for concrete diaphragm geometry with excavation height 9 m and embedded depth varying between 3 and 6 m.

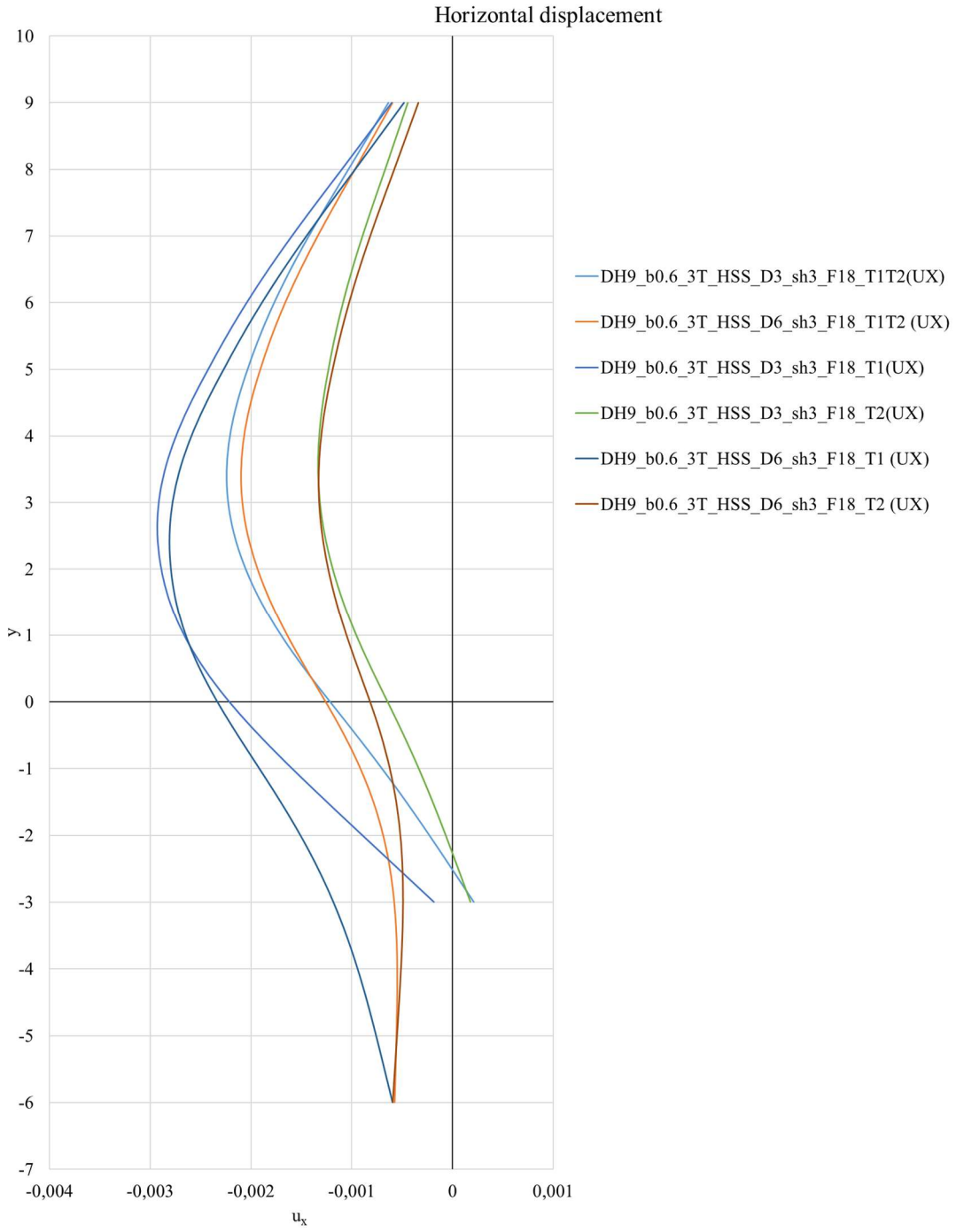

Figure 3.18(a) Horizontal displacement of diaphragm walls

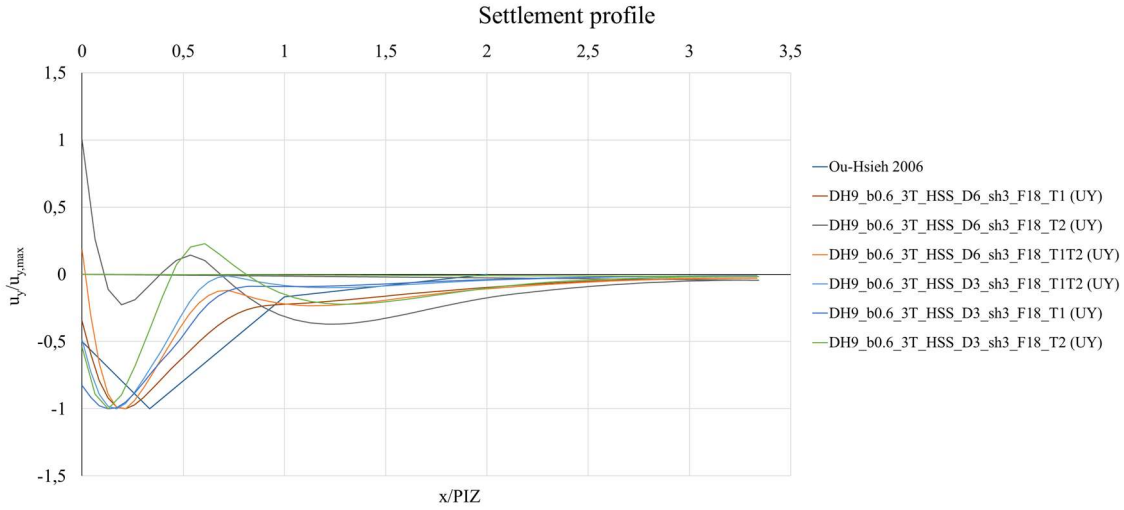

Figure 3.18(b) Settlement profile of diaphragm walls

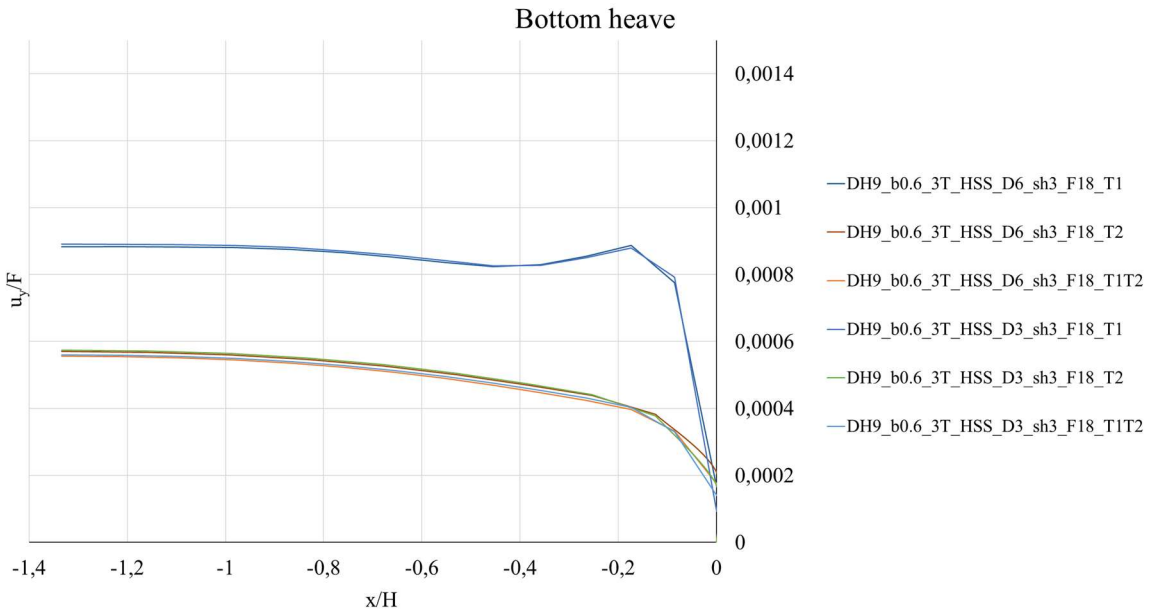

Figure 3.18(c) Bottom heave of diaphragm walls

Among the various results obtained for pile embedded walls instead, those for a series wall models of piles with a diameter of 0.6m, a spacing of 1.2m, and a height of 12m with variable embedded depths of 3 and 6m are given as examples.

In particular, Figure 3.19 (a) shows the horizontal displacement, with a trend typical of multi-anchored embedded walls. In Figure 3.19 (b) it is shown the relation between non-dimensional horizontal and vertical displacements of the retaining structures, compared with the trends proposed by Rampello (2017) and in accordance with them.

Finally Figure 3.19 (c) shows the normalized ground settlement of excavations sustained by multi-anchored embedded walls, whose profiles are found to agree with the trend of the subsidence hollow proposed by Ou (2006).

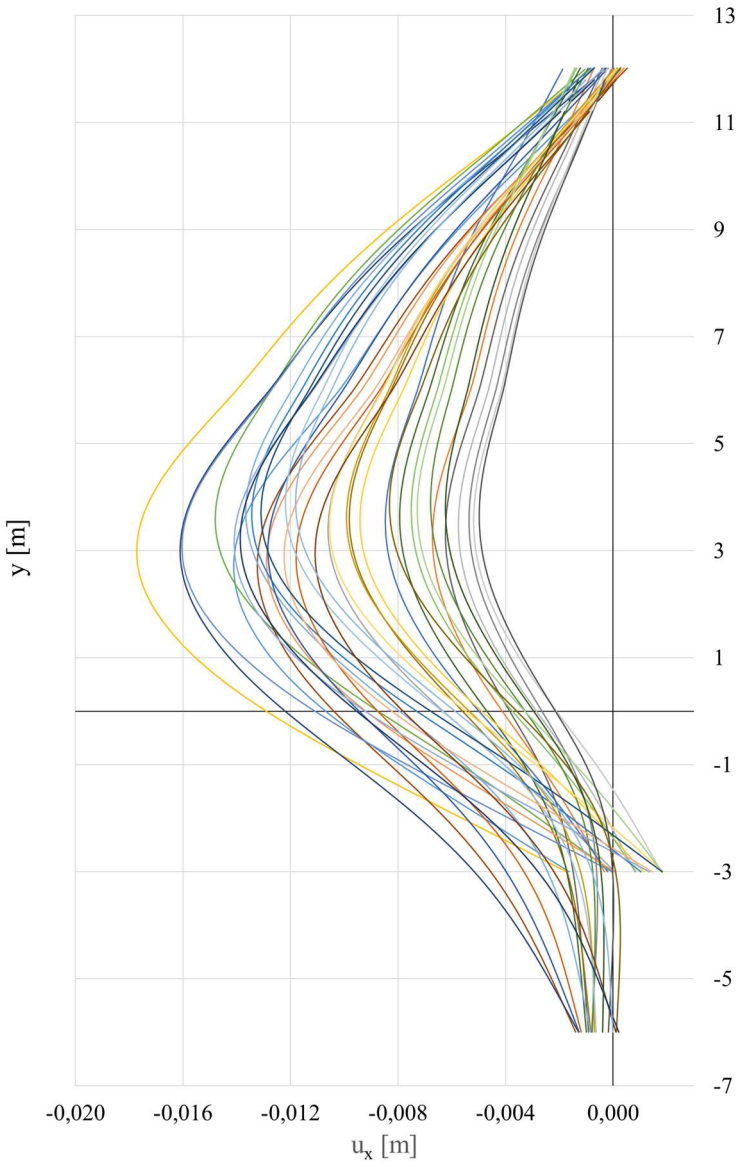

Figure 3.19 (a) Horizontal displacement of anchored pile-embedded walls

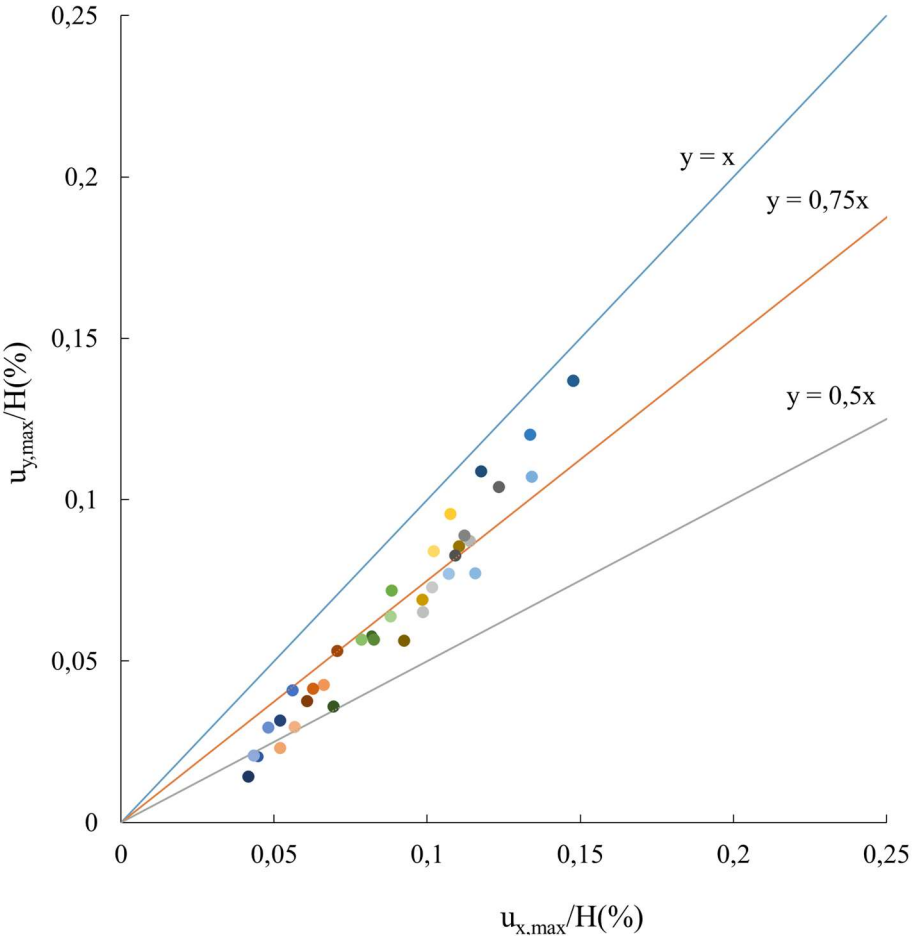

Figure 3.19(b) Relation between non-dimensional horizontal and vertical displacement of anchored pile-embedded walls

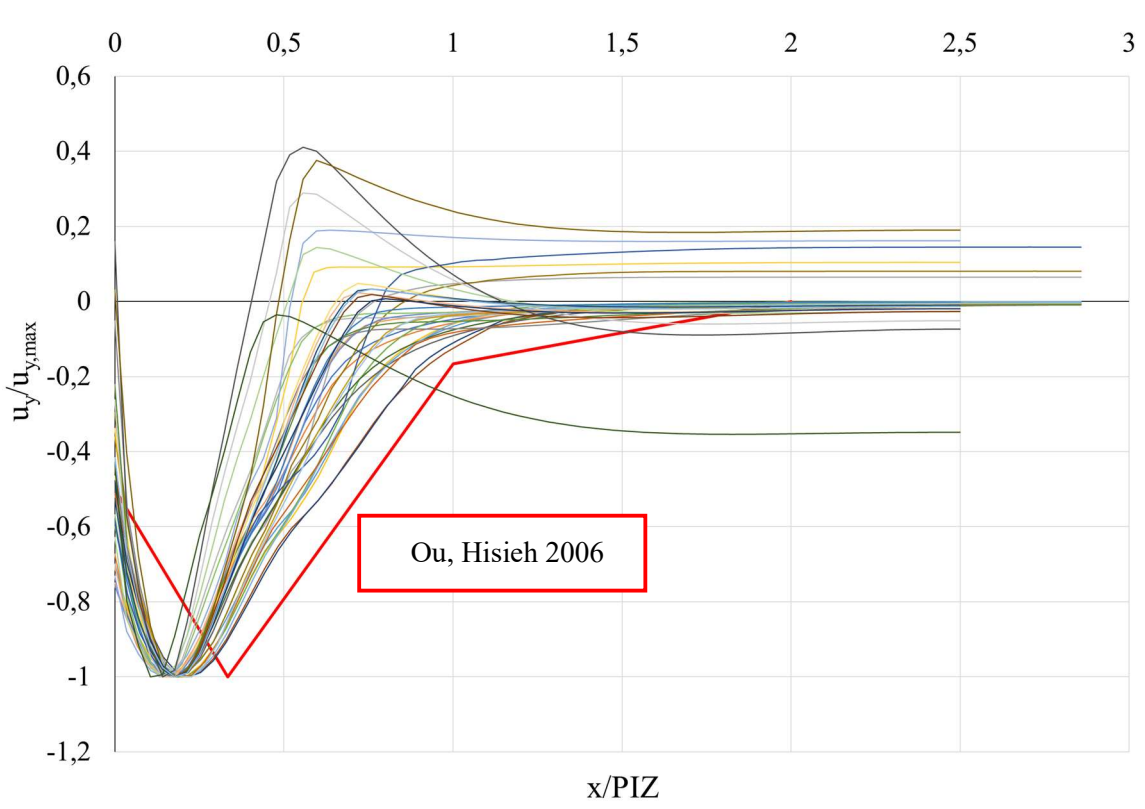

Figure 3.19 (c) Normalized ground settlement of excavations sustained by anchored pile-embedded walls

The parameterization also included the deepening under excavation with the ultimate goal also of a mesh calibration that will be later used downstream in a series of convergence analyses.

This series of analyses also resulted, through appropriate convergence analysis, in the definition of the mesh, in accordance also with the guidance provided by Potts et al. (2002).

It should be noted that the results obtained, while showing a similar trend, also show considerable variability in the absolute results in terms of horizontal and vertical displacements. This is due to the influence of various factors such as the flexural stiffness of the wall, the type of soil, the depth of excavation, the embedded depth, the type of support, etc. However, what it's wanted to put in evidence was that with an appropriate normalisation by means of the excavation height H, the results are congruent with the normalised displacement profiles and as a value of the normalised vertical displacement with respect to the normalised horizontal displacement known in the literature, such as those of Ou Hisieh from 2006 shown in Figure 3.19 (b) and 3.19 (c).

In conclusion, the numerical analyses reproduce, with an appropriate choice of geometric and mechanical parameters, an expected real experimental result.

3.5. CROSS WALL AND BUTTRESS WALL: GENERAL REMARKS

With traditional solutions it is possible to constrain the retaining wall only after the corresponding excavation depth has been reached and the corresponding displacement has been produced. The subsequent deepening of the excavation produces an increase in the displacement of the diaphragm under the level of struts/anchors. In this case the final displacement is caused for a not negligible part by the displacement occurred during the excavation phase necessary to reach the installation height of the contrast system as it is illustrated in Figure 3.20.

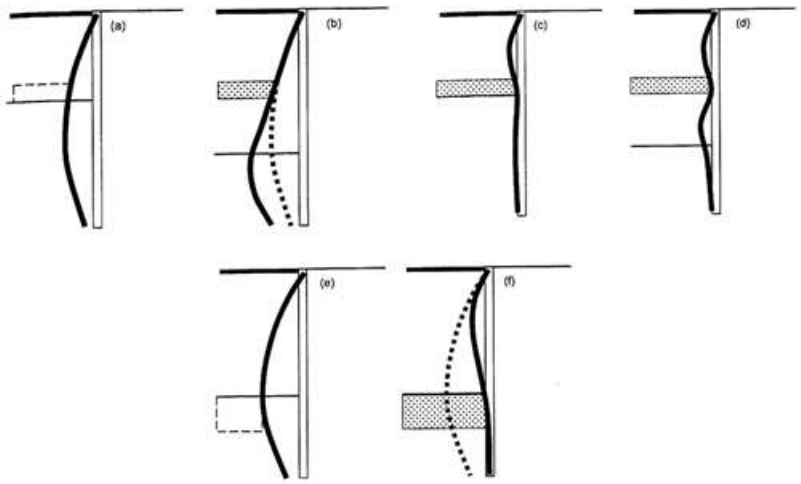

Figure 3.20 Schematic representation of the displacement of a bulkhead for different excavation sequences with realization of constraints at heights above (a, b, c, d) and below (e, f) the bottom of the excavation (Callisto, 2011)

If, on the other hand, it was possible to achieve the level of constraint before excavation, the initial phase of excavation would produce lowered displacements, deriving only from the inflection of the wall. Any increase in the excavation depth would result in further deformation of the wall, but with lower displacements than those related to the previous scheme.

Different construction methods exist in this respect and include structural inclusions connecting facing diaphragm (cross wall) and local stiffening and strengthening intervention in the soil portion that has to be excavated, also below excavation surface (buttress wall).

The basic configuration of a cross wall, reported in Figures 3.21 and 3.22, connecting two retaining walls opposite each other prior the excavation.

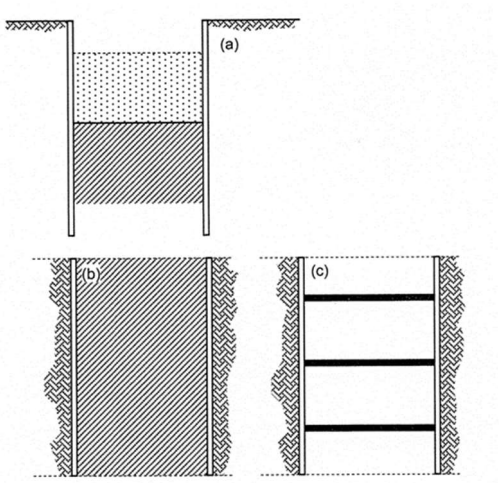

Figure 3.21 Schematic geometry of interventions linking facing walls (Callisto, 2011)

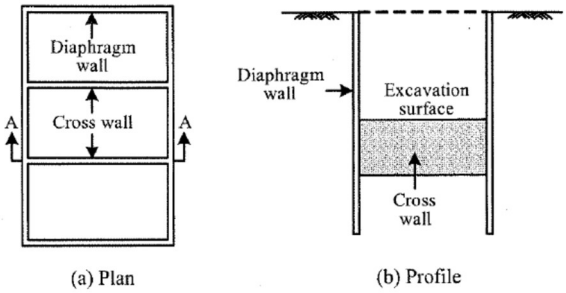

Figure 3.22 Schematic representation of a cross wall (Ou et al., 2006)

Although retaining walls have horizontal struts above the excavation level to resist lateral earth pressure, they are less capable to resist lateral earth pressure below the excavation level (Ou et al., 2006).

This might cause retaining walls to deform too much during excavation.

The cross wall works as a strut-like component which exists before excavation: along with excavation, cross wall should provide a decrease of the displacement and an overall stiffening of the soil under the bottom, also counteracting displacement components related to vertical stress. That way ground settlement outside the excavation will be reduced too, which therefore achieves the protection of adjacent buildings.

In general, these interventions can be continuous or discontinuous. In the first case a uniform constraint is provided along the retaining wall, and it implies an overall increase in strength and a reduction in permeability of the bottom of excavation improving safety against hydraulic collapse mechanisms. They can be also performed by soil improvement techniques, such as jet-grouting columns.

The contrast/constraint system can affect only the soil portion under the excavation bottom, or it can be extended above it, in which case the system must be removed during the excavation.

The discontinuous type of intervention does not significantly affect the hydraulic conditions instead and can be carried out either with soil improvement techniques or through structural elements such as rows of poles or adjacent panels of not reinforced concrete.

A different type of interventions is the construction of stiff elements in the ground area immediately downstream of the retaining wall supporting the excavation.

A buttress wall, which configuration is depicted in Figures 3.23 and 3.24, is similar to a cross wall in terms of construction: it is a concrete wall perpendicular to the retaining wall constructed before the excavation, but not encompassing the entire width of the excavation.

.

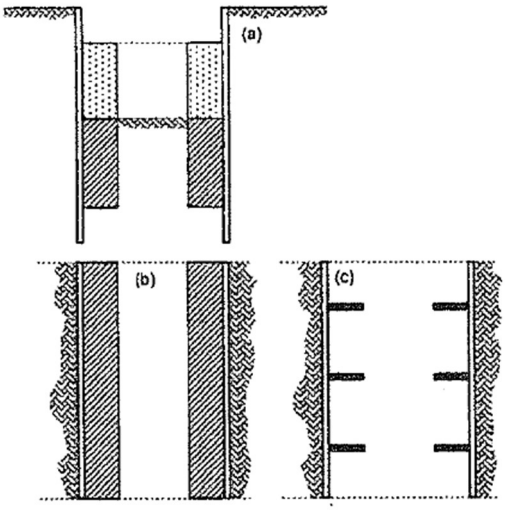

Figure 3.23 Schematic geometry of local interventions made in the soil downstream of walls (Callisto, 2011)

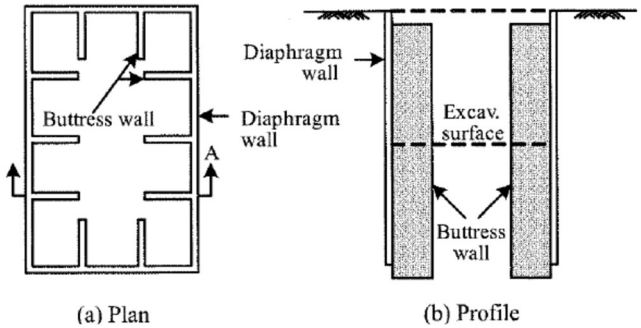

Figure 3.24 Schematic representation of a buttress wall (Ou et al., 2006)

Therefore, when the retaining wall is deformed, it will push the buttress wall to move along and a relative displacement between the buttress and the retaining wall is produced. The retaining wall moves toward the excavation zone and the buttress wall will then move to the adjacent soil.

The shear strength or frictional resistance developed on the two sides of the buttress wall will provide extra shear resistance, which will increase the overall resistance. In particular, a buttress wall linked to

the main retaining wall implies a very large increase on the bending stiffness of the wall, reducing lateral displacements.

Though the buttress wall increases lateral resistance in front of the retaining wall, it does not increase the moment resistance of the retaining wall.

On the other hand, if a buttress wall is constructed and formed a whole structure with the diaphragm wall (like a T-beam in reinforced concrete structure), the buttress wall will enhance the moment-resistance of the diaphragm wall, and the wall movement is expected to reduce to a certain extent.

Also, in this case the interventions can be continuous or discontinuous and consist of treated soil or structural inclusions.

The objective of this three-dimensional analysis, which schematises the buttressed embedded wall by means of a unit cell containing diaphragm wall and buttress, was to consider the interaction of the buttress with the ground. The three-dimensional analysis made it possible to accurately follow the geometry of the model, thus taking into account not only the increase in the bending stiffness of the wall, but also, and above all, the soil-structure interaction during each excavation phase, in particular the shear and normal stresses that develop along and in front of the buttress.

3.6. ANALYSIS AND RESULTS

As reported in previous sections, the execution in urban areas of deep excavations requires careful evaluation of displacements and consequent ground deformations, particularly in cases of proximity to pre-existing structures. The trend in current design is to use advanced numerical analyses, due to the complexity of the soil-structure interaction especially in cases where the geometry of the problem has strongly three-dimensional characteristics, as in the case of buttress walls.

3.6.1.Structure modelling

Modelling for the buttress wall response study was performed using Plaxis 3D finite element calculation software.

After appropriate convergence analysis, the mesh was defined (Figure 3.25) with an extension of 60 m at the back of the diaphragm wall, 12 m at the front and 36 m depth below the bottom of the excavation; 10-node triangular elements were used for it.

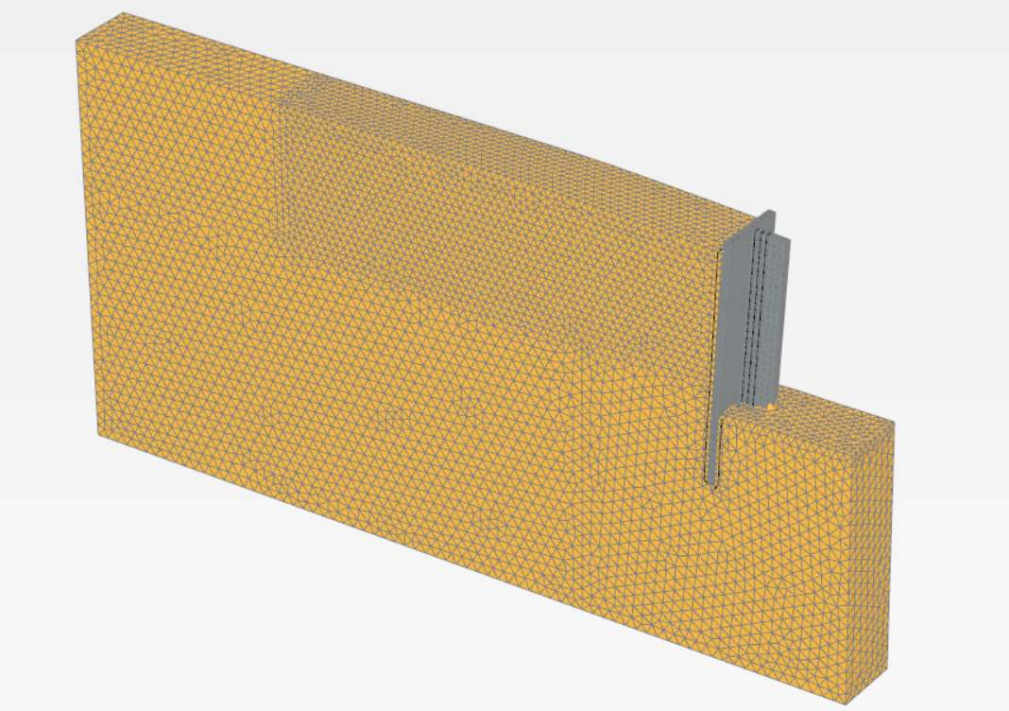

Figure 3.25 Example mesh of the three-dimensional model of the buttress wall (Plaxis 3D)

As for soil modeling, two soil types, a loose sand (T1) and a dense sand T2, modeled with the Hardening Soil Small Model, a non-linear model based on the Hardening Soil Model (HSM) (Schanz et al., 1999), were used.

In order to have a reliable tool, the parameters for the model were chosen calibrated to real soil behavior so that the numerical model reproduces the experimental result of triaxial tests on a literature soil type.

In this way, the results are not affected by the selection of model parameters.

The soils examined and their parameters are those already presented in Section 3.2.3.

Parameter	Loose sand	Dense sand	Unit
Unit weight γ	17	17.5	kN/m^3
E_{50}^{ref} (p_{ref} = 100 kPa)	20000	37000	kN/m^2
E_{ur}^{ref} (p_{ref} = 100 kPa)	60000	90000	kN/m^2
E_{oed}^{ref} (p_{ref} = 100 kPa)	16000	29600	kN/m^2
Cohesion c'	0.0	0.0	kN/m^2
Friction angle φ'	34.0	41.0	°
Dilatancy angle ψ	0.0	14.0	°
Poisson's ratio v_{ur}	0.2	0.2	-
Power m	0.65	0.5	-
K_0^{nc}	0.44	0.34	-
Tensile strength	0.00	0.00	kN/m^2
Failure ratio	0.9	0.9	-

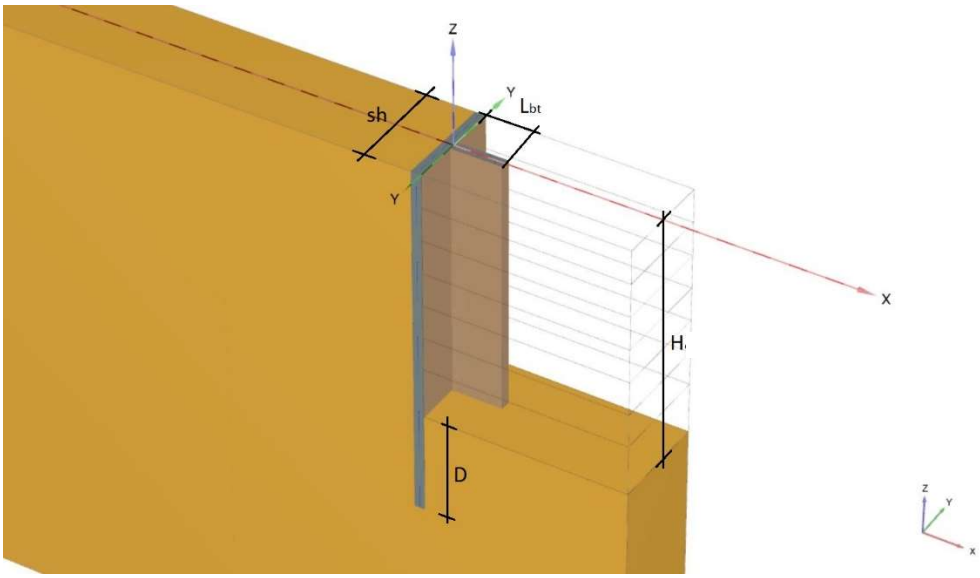

Figure 3.26 Parametric scheme of the buttress wall model

Figure 3.26, on the other hand, represents the schematic of the three-dimensional model with the quantities that are varied parametrically:

- excavation depth He=H
- diaphragm wall embedded depth D
- length of buttress wall L_{bt}
- horizontal spacing between buttress walls sh
- thickness of the buttress wall b = 0,6 m

The following table shows the list of numerical models and their parameters.

Table 3.9

Name	Excavation depth H [m]	buttress wall lenght Lbt [m]	horizontal spacing between buttress sh [m]	embedded depth D [m]	soil type
H12_nobt_T1_D6	12	-	6	6	Loose sand
H12_nobt_T2_D6	12	-	6	6	Dense sand
H12_bt1m_T1_D6	12	1	6	6	Loose sand
H12_bt1m_T2_D6	12	1	6	6	Dense sand
H12_bt2m_T1_D6	12	2	6	6	Loose sand
H12_bt2m_T2_D6	12	2	6	6	Dense sand
H12_bt3m_T1_D6	12	3	6	6	Loose sand
H12_bt3m_T2_D6	12	3	6	6	Dense sand
H12_bt2m_T2_D3	12	2	6	3	Dense sand
H12_bt3m_T2_D3	12	3	6	3	Dense sand
H12_bt1m_T2_D6_sh12	12	1	12	6	Dense sand
H12_bt3m_T2_D6_sh12	12	3	12	6	Dense sand
H15_nobt_T2_D3	15	-	6	3	Dense sand
H15_nobt_T2_D6	15	-	6	6	Dense sand
H15_bt1m_T2_D3	15	1	6	3	Dense sand
H15_bt1m_T2_D6	15	1	6	6	Dense sand
H15_bt3m_T2_D3	15	3	3	3	Dense sand
H15_bt3m_T2_D6	15	3	6	6	Dense sand

3.6.2. Comparison between 2D and 3D models

In order to carry out a validation of the three-dimensional modeling, a series of comparisons between geometries modeled two-dimensionally and three-dimensionally have been previously performed.

By way of example, the results of 2D and 3D models with a simple concrete diaphragm 0.6 m thick are compared (with no anchors and no buttress). Following Figure 3.27 and 3.28 show the results for excavation heights of 10 and 12 meters in terms of horizontal deflection of the diaphragm and ground settlement. Good agreement between 2D and 3D results is observed.

Table 3.10

Name	Excavation depth H [m]	Excavation phase [m]	embedded depth D [m]	soil type
DH12_b0.6_D6_T2_ex-10	12	-10	6	Dense sand
DH12_b0.6_D6_T2_ex-12	12	-12	6	Dense sand
H12_nobt_D6_T2_ex-10	12	-10	6	Dense sand
H12_nobt_D6_T2_ex-12	12	-12	6	Dense sand

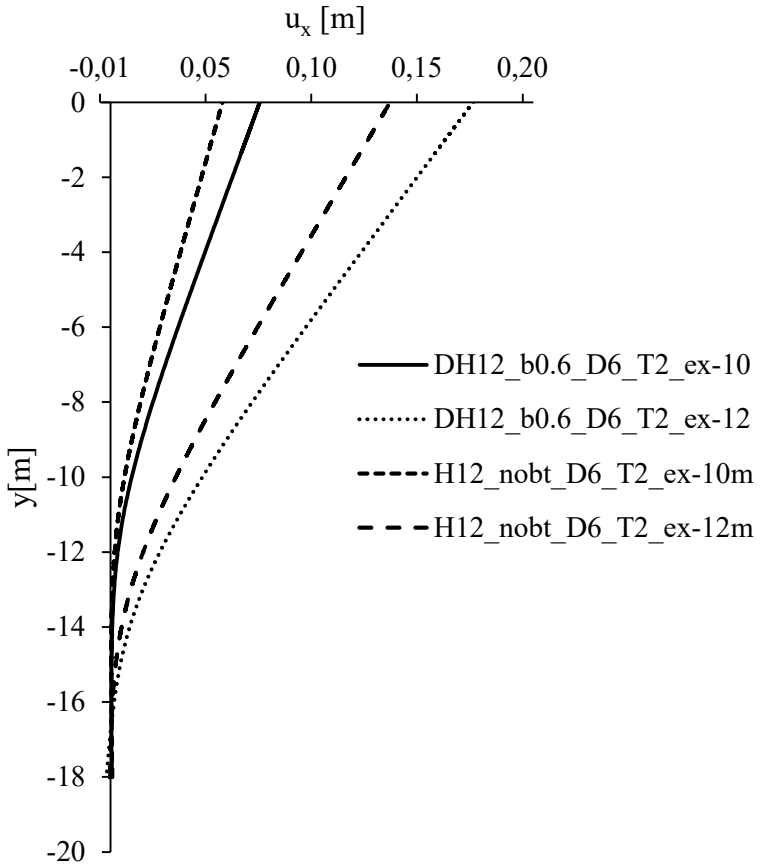

Figure 3.27 Horizontal deflection of diaphragm of 2D and 3D models (see Table 3.10)

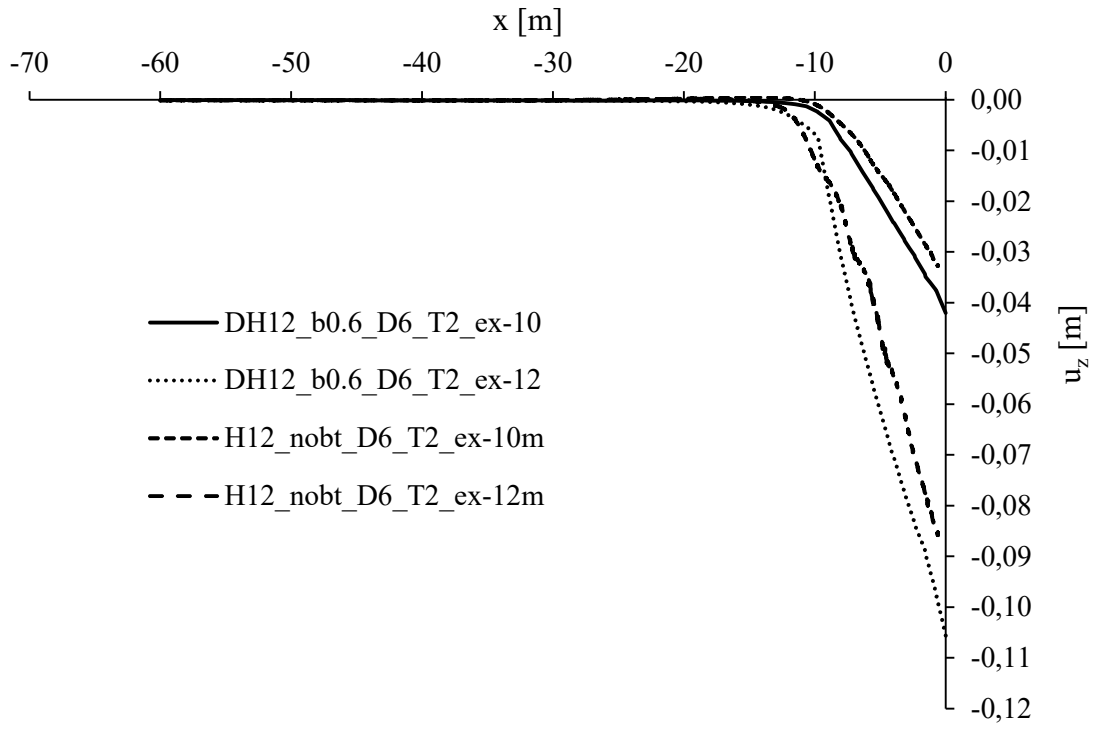

Figure 3.28 Ground settlement of 2D and 3D models (see Table 3.10)

It was also possible to compare different design solutions, such as a diaphragm constrained with anchors and a concrete diaphragm provided with buttress walls of different lengths L_{bt}.

Table 3.11

Name	Excavation depth H [m]	Excavation phase [m]	horizontal spacing between buttress/anchors [m]	buttress wall lenght Lbt [m]	embedded depth D [m]	soil type
DH12_b0.6_sh6_T2_ex-12	12	-12	6	-	6	Dense sand
H12_nobt_D6_T2_ex-12	12	-12	6	-	6	Dense sand
H12_bt1m_D6_T2_ex-12	12	-12	6	1	6	Dense sand
H12_bt2m_D6_T2_ex-12	12	-12	6	2	6	Dense sand
H12_bt3m_D6_T2_ex-12	12	-12	6	3	6	Dense sand

The graphs shown in Figures 3.29 and 3.30 compare the horizontal displacement profiles of the retaining structure and the ground settlement at the back for these design solutions.

The qualitative difference in the deformation of the diaphragm appears evident, which in the case of using the buttress wall realizes a cantilever deformation (typical of the cantilever beam), while in the case of the tie-rod restraint a deeper kinematics is activated in which the maximum displacement does not occur at the top but at a certain depth.

Starting from the same concrete diaphragm, with the same depth and excavation height, it turns out that a buttress wall of at least 3 meters in length is required to achieve comparable displacements.

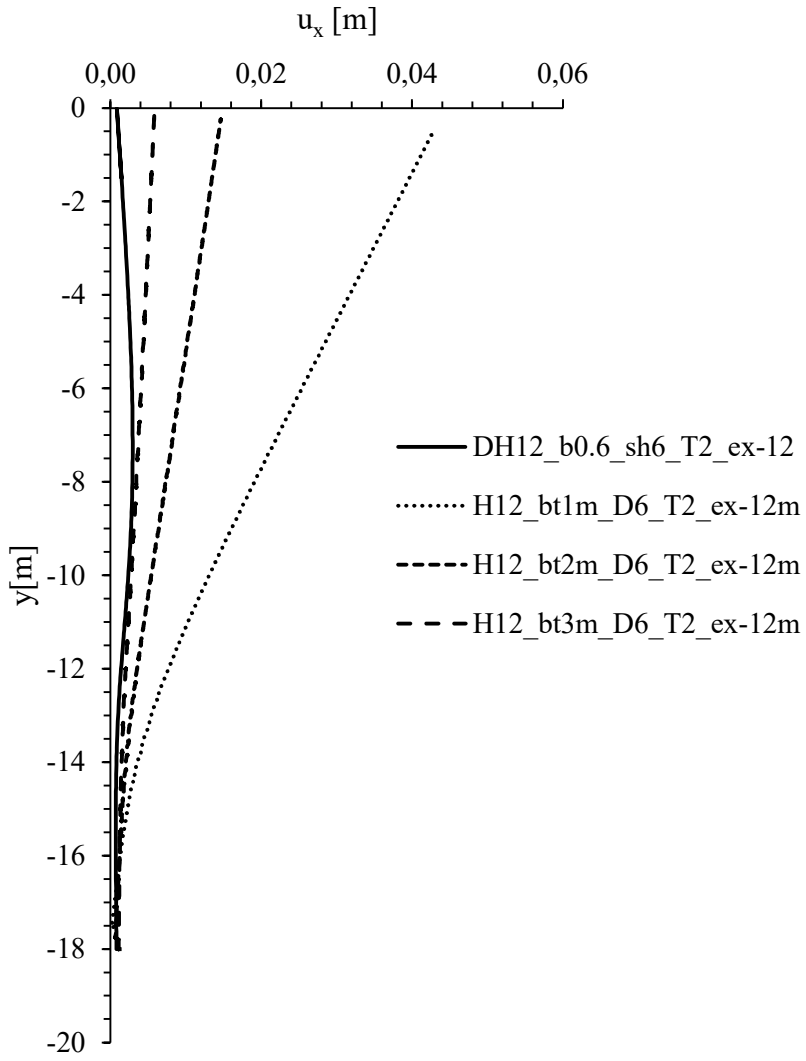

Figura 3.29 Horizontal deflection of anchored diaphragm (solid line) and buttressed wall models (see Table 3.11)

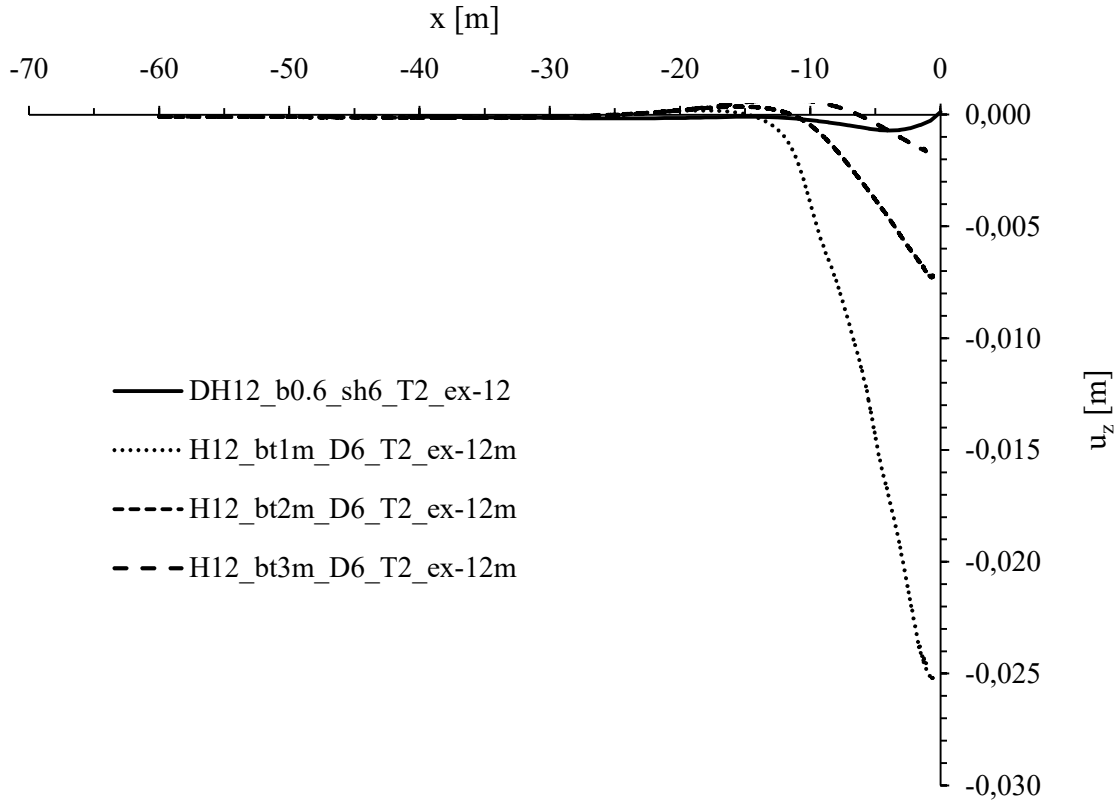

Figura 3.30 Ground settlement of anchored diaphragm (solid line) and buttressed wall models (see Table 3.11)

3.6.3. Maximum ground surface settlement

Still regarding the displacement analysis, as reported in the literature, in general the maximum displacement at ground level ($u_{z,max}$) can be estimated in relation to the value of the maximum wall deflection ($u_{x,max}$). Figure 3.30 shows the dimensionless relationship between $u_{z,max}$ and $u_{x,max}$ for the sixteen models summarized in the table above.

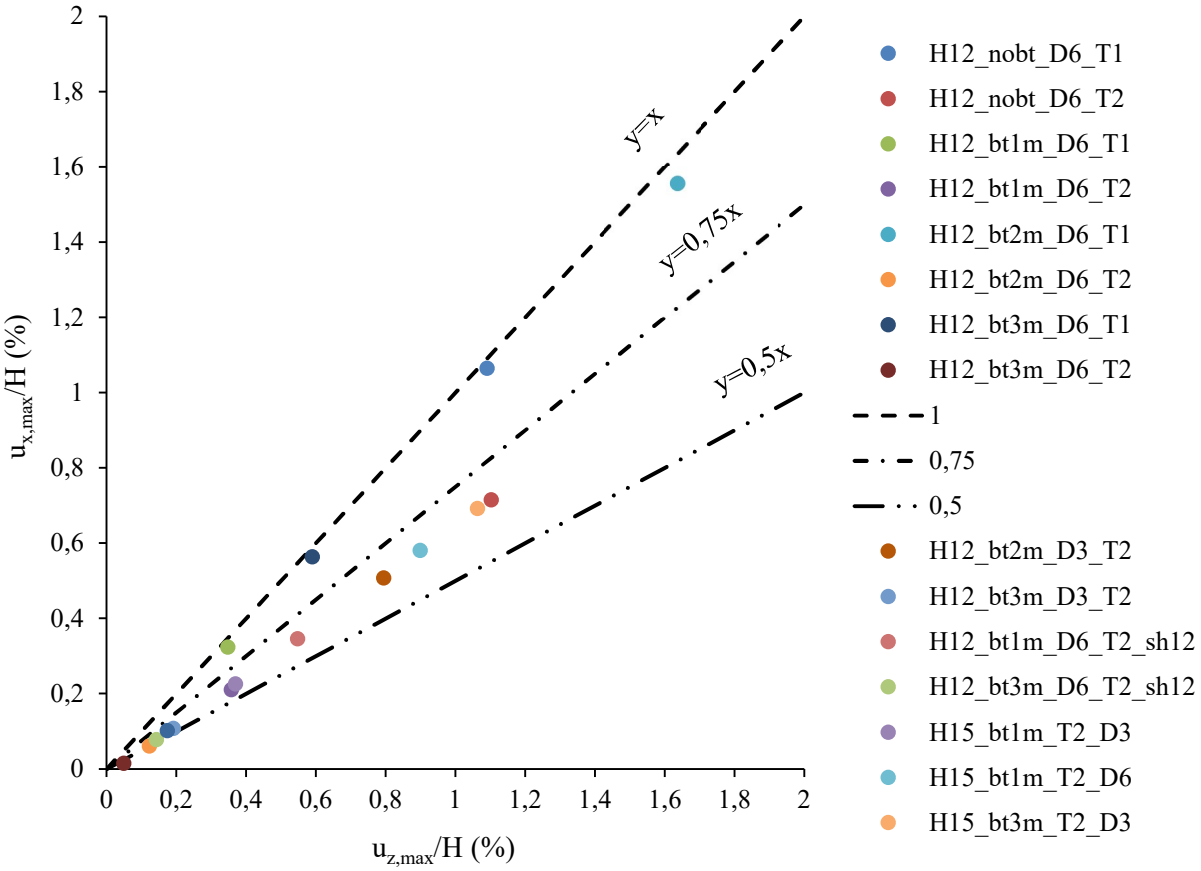

Figure 3.31 Relationship between maximum horizontal displacement and maximum subsidence at ground level (see Table 3.9)

As shown in the figure, in most cases $u_{z,max}$ is equal to (0.5-0.75) $u_{x,max}$, and the upper limit is $u_{z,max}$ = $u_{x,max}$. The value of $u_{z,max}$ is almost equal to $u_{x,max}$ for cases where the soil is of poor quality (e.g. T1 cases).

The results obtained are congruent with those shown in Figure 3.19 (b) as they fall in the range between y=x and y= 0.5x.

The maximum lateral wall deflection can be obtained by performing a lateral deformation analysis, e.g., finite element method or the beam on elastic foundation method, with good accuracy and can also be estimated by referring to the maximum excavation depth (H). Other factors, such as soil conditions, construction sequence, excavation width and wall stiffness, may also affect the value of $u_{x,max}$.

The following graphs, on the other hand, show the relationship between the maximum horizontal displacement of the diaphragm and the excavation depth: as can be seen, $u_{x,max}$ increases as the excavation depth increases.

Furthermore, for the same excavation depth, the horizontal displacement decreases as the length of the buttress wall increases and increases as the horizontal spacing (sh) between buttresses increases (Figures 3.33 and 3.34).

Finally, as the embedded depth increases, the horizontal displacement decreases (Figure 3.35).

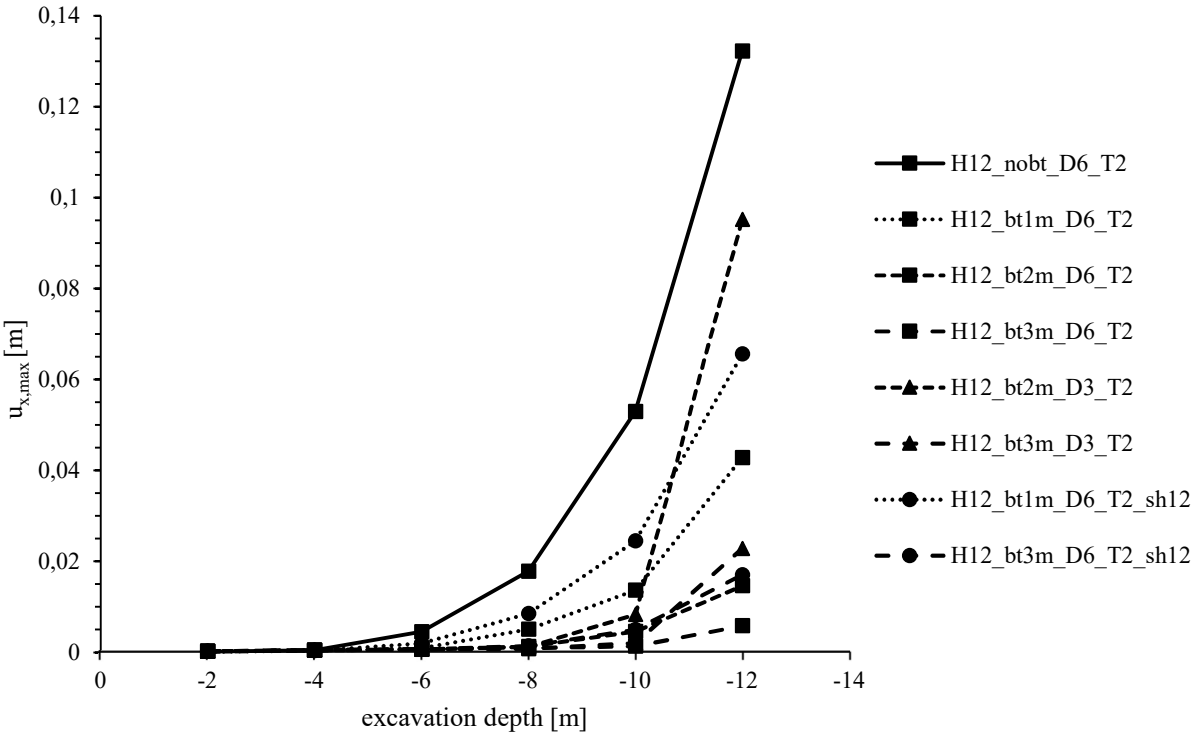

Figure 3.32 Relationship between the maximum horizontal displacement of the support structure and the excavation depth (see Table 3.9)

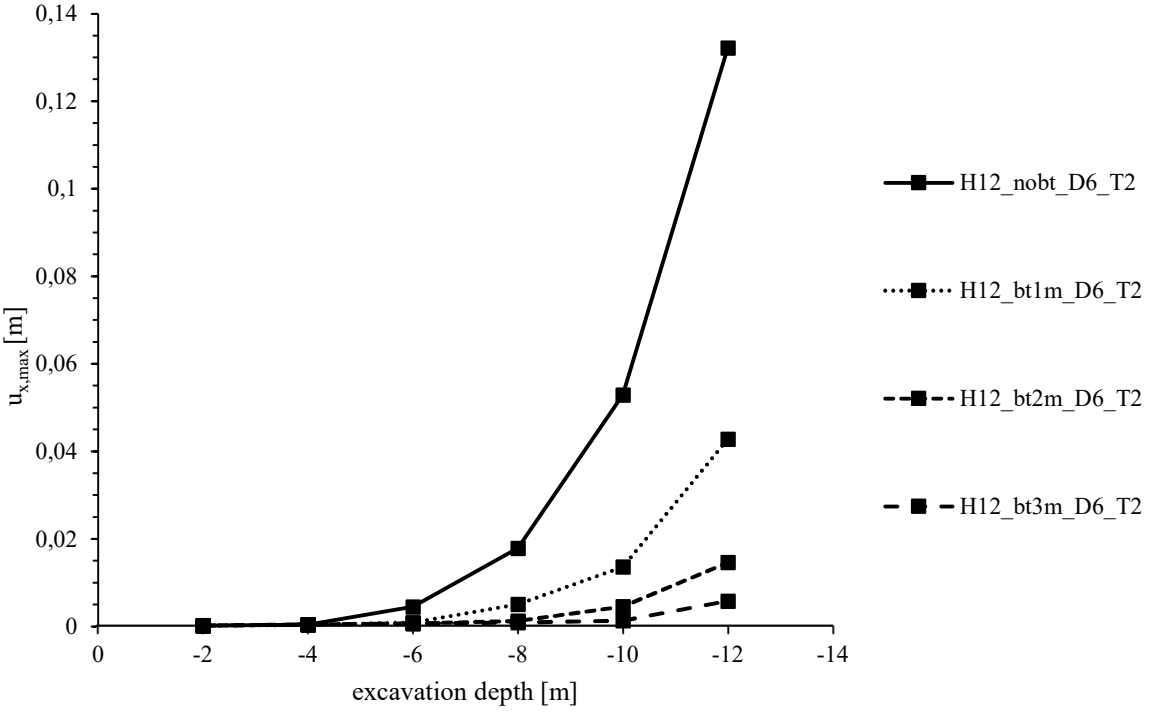

Figure 3.33 Relationship between the maximum horizontal displacement of the support structure and the excavation depth (as the length of the buttress increases). See Table 3.9

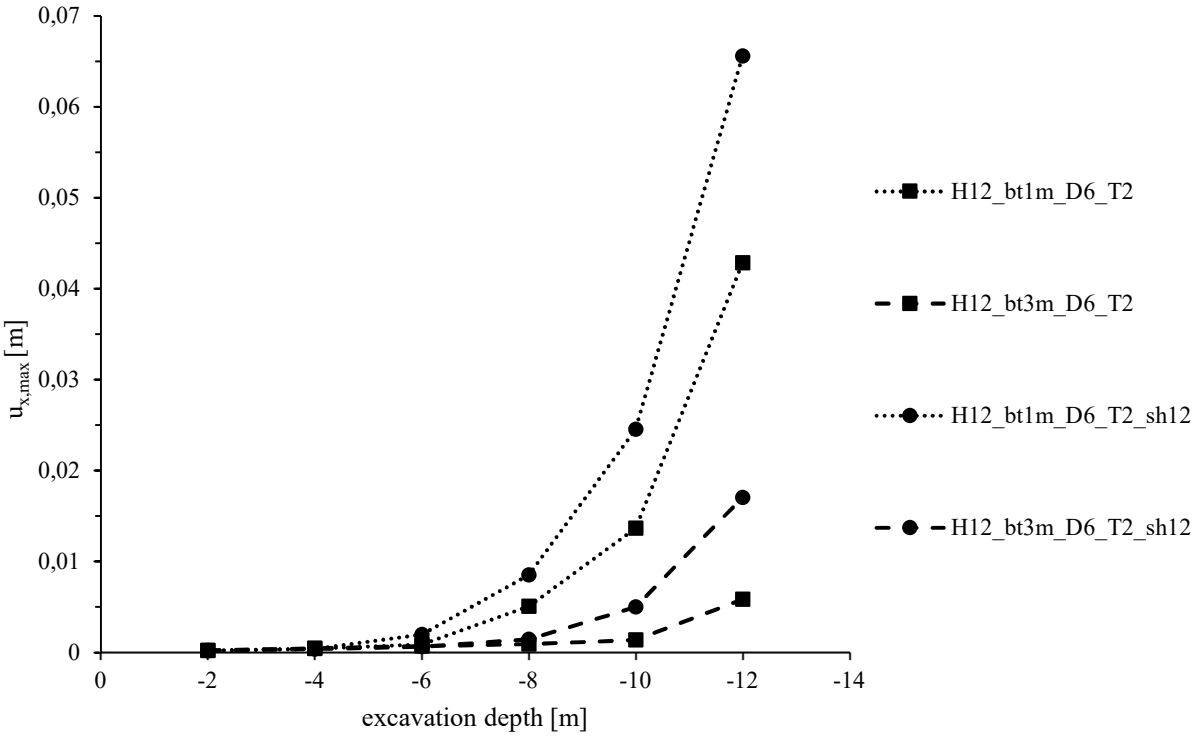

Figure 3.34 Relationship between the maximum horizontal displacement of the support structure and the depth of excavation (as the horizontal spacing between buttresses increases). See Table 3.9.

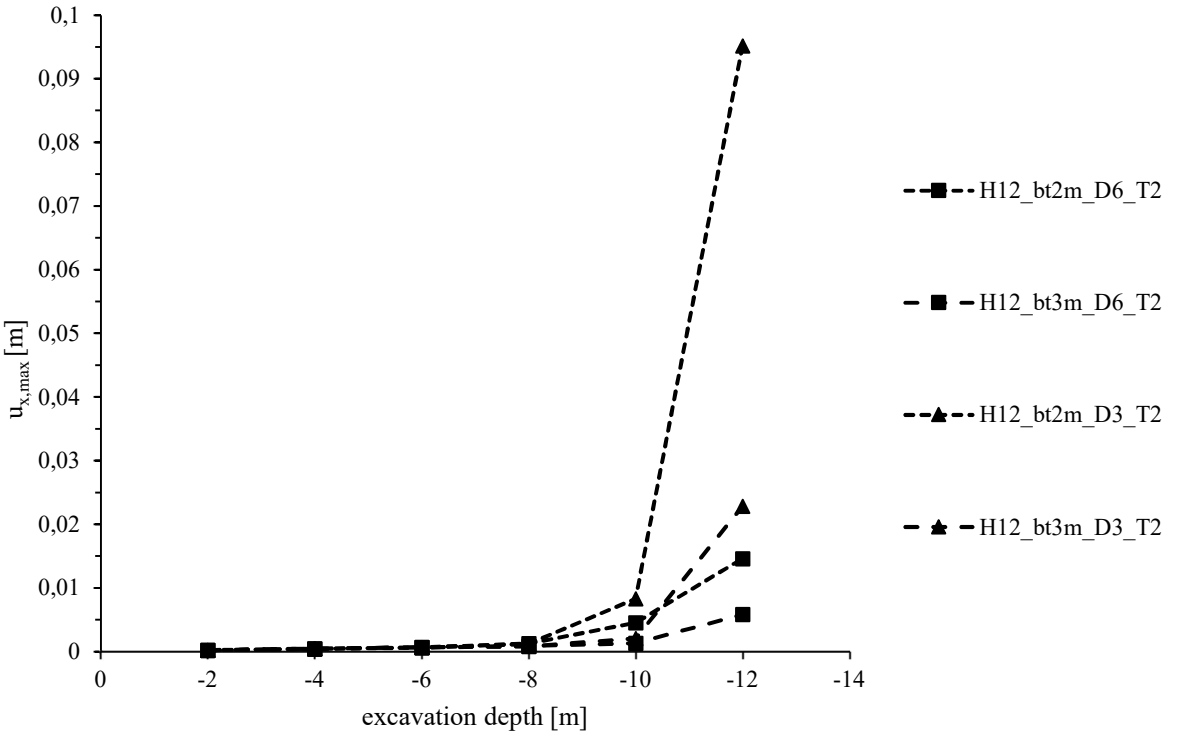

Figure 3.35 Relationship between the maximum horizontal displacement of the retaining structure and the depth of excavation (as embedded depth increases) See Table 3.9.

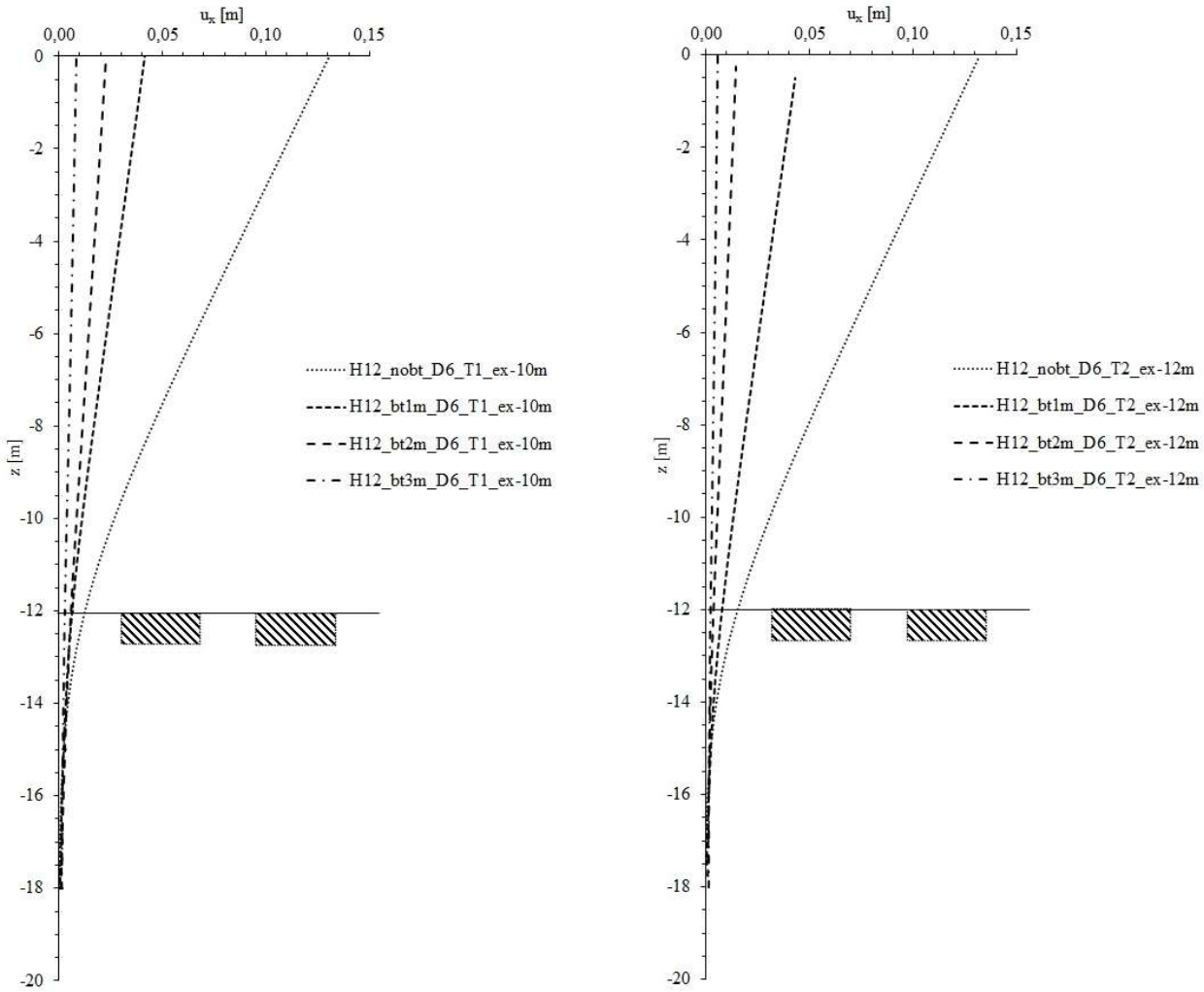

Figure 3.36 Comparison of wall deformations for different lengths of buttressed wall in loose sand (T1) and dense sand (T2) excavations (see Table 3.11).

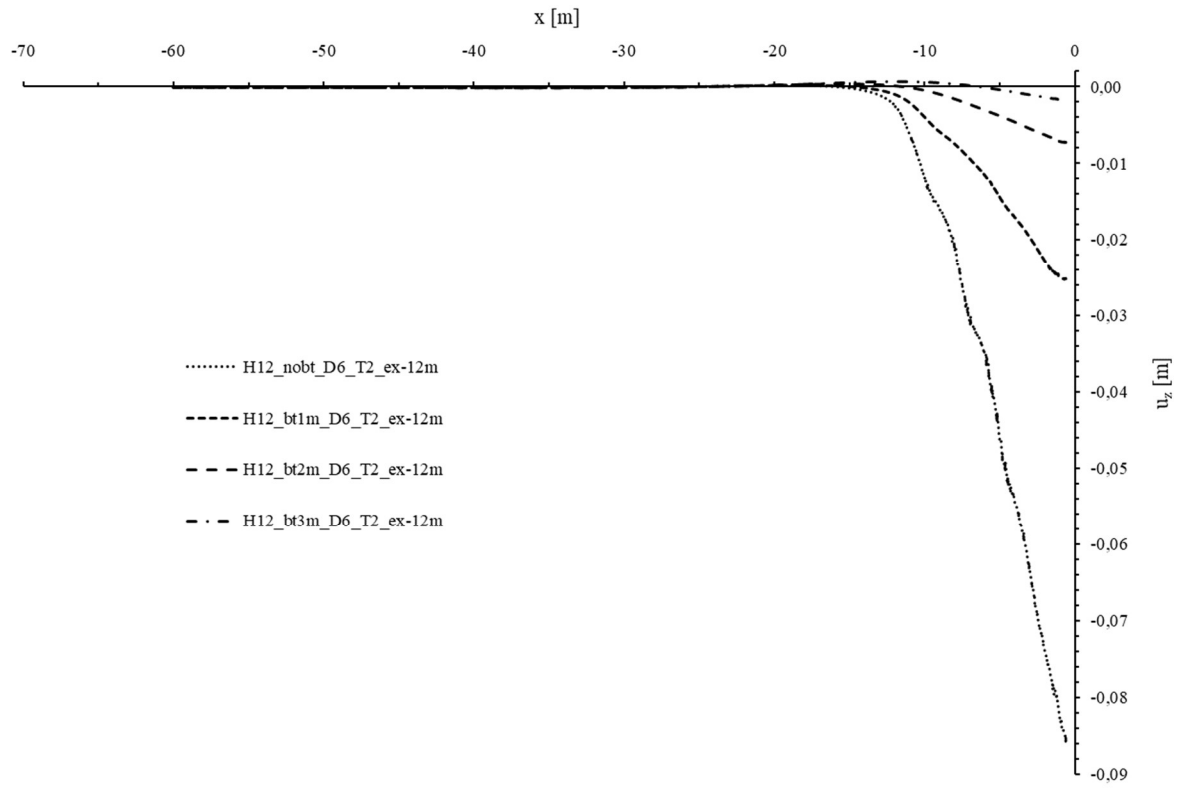

Figure 3.37 Comparison of ground subsidence at ground level for different lengths of buttressed wall in dense sand excavations (see Table 3.11).

Figure 3.36 shows the variation in wall deflection for scenarios with buttress walls with L_{bt} = 1, 2, 3 m and without buttress, respectively. The value of the horizontal wall displacement decreases with increasing buttress wall length. Similar and consistent results are obtained with the subsidence profiles shown in Figure 3.37.

3.6.4. Horizontal displacements vs. buttressed wall geometry

The graphs in Figures 3.38 and 3.39 show the trend of the horizontal displacement of the diaphragm in relation to the depth of the wall, both divided by the current excavation depth H. It can be seen that the diaphragm inflexion decreases with increasing buttress wall length. It is also shown that the inflexion of the structure decreases as D increases and that, for a fixed value of D/H, ux/H increases as the ratio of buttress length to current excavation depth bt/H decreases.

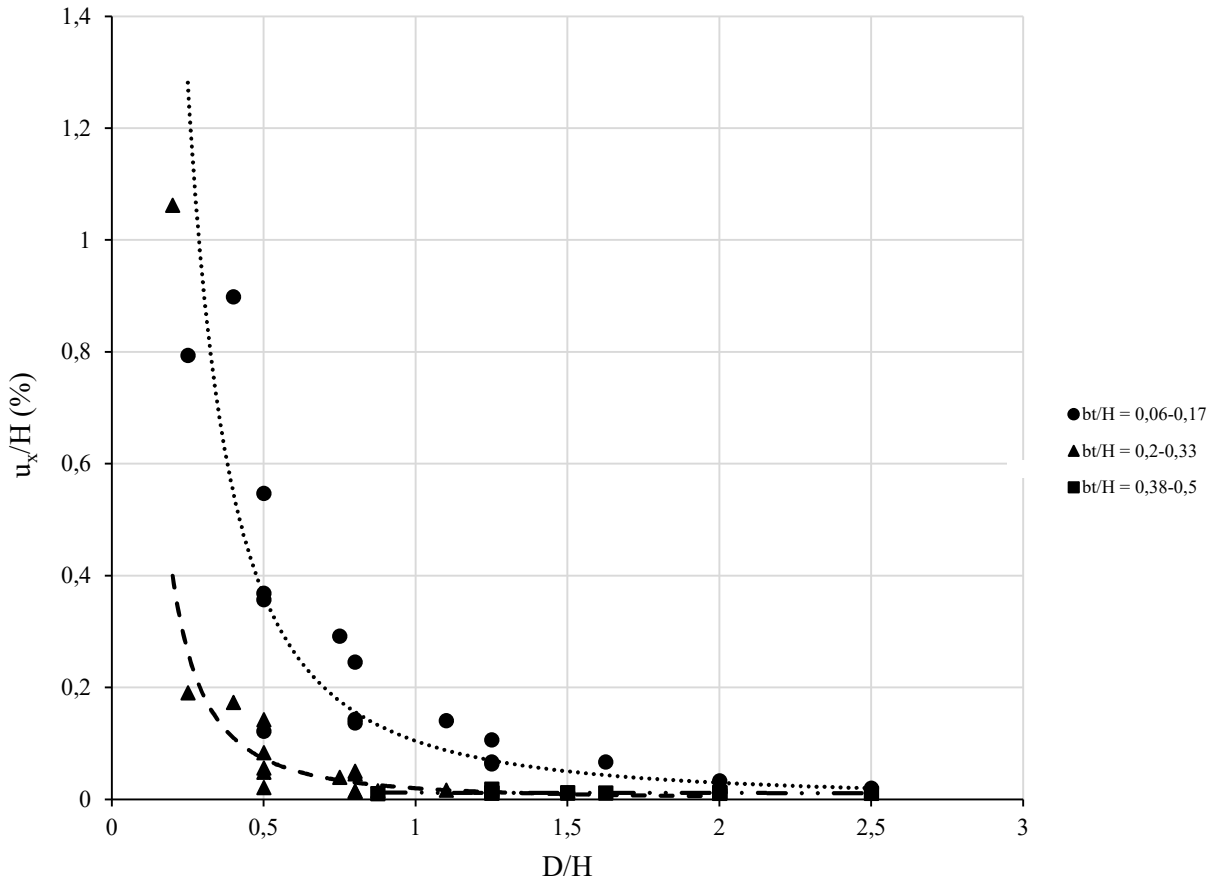

Figure 3.38 Non-dimensional relationship between horizontal displacement of the diaphragm in relation to wall deepening

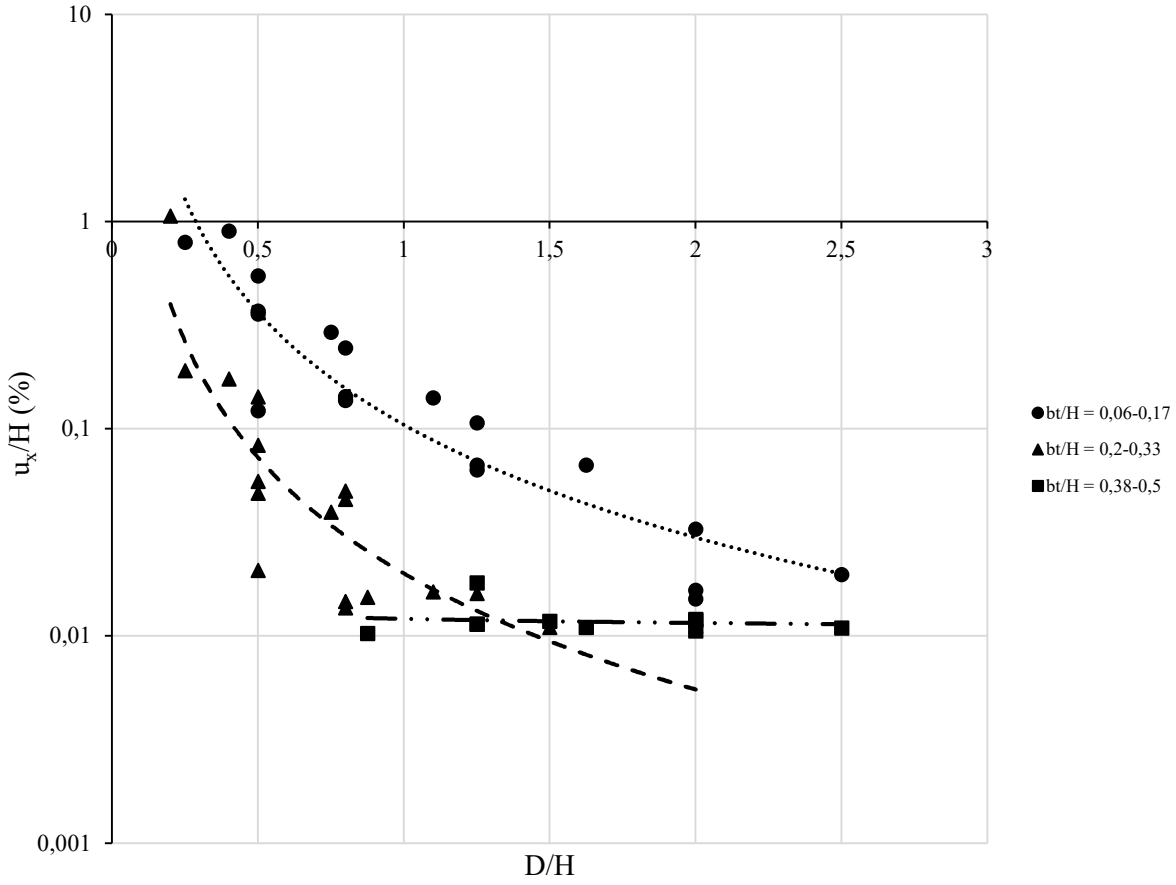

Figure 3.39 Non-dimensional relationship between horizontal diaphragm displacement in relation to wall deepening in semilogarithmic scale

The graphs in Figure 3.40 show the trend of the horizontal displacement of the diaphragm in relation to the horizontal spacing between buttresses, both divided by the current excavation depth H, comparing the results of the models where the only parameter to differ is sh.

It can be seen that the deflection of the structure decreases as the ratio sh/H increases (keeping sh constant) and, for a fixed value of sh/H, ux/H increases as the spacing between buttresses increases.

Similar results are obtained in Figures 3.41 and 3.42, where the models are compared as the length of the buttress changes: the inflexion of the structure decreases as sh increases and, for a fixed value of sh/H, ux/H increases as the length of the buttress decreases.

The graph in Figure 3.43 shows a different trend of ux as a function of sh. Looking at models with the same buttress wall length and the same wall depth, it can be seen that for the same excavation depth, the ratio ux/H increases as the ratio sh/H increases.

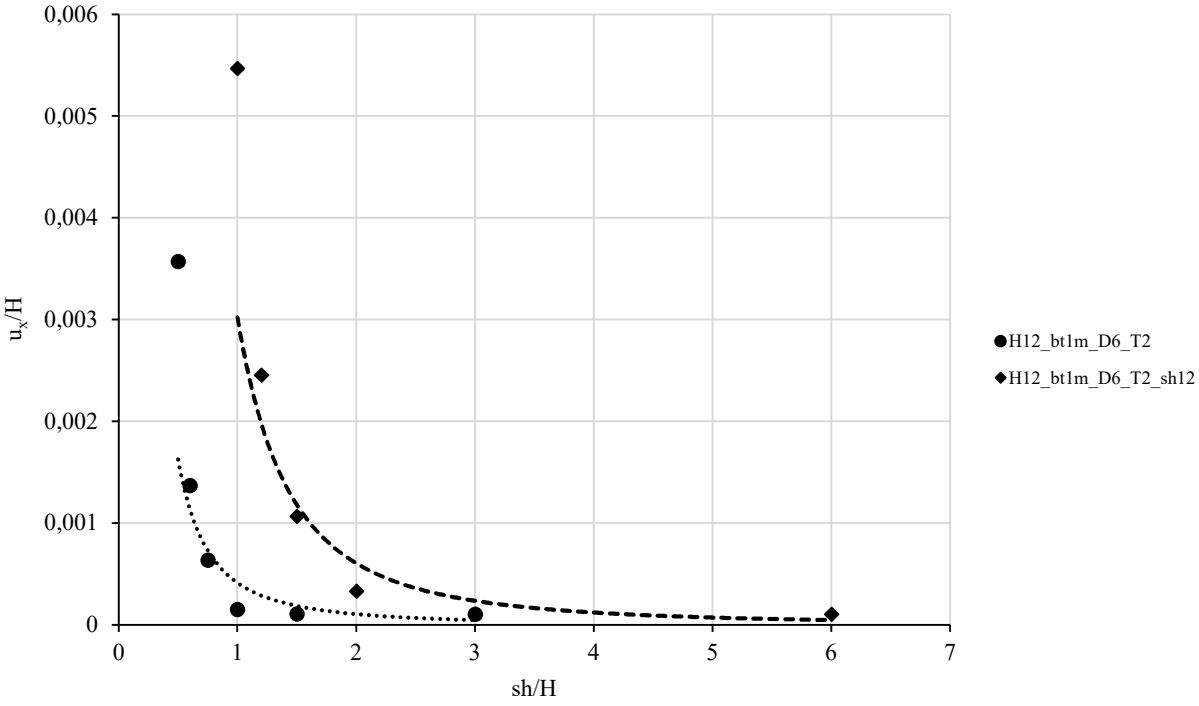

Figure 3.40 Dimensionless relationship between the horizontal displacement of the diaphragm and the horizontal spacing between buttress walls

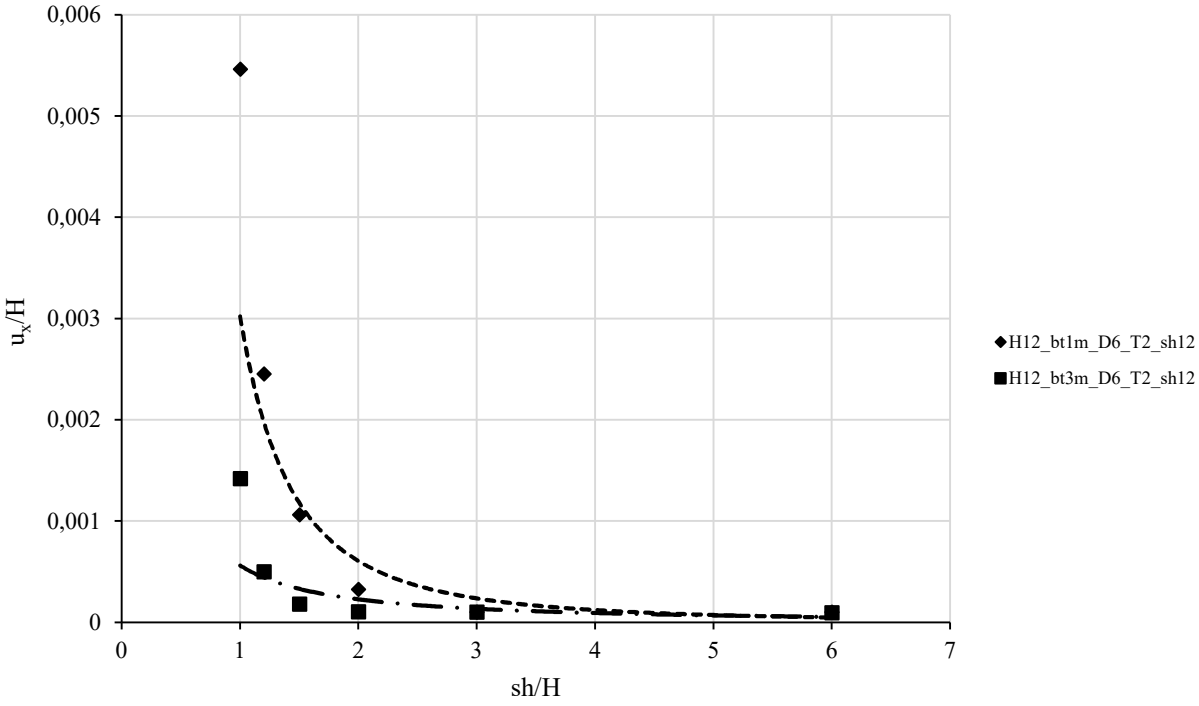

Figure 3.41 Dimensionless relationship between the horizontal displacement of the diaphragm and the horizontal spacing between the buttress walls

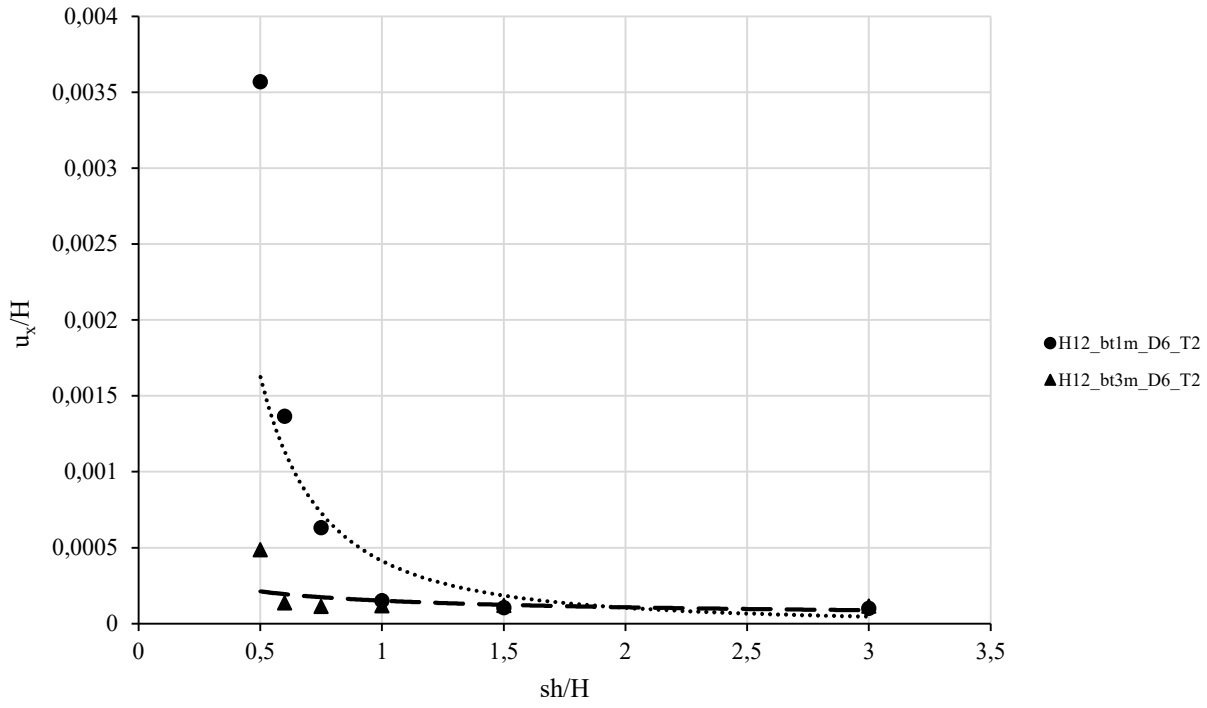

Figure 3.42 Dimensionless relationship between the horizontal displacement of the diaphragm and the horizontal spacing between buttress walls

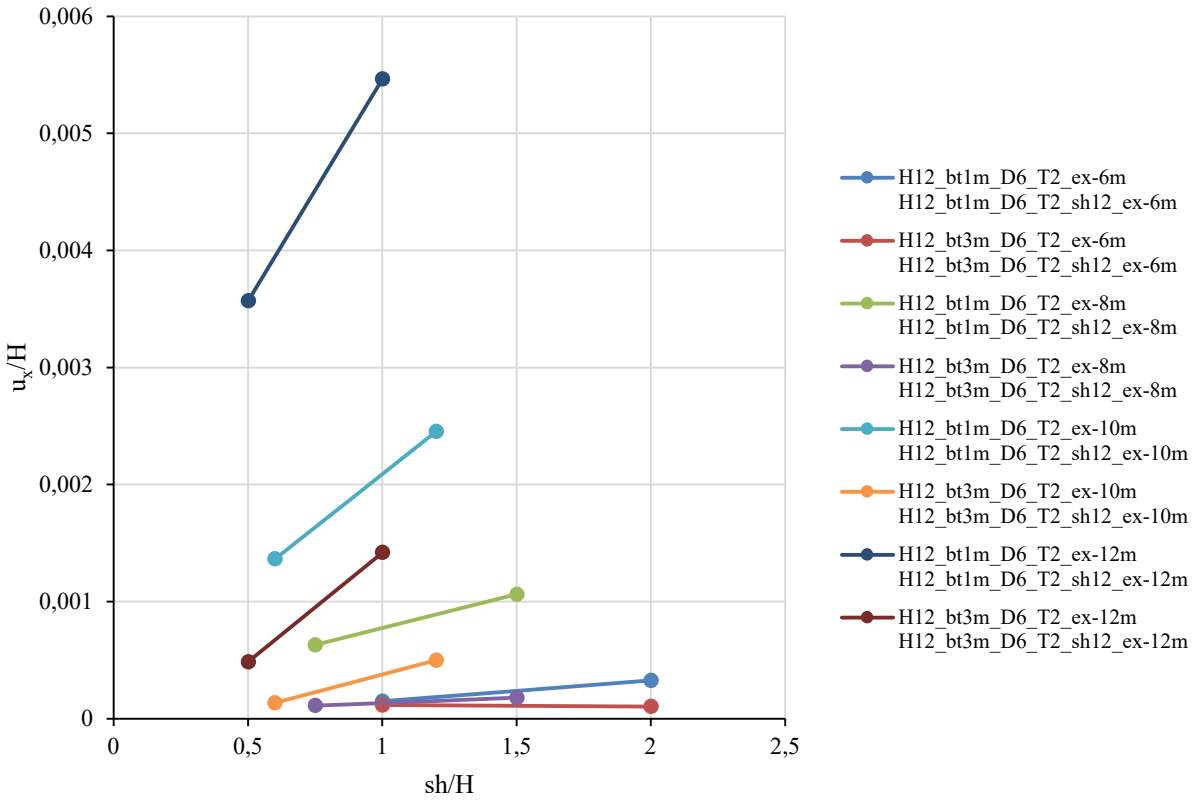

Figure 3.43 Dimensionless relationship between the horizontal displacement of the diaphragm and the horizontal spacing between buttress walls (see Table 3.9).

3.6.5. Buttress wall efficiency

In order to evaluate the effectiveness of buttress walls quantitatively, it is defined a ratio of reduction in the maximum wall deflection as:

$$Bte = \frac{u_{x,max,nobtw} - u_{x,max,btw}}{u_{x,max,nobtw}} * 100$$

Where $u_{x,max,nobtw}$ is the maximum displacement of the diaphragm wall with the assumption of no buttress walls and $u_{x,max,btw}$ is the deflection of the diaphragm wall with buttress walls.

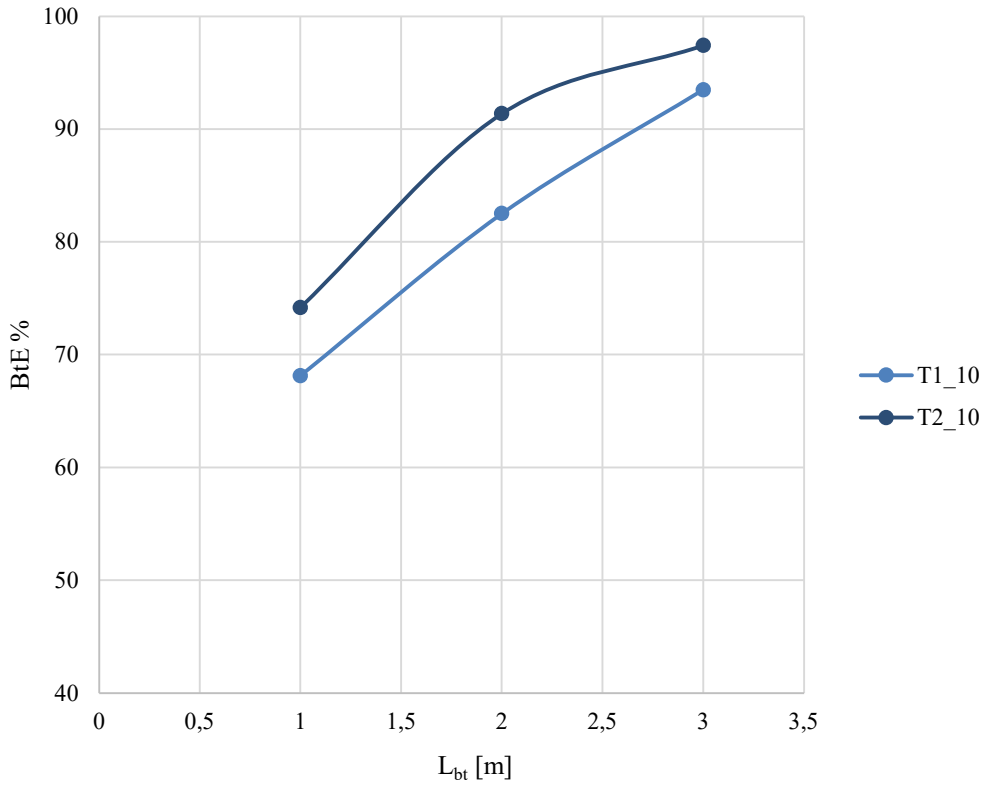

Figure 3.44 Coefficient of buttress wall efficiency for buttress wall models with Lbt=1,2,3m, excavation height 15m, deepening D=3m for excavation stages of -10 m, varying type of soil T1 or T2

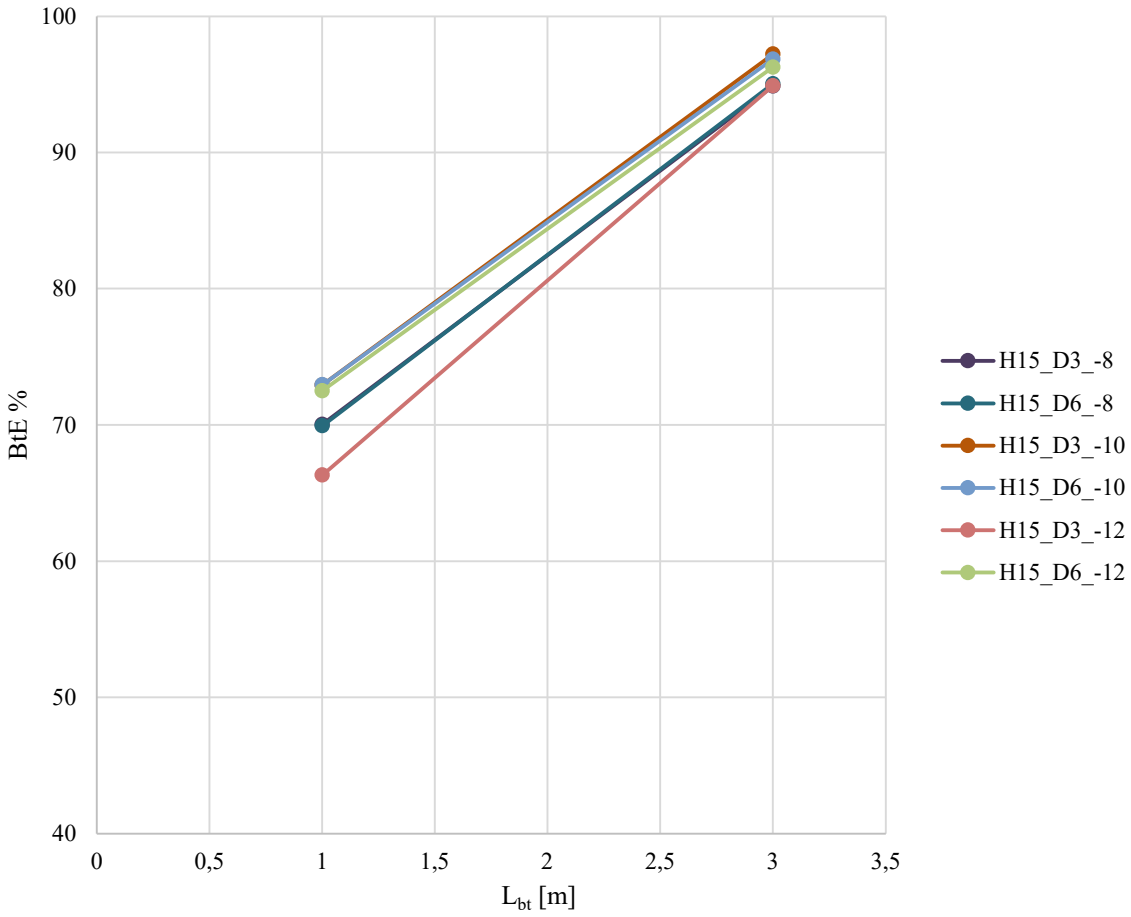

Figure 3.45 Coefficient of buttress wall efficiency for buttress wall models with Lbt=1,2,3m, excavation height 15m, deepening D=3 and 6 m for excavation stages of -8, -10 and -12 m

The graph shows the extent of reduction in BtE value due to the installation of buttress wall, indicating that the greater the length Lbt, the greater the reduction in wall deflection. The rate of reduction decreases as the length of the buttress wall increases.

This effect is more evident for soil with better mechanical properties (Figure 3.44) and does not depend on the value of D (Figure 3.45).

3.6.6.Conclusions

Traditional solutions (such as struts and anchors) have a limited ability to reduce displacements related to the change in total horizontal and vertical stresses following the execution of an excavation because these are systems that can only be realized after excavation, when a significant amount of displacement has already occurred. Different reinforcing solutions that can be installed before excavation execution and thus counteract a significant portion of induced displacement are cross walls connecting face bulkheads and buttress walls, local stiffening and strengthening interventions in the portion of the ground to be excavated.

The focus of the research was on this second category of structures.

In general, analyses for evaluating excavation-induced effects start from the assumption of simple deformation conditions. In the case of continuous elements this assumption may still be true, considering the area affected by the intervention as homogeneously equivalent, but if the interventions are discontinuous as in this case the problem has strongly three-dimensional characteristics.

A series of numerical FEM analyses were then developed to study the performance of "non-traditional" solutions, initially comparing two- and three-dimensional modelling results, followed by a parametric study to evaluate the influence of geometric parameters on the stiffening of the retaining structure and the reduction of displacements to develop design criteria.

From the results produced, indications are obtained on the magnitude of the displacements that may occur and the type of geometric solution to be adopted under similar conditions; thus, the possibility of having feedback to verify that the results obtained even from less in-depth analysis have realistic values and indications for a preliminary design of this type of structures.

4. MODELING OF THE RESPONSE OF GRAVITY DOCKS SUBJECTED TO EXCAVATIONS AND LOCALIZED EROSION PHENOMENA

4.1. INTRODUCTION

The retrofitting of port structures such as mooring docks, which are subject to potential stability or displacement problems caused by excavation or erosive phenomena at the foot, is often carried out with structural interventions of onerous design, execution and economic demands. In the case of quay wall, some solutions may not be feasible, such as those involving reinforcement of the passive zone, which is not present in gravity support works. This chapter discusses this aspect, studying the response of a typical dock subjected to excavation at the foot, aimed at simulating localized erosion phenomena or a deepening of the seabed. Some results carried out by numerical FEM analysis are reported, with the purpose of analyzing the deformation and displacement mechanisms of the sandy or silt-clay type fill and foundation soil, and an examination of the local and global response of the structure in relation to geotechnical soil improvement interventions, to obtain results on the displacements to which the structure may be subjected as well as the definition of sizing and optimization criteria for the intervention.

The purpose of this study is to verify the problem of excavation at the foot of docks with the aim of obtaining displacement envelopes similar to those available in the framework of deep excavation in terms of extent and amount of displacement, ratio of vertical to horizontal displacements etc. More generally, the effort is to replicate, with the same procedure (thus taking into account the geometry of the problem, the reinforcement intervention at the footing...) the background known for the excavation problem; just as a reinforcement system may be present for the latter, so a dock subjected to excavation may be subject to improvement interventions.

4.2. HARBOUR STRUCTURES: GENERAL REMARKS

4.2.1. General remarks

The harbour system is one of the strategic logistic infrastructures for a country (like Italy for example) that imports raw materials and exports its products in the world market.

The sea transport is the system of cargo transport characterized from the minor energy spending and from the less unitary cost and represents the modality of greater interest for the worldwide transports of goods.

In the last century the dimension of transport ships has exponentially grown and consequently the required harbour infrastructures to guarantee the mooring of the modern vessels.

Figure 4.1 illustrates the evolution of port infrastructure linked to the characteristics of the ships showing historical development of the container capacity of vessels compared with their draught.

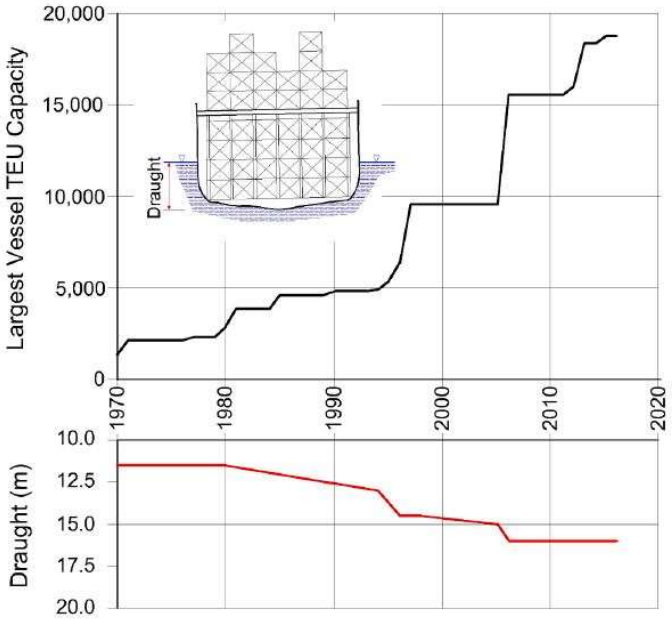

Figure 4.1 Evolution of vessels TEU capacity and corresponding draught (Hacegaba, 2014)

A current quay structure employed for cargo-handling needs a seabed depth ranging from 12m to 20m and a deck height ranging from 2.5m to 5.0m above sea level.

Considering the large number of existing ports in Europe, and the fact that it is difficult to find other sites on which to plan a new one, solutions must be found for upgrading existing structures to actual requirements. This is particularly true for Italian ports, which were usually constructed in past centuries and are part of very large urban zones, where the possibility of expansion into new areas is minimal (Ruggeri et al. 2019).

The upgrading of a quay wall is an actual important issue, but rarely addressed in literature. It needs the consideration of several factors, including the deepening of the seabed, increased terrain loads, the use of large cranes (often heavy mobile cranes) and the availability of strong mooring bitts.

Bauduin et al. (2017) classify the entity of improvements by distinguishing between:

- restoration, in which the existing structures are essentially reused;
- medium upgrade, in which the existing structures are still used, but it is necessary to supplement them with new structures;
- intensive upgrade, in which the existing structure is fully disregarded and the new structures have to sustain the full impact of all actions.

Finally, a relevant aspect for design of upgrading intervention is their cost: it is related, among others, to the evolution of the mandatory codes for construction.

Given the increasing demand for safety in public infrastructures by the society, always particularly sensitive to their performance during earthquakes (Scarpelli et al., 2011, 2012), any new updating of the codes implies an increase significantly in the strength of the structures. Consequently, improvement intervention on old structures become very expensive just because of the increasing safety demand in technical codes, even in the absence of any relevant modification in the use of the infrastructure.

4.2.2. Classification of quay walls

According to Tsinker (1997) a dock indicates a marine structure for safe mooring of a ship, accommodating cargo-handling equipment, the loading or unloading of a cargo, supply and repair of ships and the boarding or disembarkation of passengers.

It is customary to distinguish different types of docks between:

- quays: structure of timber, masonry, cement or other material built along the navigable waterway, able to offer a permanent safe mooring to vessels and that allow to carry out all the tasks of service and storage for port traffic;
- piers (or jetties): a construction projected out onto the water and able to accommodate vessels on one or both sides. They differ from the quays for the limited or absent storage capacity of the goods and in many cases, they do not allow a permanent mooring;
- dolphins: isolated marine structures for mooring vessels; more than one dolphin must be used to moor a ship.

The choice of a good technical solution for the construction of a quay must consider different aspects whose most important are (Scarpelli et al. 2017):

- environmental aspects, such as tidal entity, geotechnical soils characteristics and waves energy;
- management aspects, such as the size of the project vessel, the type of transported cargo, the way the cargo is handled, the type of cargo-handling equipment operating on the service area;
- economic aspects, such as the availability of building materials, and construction time in relation to the needs of commercial traffic.

From a structural point of view, the classification recommended by Thoresen (2003) groups quay walls into two main categories:

- solid berth structures: a vertical front wall constructed to resist both the horizontal load from the fill and the live load on the apron;
- open berth structures: a load-bearing slab on columns/piles that covers the slope between seabed and apron.

Solid berth structures can be divided into gravity-wall structure and sheet-pile-wall structures, based on the principle that lends stability to the wall.

The gravity-wall (Figure 4.2) structure balances the horizontal action with its own deadweight and bottom friction. Typical solutions consist of concrete blocks or caissons and always require a rubble rock-fill behind the blocks to limit the horizontal pressure of the soil. They are the primary option if the foundation soil is firm because it requires only moderate maintenance, thanks to a massive structural section. Moreover, it is the solution under which construction of an anti-reflective wave chamber is easiest.

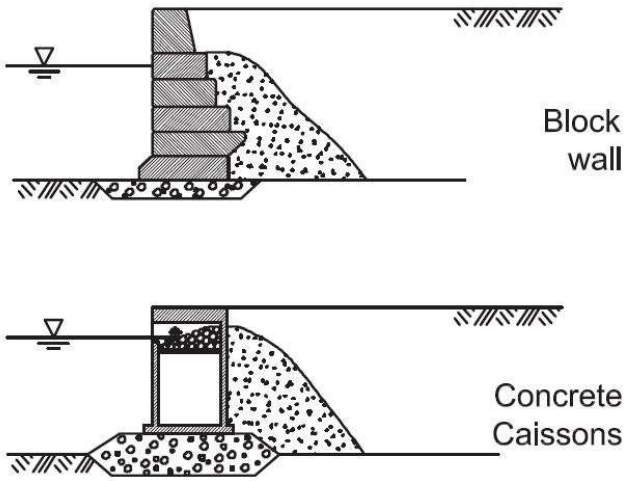

Figure 4.2 Gravity wall examples

Sheet-pile walls (Figure 4.3) are made up by relatively thin walls of steel, reinforced concrete or timber supported by anchors and passive soil pressure in front of the wall. Anchors can transmit the tensile force directly to the soil or to other anchoring structures. Currently, the most widely used sheet walls are steel-sheet piles, thanks to the highly flexible profiles offered by industrial production. However, the slenderness of the profiles calls for care to be taken in aggressive environments and it is not easy to build anti-reflective wave chambers.

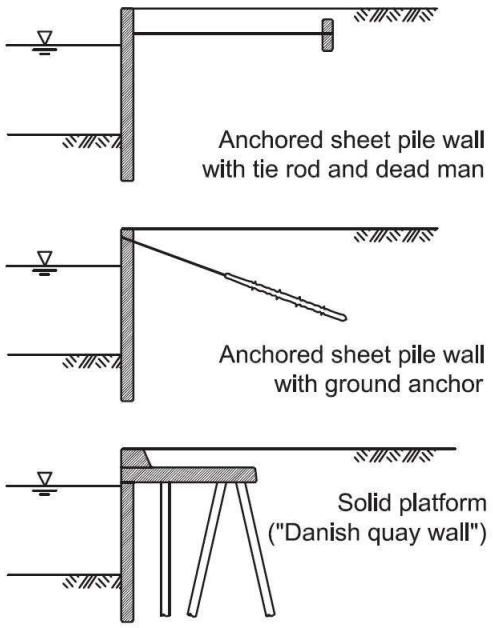

Figure 4.3 Sheet pile wall examples

Among solid berth structures solutions, there is so-called “Danish quay wall”, consisting of a sheet-pile wall retained by a platform set on inclined piles that makes possible the transmission of overloads on the deck to a deep bearing soil stratum, decreasing the soil pressure on the wall.

The solution represented by open-berth structures (or jetties) separates the berthing actions in two parts: the seabed is shaped in a slope, to remove the horizontal soil pressure on the structures, while a concrete slab set on piles is placed over the slope, providing the berth for vessels (Figure 4.4).

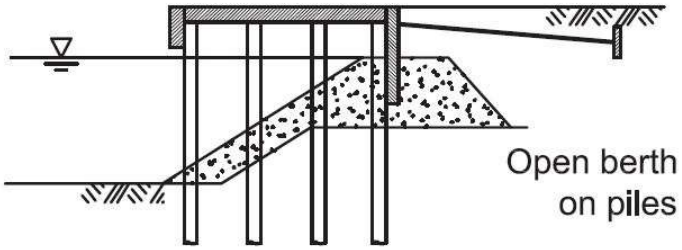

Figure 4.4 Open berth structure example

This solution provides to reach very deep seabed, can be designed for high-performance in the event of an earthquake or tsunami, thanks to the relatively light-weight structures employed and ensure an optimal absorption of the marine waves. On the other hand, the large number of structural elements exposed to the marine environment and their slenderness makes this solution sensitive to ageing and difficult to maintain.

4.2.3. Retrofitting of quay walls: general aspects

The main circumstances that could require a structural intervention to enhance the performance of a quay wall are (Ruggeri et al., 2019):

- deterioration of the structures (due to the ageing of the works);
- deepening of the seabed;
- erosion of the seabed (e. g. ship propeller action)
- increased berthing forces;
- increased loads on the deck (increased overloads or the employment of heavy cranes);
- changes in technical code requirements, especially with regard to safety standards for public works and/or changes in the natural actions to be considered (i.e. seismic safety).

Limiting the investigation to solid-berth structures, and considering them as a retaining wall essentially, three strategies of intervention to improve performance may be identified:

1) reduction of stress, especially horizontal soil pressure;
2) increase in strength resources in the foundation zone;
3) strengthening of quay wall structures.

Typically, any improvement work requires a combination of more than one strategy to gain the best result.

Point 1 deals with the reduction of soil pressures and includes interventions aimed at transferring the surface loads at a depth (relieving platform built behind the vertical wall and soil-improvement treatments, such as jet grouting or deep-mixing columns installed in the active volume of the wall).

A different way to reduce active soil pressure is the substitution of the first meters of soil below the deck with lightweight material (i.e. expanded clay aggregate).

Point 2 focuses on increasing the strength resources in the passive and foundation zones. Techniques normally employed in such interventions are weighting of the soil at the toe with the addition rocks, or partially substituting soft soil with gravel, or treating soil volume with jet grouting by means of deepmixing techniques to enhance strength and stiffness.

Point 3 includes strengthening intervention on the structures. Concrete blocks are frequently connected by vertical steel rods, with an underpinning of micro-piles, in order to prevent displacement of the individual blocks and improve the overall stability of the construction.

For sheet-pile walls, the typical approach is to reinforce the anchoring systems by adding new anchors or strengthening the existing steel bars and retaining walls. Strengthening of the structural section of the main wall can also enhance the performance of the retaining system.

Certainly they are the typology, the importance of the existing work and the increment of demanded performance that determine the entity of the reinforcement intervention; in this case it is not uncommon to prefer to replacing the old structures or incorporating them in a new construction.

4.3. STUDY OF THE PERFORMANCE OF A GRAVITY QUAY

4.3.1. Introduction

As described in previous paragraph, in last few years we can assist very frequently to the need to operate relevant and extended dredgings in the harbour areas, because of the increment of the dimensions of the cargo and passengers' ships. (Scarpelli et al., 2017). It follows the need to upgrade port infrastructure (breakwaters, docks), a requirement that presupposes, mainly, a deepening of the seabed. Moreover, the cases of loss of stability of portions of existing docks are more and more frequent and are linked to phenomena of localized erosion, caused at foundation level by the propulsive action of the ships.

Even in the presence of massive and rigid structures, the removal of vertical stress from the bottom induces deep movements and possible instability phenomena. In addition to traditional reinforcement interventions, other solutions can be investigated by increasing the resistance and stiffness at the foot of the structures, acting on the ground-system foundation through an improvement of the mechanical response of the soils or the insertion of structural "inclusions" (Ruggeri et al., 2014; Sauvageon & Berardi, 2021, Sauvageon, 2021).

In Figure 4.5 two examples of quay walls located in the Port of Genoa (Eritrea Pier and San Giorgio Pier) are shown; in both cases consolidation works using jet grouting technique have been planned.

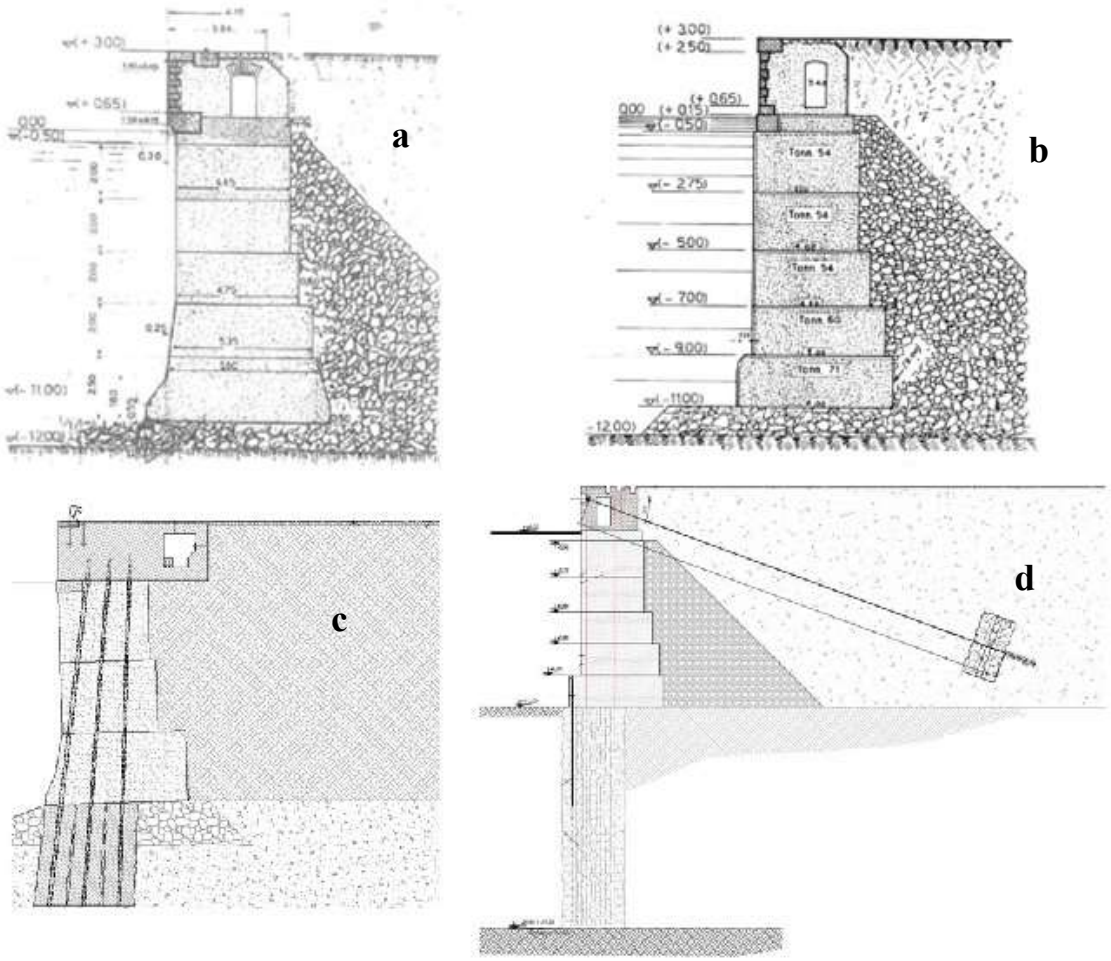

Figure 4.5 Examples of actual intervention of jet grouting. Eritrea Pier (a) and San Giorgio Pier (b) in Port of Genoa and the corresponding interventions (c) and (d)

Through finite element numerical modelling, the study addresses the analysis of the above-mentioned mechanisms, taking into account, among other aspects, the capability of the soil construction model to reproduce these phenomena and the interaction of the soil with the structural elements, with the aim of defining general modelling criteria, obtaining possible deformation modes and providing general displacement profiles to assess expected effects and, finally, providing guidance on possible geotechnical interventions.

The object of the study is a quay wall, having typical size and characteristics of existing quays in commercial and passengers' ports, built before the advent of ships having greater draught and with propulsive systems significantly different to the current ones (Tsinker, 1997). The objective is to simulate the response of a representative case of a possible real situation.

4.3.2.Structure modelling

The structural typology chosen is a gravity quay wall, whose scheme is as shown in Figure 4.6. The structural scheme adopted was developed considering the typical block wall quay standards, which have

a seabed depth of interest such as to have to provide the need of a deepening of the seabed or be able to be subjected to localized erosion phenomena at the foot.

The structure consists of 5 overlapping concrete blocks resting on a gravel basement, with an abutment on the back inside the soil backfill.

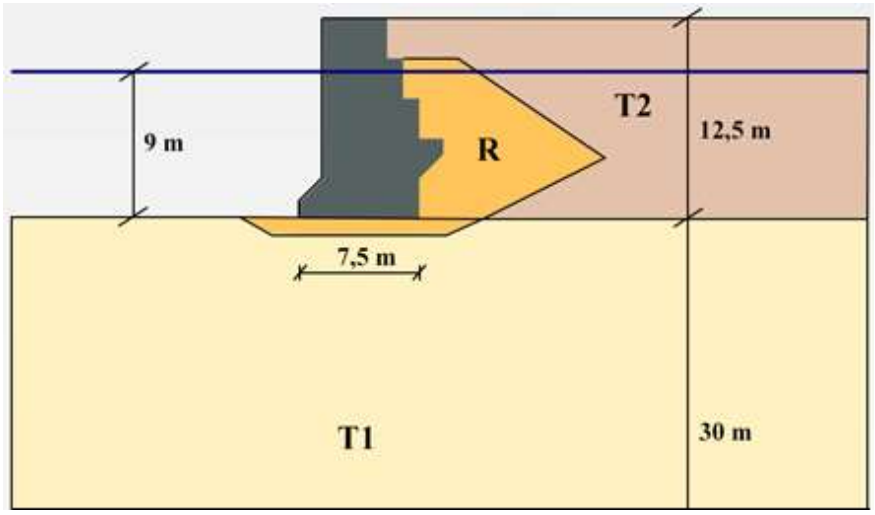

Figure 4.6 Geometric scheme of the quay wall and soil stratigraphy

The quay has been modelled since its construction, including the placement of the backfill and inserting interfaces between the structure and the soil, to obtain a stress state and representative deformation for various stages of the analysis. The excavation at the foot of the quay, that takes place step by step until the failure condition is reached, has been then schematized and was executed every 0,5 m in two modalities, vertical wall and sloped as it is shown in Figure 4.7

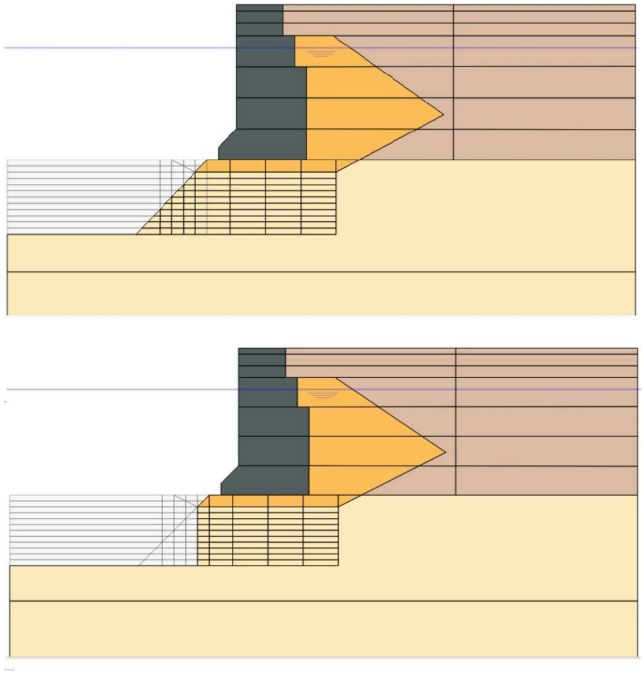

Figure 4.7 Sloped and vertical excavation schemes

4.3.3.Soil behavior modelling

As regards soil behavior modelling, sandy and clayey silt soils are adopted in numerical analyses, carried out by Plaxis, and the soils have been modelled respectively by Hardening Soil Small, a non-linear strain hardening plastic model with the possibility of following loading and unloading cycles, and the Soft Soil model, best suited to simulate the behavior of compressible soils typical of the seabed. The parameters used for modeling have been calibrated from experimental results (oedometric and triaxial tests) and are reported in the following tables. The soil that was modelled as 'Soft Soil' is actually the soil of a seabed within a harbour; it was taken as a reference to represent real situation for the particular problem here analyzed. It is worth knowing that the parameters used in the numerical model have been calibrated and obtained from actual laboratory tests carried out on undisturbed specimens (see also Figures 4.9, 4.10, 4.11).

Table 4.1 Parameters of Hardening Soil Small model

	γ [kN/m^3]	E_{50}^{ref} [kN/m^2]	E_{ur}^{ref} [kN/m^2]	E_{oed}^{ref} [kN/m^2]	c' [kN/m^2]	φ' [°]	ψ [°]	ν [-]	G_0^{ref} [kN/m^2]	$\gamma_{0.7}$ [-]
Loose sand (T1)	17	20000	60000	16000	1	34	0	0.20	70000	0.0001
Dense sand (T2)	17.5	37000	90000	29600	1	41	14	0.20	112500	0.0002
Embankment (R)	18.5	37000	29600	29600	1	44	7	0.20	70000	0.0001

Table 4.2 Parameters of Soft Soil model

	γ [kN/m^3]	λ^* [-]	κ^* [-]	c'_{ref} [kN/m^2]	φ' [°]	ψ [°]
Soft clay (T1)_L4	18	0.050	0.018	8	30	0

For the concrete constituting the quay it was considered an elastic material characterized by the weight of the volume unit γ =24 kN/m^3 and elastic module E=31500 MN/m^2. Considering the case study of the gravity quay, the improvement intervention at the foundation ground can be carried out by technique of jet-grouting, executed from pontoon and from plan descent, crossing the dock structure. That said, the area of intervention was modelled with clusters of soil with linear elastic behaviour, characterized by a unit weight of volume equal to 18,7 kN/m^3 and elastic module E_{eq}=300 MN/m^2 in models with a dense sand foundation soil, and with a weight of 19,5 kN/m^3 and elastic modulus E_{eq}=140 MN/m^2 in those with a silty clay foundation soil. All the parameters adopted for the natural soil and for the improved soil have been defined by calibrating the model from real experimental results.

The equivalent modulus of the improved soil was defined from an average value of the elastic modulus of the soil Es, the elastic modulus of the jet grouting columns E_j and the ratio of the area of the improved soil to that of the virgin soil A_j/A_s:

$$E_{eq} = E_s + \left(E_s - E_j\right)\frac{A_j}{A_s}$$

In the case of the soft silty soil, for example, a uniaxial compressive strength of the jet-grouting q_u =2 MN/m^2 was assumed; the ratio E_j/σ_j =200 and the column diameter D_j=0.5 m with spacing s_j=1.5D_j; for the soil an elastic modulus Es=1.2 MN/m2 was assessed.

A similar procedure (with different values, suitable for sandy soil) led to the value Eq=300 MN/m2

The HSS-modeled soils examined here and their parameters are those already presented in Section 3.2.3.

Soft Soil model

The Soft Soil model is a Cam-Clay type model especially introduced for primary compression of near normally consolidated clay-type soils. In fact, as soft soil it can be considered near-normally consolidated clays, clayey silts and peat. A particular feature of such materials is their high degree of compressibility. This is best demonstrated by oedometer test data as reported for instance by Janbu (1985). Considering tangent stiffness moduli at a reference oedometer pressure of 100 kPa, he reports for normally consolidated clays E_{oed} = 1 to 4 MPa, depending on the clay considered. The differences between these values and stiffnesses for NC-sands are considerable and for them the values are in the range of 10 to 50 MPa, at least for non-cemented laboratory samples.

Therefore, in oedometer testing normally consolidated clays behave ten times softer than normally consolidated sands. This illustrates the extreme compressibility of soft soils (Plaxis Manual)

A feature of soft soils is the linear stress-dependency of soil stiffness. The oedometer modulus Eoed is given by:

$$E_{oed} = \frac{-\sigma_1'}{\lambda^*}$$

where:

$$\lambda^* = \frac{p^{ref}}{E_{oed}^{ref}}$$

For lots of practical soft-soil studies, the modified compression index λ^* will be known and the oedometer modulus can be computed from the relationship:

$$E_{oed}^{ref} = \frac{p^{ref}}{\lambda^*}$$

It is important to note that most soft soil problems can be analysed using the Hardening Soil model, but this model is not suitable when considering very soft soils with a high compressibility, i.e $E_{oed}^{ref} / E_{50}^{ref} <$ 0.5.

For such soils indeed, the Soft Soil model may be used.

Some properties of Soft Soil model are:

- stress dependent stiffness (logarithmic compression behaviour)
- distinction between primary loading and unloading-reloading
- memory for pre-consolidation stress
- failure behaviour according to the Mohr-Coulomb criterion

The parameters of the Soft Soil model, summarised in the table below, include the compression and swelling indices, typical of soft soils, and the failure parameters of the Mohr-Coulomb model.

Table 4.3 Soft Soil model parameters

Modified compression index	λ^*	[-]
Modified swelling index	κ^*	[-]
Poisson's ratio for unloading / reloading	ν_{ur}	[-]
Effective cohesion	C	[kN/m^2]
Friction angle	Φ	[°]
Dilatancy angle	Ψ	[°]
Tensile strength	σ_t	[kN/m^2]

Modified compression index and modified swelling index can be obtained from an isotropic compression test including isotropic unloading. When plotting the logarithm of the mean stress as a

function of the volumetric strain for clay-type materials, the plot can be approximated by two straight lines (Figure 4.8).

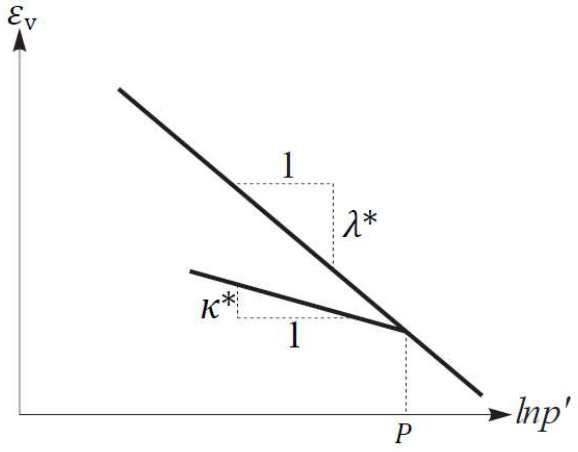

Figure 4.8 Logarithmic relation between volumetric strain and mean stress

The slope of the primary loading line gives the modified compression index, and the slope of the unloading (or swelling) line gives the modified swelling index. There is a difference between the modified indices κ* and λ* and the original Cam-Clay parameters κ and λ. Indeed, the latter parameters are defined in terms of the void ratio, e, instead of the volumetric strain, ε_v.

Apart from the isotropic compression test, the parameters κ* and λ* can be obtained from a one-dimensional compression test. Relationships exist with the internationally recognised parameters for one-dimensional compression and swelling, C_c and C_s:

$$\lambda^* = \frac{\lambda}{(1+e)} \qquad \kappa^* = \frac{\kappa}{(1+e)}$$

$$\lambda^* = \frac{C_c}{2{,}3\ (1+e)} \qquad \kappa^* = \frac{C_s}{2{,}3\ (1+e)}$$

The choice of parameters for the Soft Soil model was based on the results of oedometric tests on three soils: very compressible medium plasticity silty clay (L1), silty clay (L3) and very compressible clay (L4).

All the undisturbed samples of these three soils were taken from boreholes during a geotechnical investigation performed on the seabed of an Italian harbour, where new docks were to be built.

The graphs in Figures 4.9, 4.10 and 4.11 show, in terms of oedometric curve e-log σ'_v, the result of the calibration of the parameters for Soft Soil model carried out through Plaxis Soil test function. The experimental laboratory data are therefore representative of the case object of the study.

For the numerical analyses performed the L4 soil type has been chosen. The parameters are reported in Table 4.2.

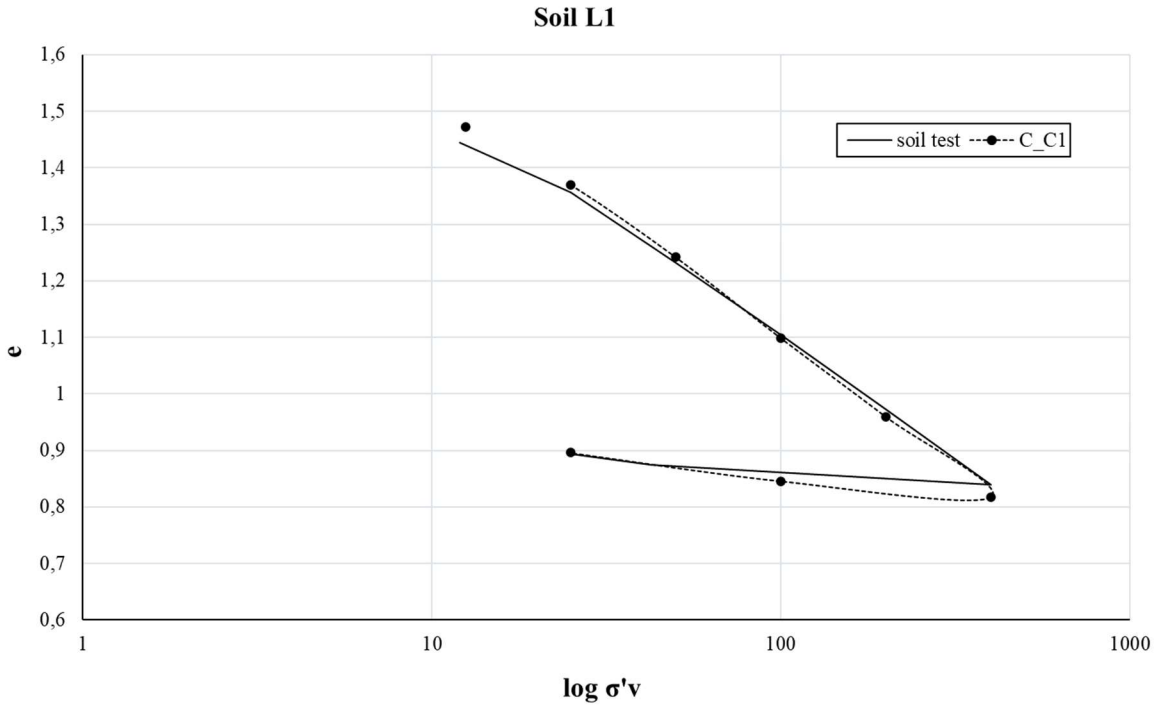

Figure 4.9 Calibration curve C-C1 (L1) (solid line Plaxis soil test, dotted line experimental curve)

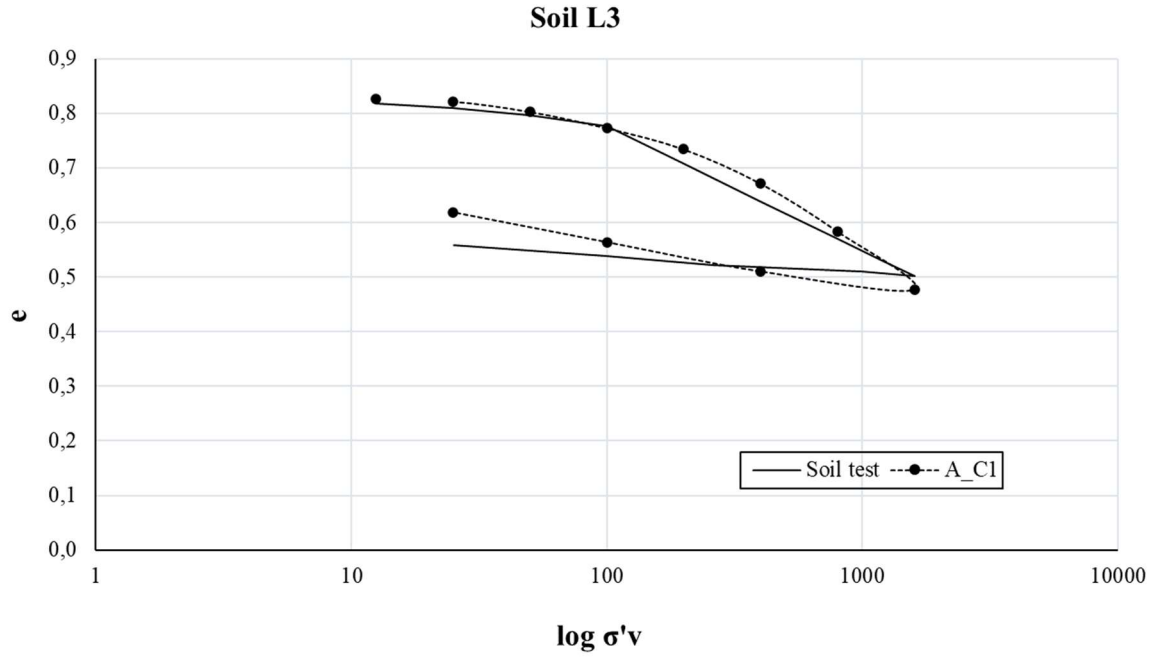

Figure 4.10 Calibration curve A-C1 (L3) (solid line Plaxis soil test, dotted line experimental curve)

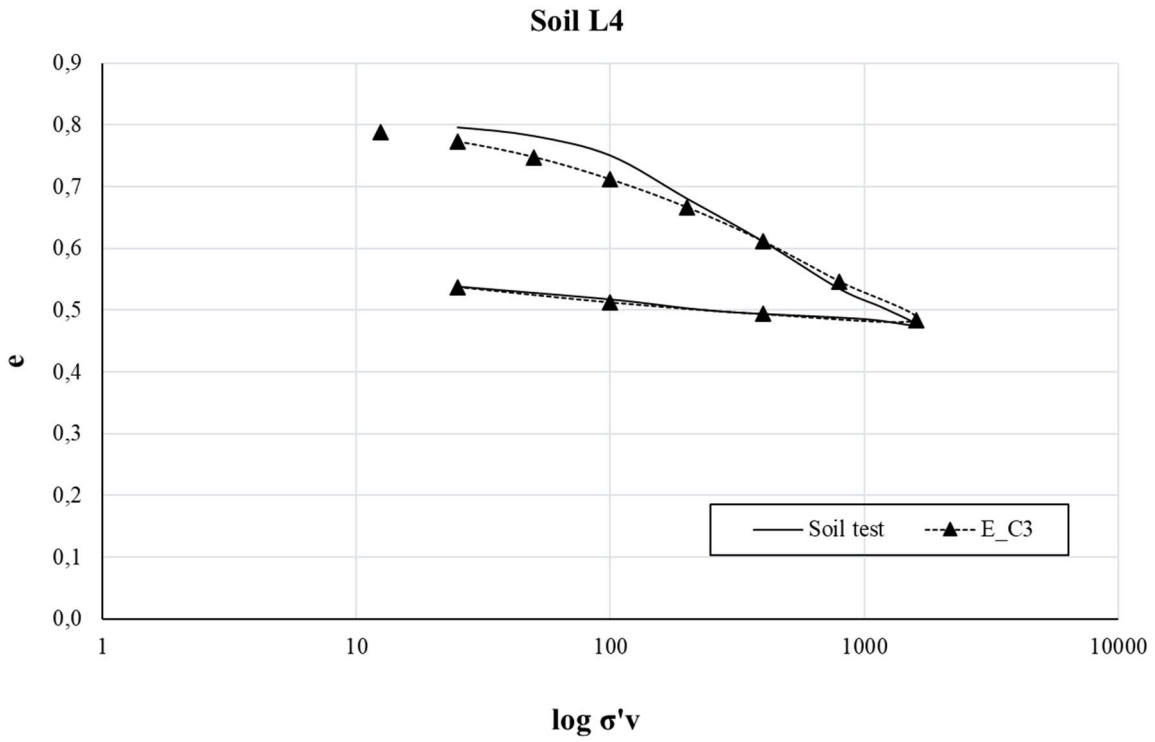

Figure 4.11 Calibration curve E-C3 (L4) (solid line Plaxis soil test, dotted line experimental curve)

In order to improve the mechanical response of the foundation soil and the structure as a whole, two different main intervention schemes have been defined, a treatment of "columnar" type (columnar improvement C) and one of "horizontal" type (horizontal improvement H) as shown in Figure 4.12.

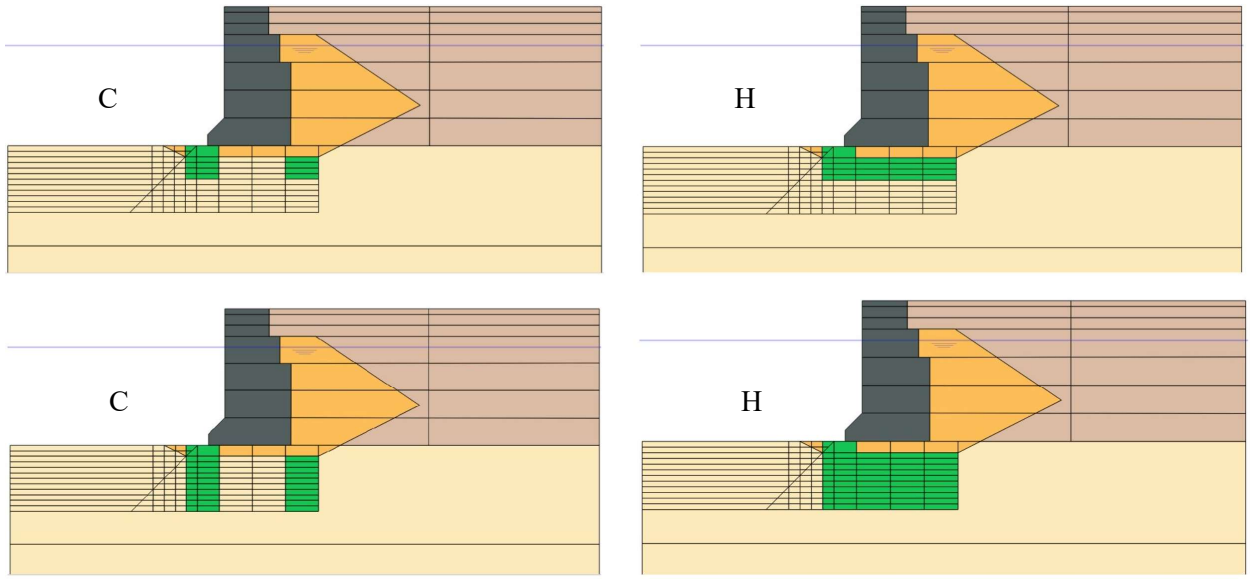

Figure 4.12 Schemes of improvements (columnar C and horizontal H)

The portion of soil affected by the improvement is gradually extended in 1-meter steps up to 6 meters under the seabed for both the improvements. The excavation is simulated as a vertical and sloped, step by step every 0.5 meters since the failure condition is reached. The analyses were carried out under drainage conditions in the case of sandy soil and simulating phases of consolidation for the clay soil. Consolidation phases of the stages of the quay construction were carried out in a single time interval of 30 days, whereas consolidation calculation of excavation phases were carried out in two steps of time interval of overall 12 days.

Table 4.4 shows the summary of the calculation phases of the quay wall models: the first twelve stages regard the construction of the structure, after the improvement stages and next the various excavations phases, plastic for Hardening Soil Small models and consolidation for Soft Soil models and relating safety analyses.

Safety analysis was performed by "phi-c reduction" procedure, which involves the progressive reduction of soil strength parameters tanφ and c until incipient failure of the structure occurs.

The total multiplier $\sum Msf$ is used to define the value of the soil strength parameters at a given stage in the analysis:

$$\sum Msf = \frac{tan\varphi_{input}}{tan\varphi_{reduced}} = \frac{c_{input}}{c_{reduced}} = \frac{s_{u,input}}{s_{u,reduced}} = \frac{tensile\ strength_{input}}{tensile\ strength_{reduced}}$$

where the strength parameters with the subscript 'input' refer to the properties entered in the material sets and parameters with the subscript 'reduced' refer to the reduced values used in the analysis. $\sum Msf$ is set to 1.0 at the start of a calculation to set all material strengths to their input values (Plaxis Manual).

Table 4.4 Calculation phases for quay wall models

Phase name	**Phase description**	**Calculation type Hardening Soil Small Models**	**Calculation type Soft Soil Models**
Initial phase		K0 procedure	K0 procedure
Phase_1	Construction of the basement	Plastic	Consolidation (30 d)
Phase_2	Placement of the first block	Plastic	Consolidation (30 d)
Phase_3	Placement of backfill corresponding to first block	Plastic	Consolidation (30 d)
Phase_4	Placement of the second block	Plastic	Consolidation (30 d)
Phase_5	Placement of backfill corresponding to second block	Plastic	Consolidation (30 d)
Phase_6	Placement of the third block	Plastic	Consolidation (30 d)
Phase_7	Placement of backfill corresponding to third block	Plastic	Consolidation (30 d)
Phase_8	Placement of the fourth block	Plastic	Consolidation (30 d)
Phase_9	Placement of backfill corresponding to fourth block	Plastic	Consolidation (30 d)

Phase_10	Placement of the fifth block	Plastic	Consolidation (30 d)
Phase_11	Placement of backfill corresponding to fifth block	Plastic	Consolidation (30 d)
Phase_12	-	Safety	Safety
improvement	Jet-grouting intervention	Plastic	Plastic
-0.5	Excavation down to -0.5 m	Plastic	Consolidation (2+10 d)
safety -0.5	-	Safety	Safety
-1	Excavation down to -1 m	Plastic	Consolidation (2+10 d)
safety -1	-	Safety	Safety
-1.5	Excavation down to -1.5 m	Plastic	Consolidation (2+10 d)
safety -1.5	-	Safety	Safety
-2	Excavation down to -2 m	Plastic	Consolidation (2+10 d)
safety -2	-	Safety	Safety
-2.5	Excavation down to -2.5 m	Plastic	Consolidation (2+10 d)
safety -2.5	-	Safety	Safety
-3	Excavation down to -3 m	Plastic	Consolidation (2+10 d)
safety -3	-	Safety	Safety
-3.5	Excavation down to -3.5 m	Plastic	Consolidation (2+10 d)
safety -3.5	-	Safety	Safety
-4	Excavation down to -4 m	Plastic	Consolidation (2+10 d)
safety -4	-	Safety	Safety
-4.5	Excavation down to -4.5 m	Plastic	Consolidation (2+10 d)
safety -4.5	-	Safety	Safety
-5	Excavation down to -5 m	Plastic	Consolidation (2+10 d)
safety -5	-	Safety	Safety
-5.5	Excavation down to -5.5 m	Plastic	Consolidation (2+10 d)
safety -5.5	-	Safety	Safety
-6	Excavation down to -6 m	Plastic	Consolidation (2+10 d)
safety -6	-	Safety	Safety

4.3.4. Analysis and results

In absence of consolidation of the soil with jet-grouting intervention, numerical analyses indicate an excavation depth at the foot not exceeding one meter due to local plastification associated to rigid rotations of the quay towards the sea front.

Adopting the different configurations of foundation soil improvement, the excavation depths reached before collapse, as expected, increase significantly as the area affected by the treatment increases and depending on the case, reached and exceed 6 m depth, with safety factor FS associated with the phase preceding the collapse of a value equal to or greater than the unit.

The following table 4.5 shows a summary of the various models analysed, with different schemes of improvement (O = horizontal and C = columnar): H_i is the thickness of the improved soil, $H_{d,max}$ is the final excavation depth and FS is the corresponding safety factor for a general failure as shown below.

Table 4.5

			H_i [m]	excavation	$H_{d,max}$ [m]	FS
Hardening Soil Small	**Improvement_1**	O	3	sloped	-6	1,064
	Improvement_2	O	3	vertical	-4,5	0,992
	Improvement_3	C	3	vertical	-2,5	1,078
	Improvement_4	C	3	sloped	-3	1,074
	Improvement_5	C	4	sloped	-3	1,032
	Improvement_6	C	5	sloped	-3	1,058
	Improvement_7	C	6	sloped	-3,5	1,077
	Improvement_8	C	6	vertical	-3,5	1,055
	Improvement_9	C	5	vertical	-3	1,029
	Improvement_10	C	4	vertical	-2,5	1,078
	Improvement_11	O	6	sloped	-6	1,065
	Improvement_12	O	6	vertical	-6	1,216
	Improvement_13	O	4	vertical	-5	1,112
	Improvement_14	O	5	vertical	-6	1,075
	Improvement_15	O	4	sloped	-6	1,073
	Improvement_16	O	5	sloped	-6	1,065

			H_i [m]	excavation	$H_{d,max}$ [m]	FS
Soft Soil	**Improvement_1**	O	3	sloped	-6	1,153
	Improvement_2	O	3	vertical	-5	1,112
	Improvement_3	C	3	vertical	-3	0,9853
	Improvement_4	C	3	sloped	-4	0,9825
	Improvement_5	C	4	sloped	-4	1,006
	Improvement_6	C	5	sloped	-5	1,03
	Improvement_7	C	6	sloped	-6	1,053
	Improvement_8	C	6	vertical	-4,5	1,085
	Improvement_9	C	5	vertical	-3,5	1,076
	Improvement_10	C	4	vertical	-2,5	1,068
	Improvement_11	O	6	sloped	-6	1,314
	Improvement_12	O	6	vertical	-6	1,207
	Improvement_13	O	4	vertical	-6	1,055
	Improvement_14	O	5	vertical	-6	1,16
	Improvement_15	O	4	sloped	-6	1,208
	Improvement_16	O	5	sloped	-6	1,248

In addition, there are two main mechanisms that can be observed at the collapse, not closely related to the type of foundation soil, but to the improvement configuration (columnar rather than horizontal), as shown in Figures 4.13 and 4.14.

The first mechanism, associated to a global counterclockwise rotation of the structures and an horizontal improvement, has a sliding wedge and a failure surface that pass under the bottom of the improved- layer. In fact, as the thickness of the treatment increases, this surface moves deeper.

The second mechanism, associated to a global clockwise rotation of the structures and a columnar improvement, presents a circular surface that passes between the treatment columns and whose depth increases again with the thickness of the improved zone.

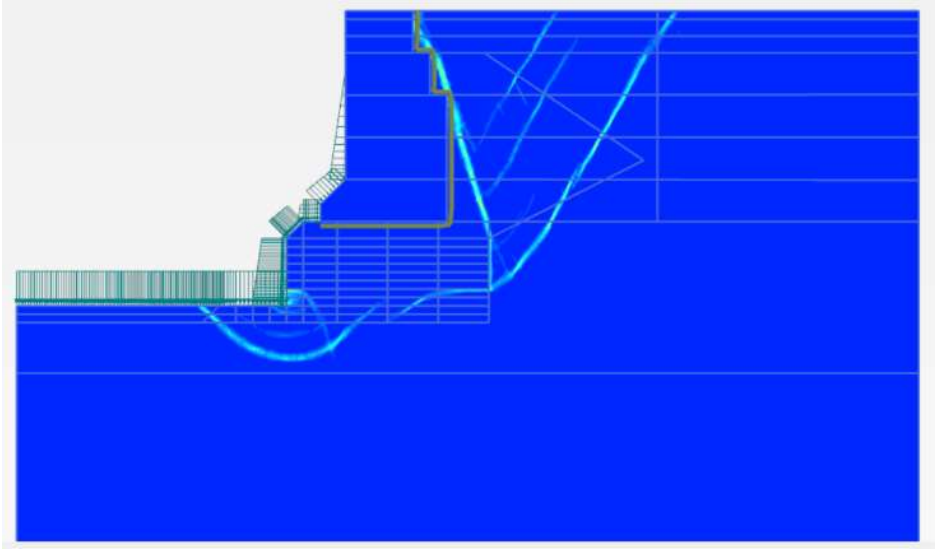

Figure 4.13 Mechanism of potential instability referred to the case “horizontal improvement.”

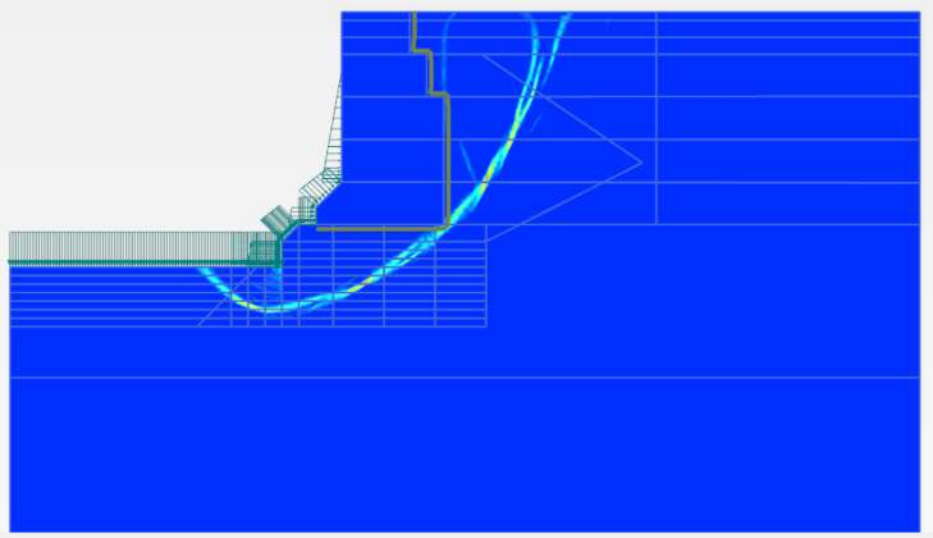

Figure 4.14 Mechanism of potential instability referred to the case “columnar improvement.”

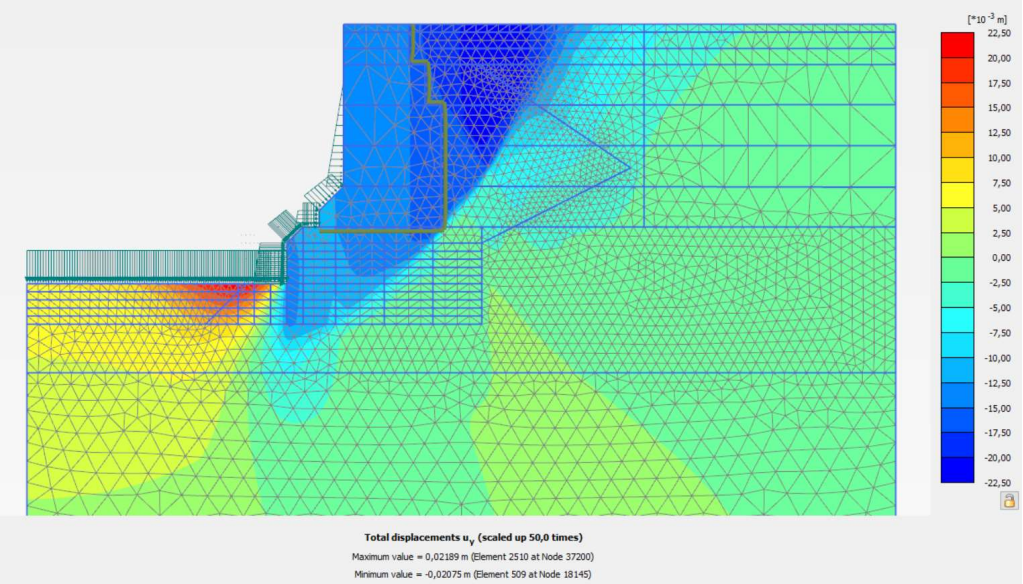

Figure 4.15 Example of distribution of vertical displacement

In Figure 4.15 is shown an example of the vertical displacements with the color map that indicates their values in Plaxis output. The greatest displacements are localized at the foot of the quay and immediately behind it. From a first observation of the settlement profiles, it is noted that for models with soft soil seabed, with the exception of the profiles corresponding to the initial excavation phases, there is a different shape of the profile depending on the type of columnar or horizontal treatment as it will be explained in the following.

For each model, the ground settlement profile on the back of the quay wall has been extracted, for every excavation phase. As expected, the value of the maximum settlement $u_{y,max}$ is dependent on the excavation depth H_d, and it increases as the excavation phases progress.

The results of a trend of the values of the dimensional maximum vertical displacements, as a function of the current excavation depth are reported in Figures 4.16 and 4.17. As expected, it is evident how the values of displacements in soft soil models are an order of magnitude higher than HSS displacements.

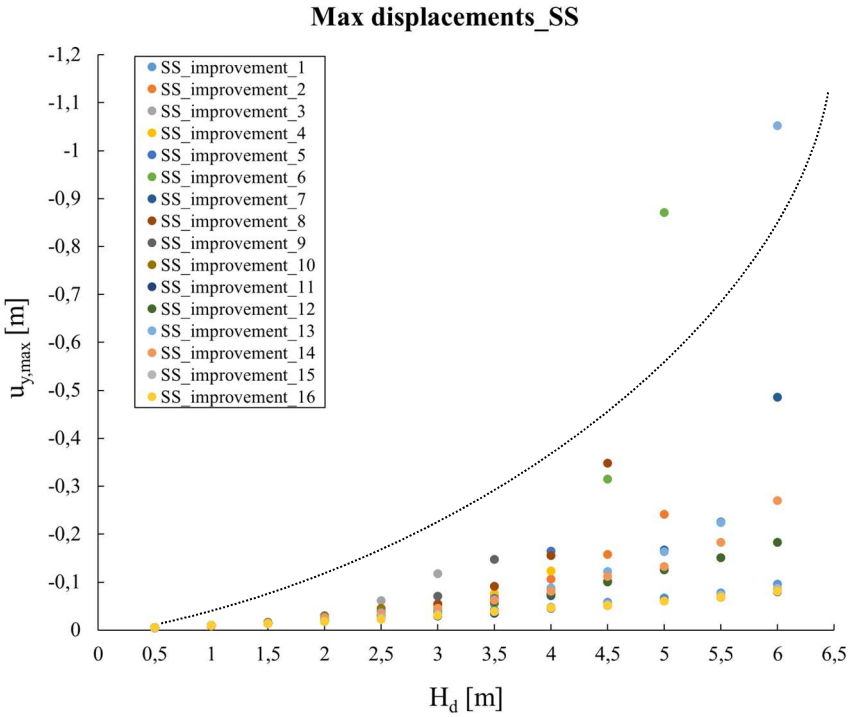

Figure 4.16 Maximum ground settlement related to current excavation depth for Soft Soil models (see table 4.5)

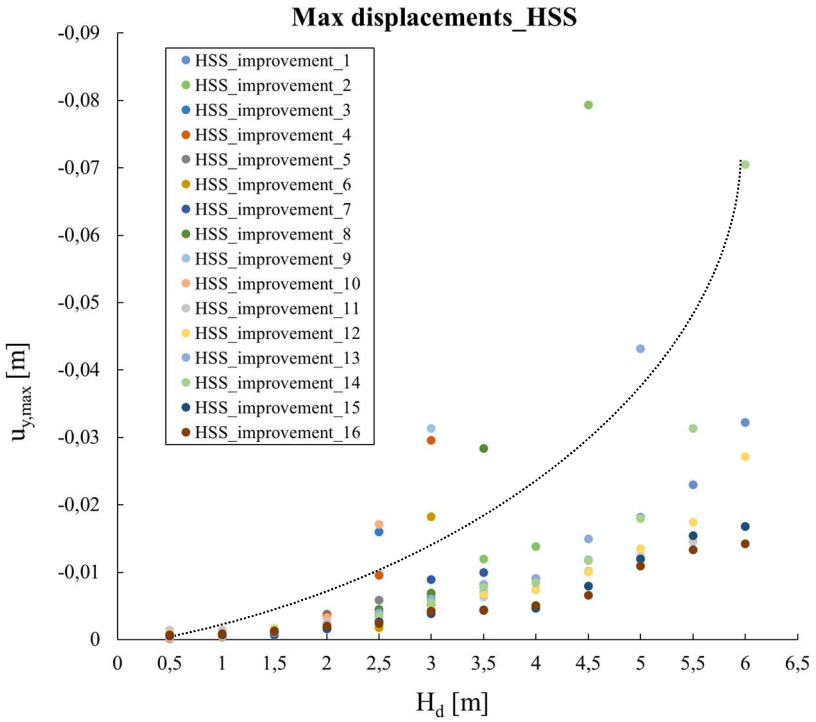

Figure 4.17 Maximum ground settlement related to current excavation depth for Hardening Soil Small models (see table 4.5)

Through the analysis of progressive displacements in different phases of excavation, extracting the vertical displacement values, it was also possible to obtain some envelopes of the ground displacement behind the dock. The results are expressed as the non-dimensional ratio u/u_{max} as a function of the ratio between x and H_p, where x is the horizontal coordinate at ground level and H_p is the height of the dock H plus the current depth of excavation H_d ($H_p = H + H_d$, see Figure 4.18).

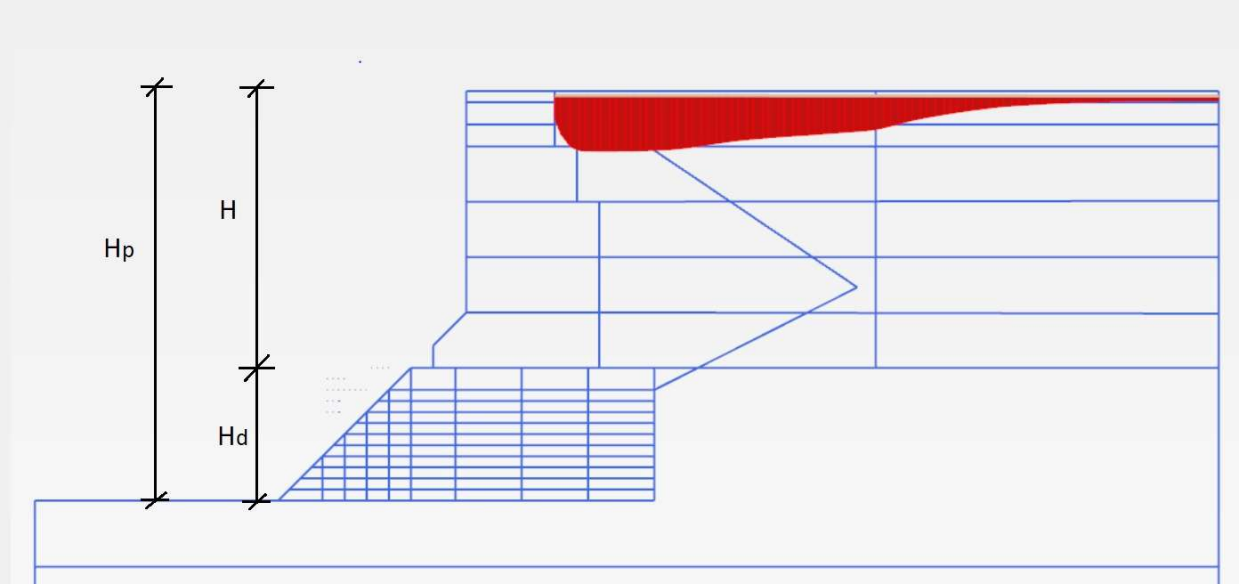

Figure 4.18 Example of ground settlement profile

The results are illustrated in following graphs (Figure 4.19 to 4.29). The settlement profiles were grouped on the basis of the type of seabed soil, the columnar or horizontal improvement and the value of the safety factor FS.

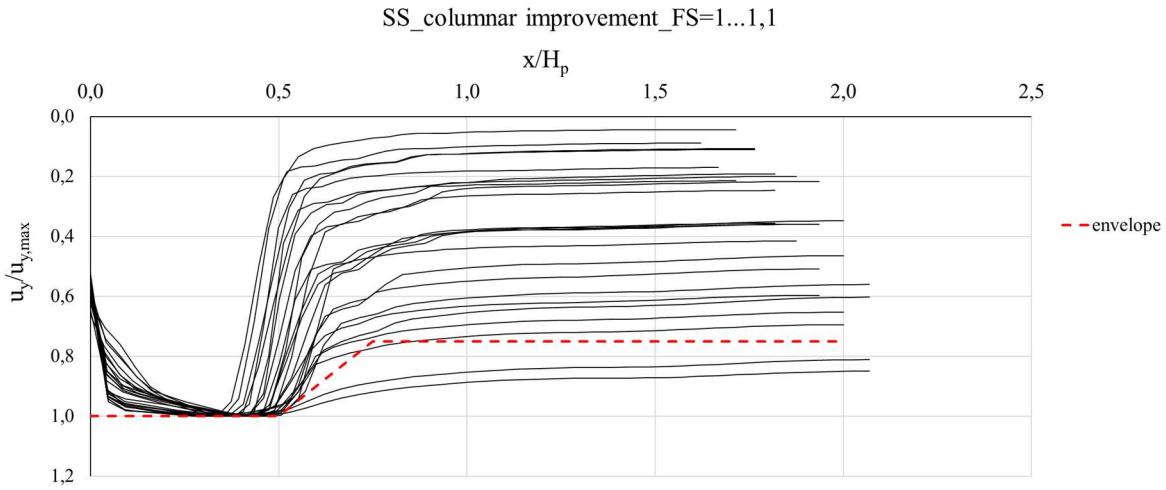

Figure 4.19 Envelope for settlement profile of Soft Soil columnar improvement models with FS value from 1 to 1.1.

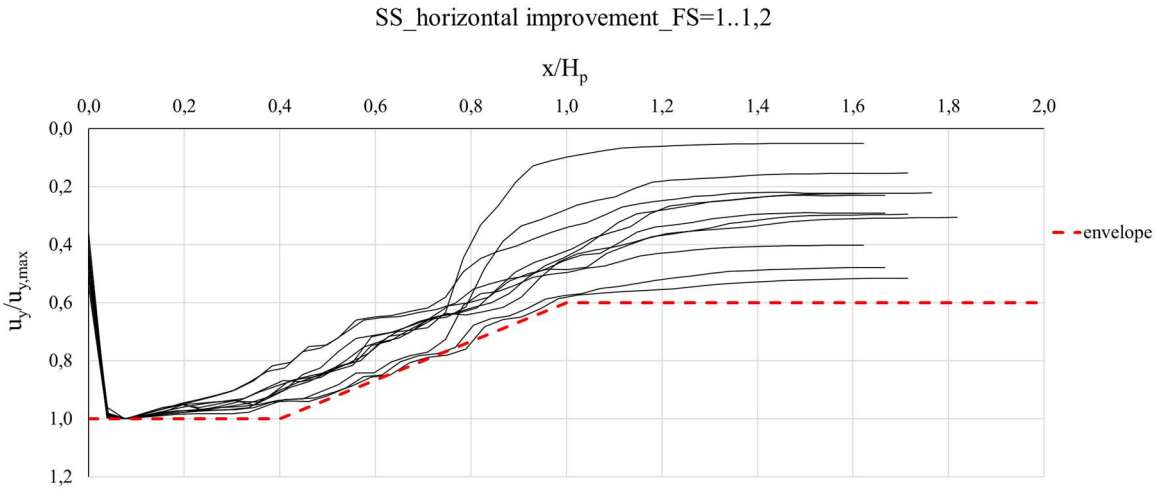

Figure 4.20 Envelope for settlement profile of Soft Soil horizontal improvement models with FS value from 1 to 1.2.

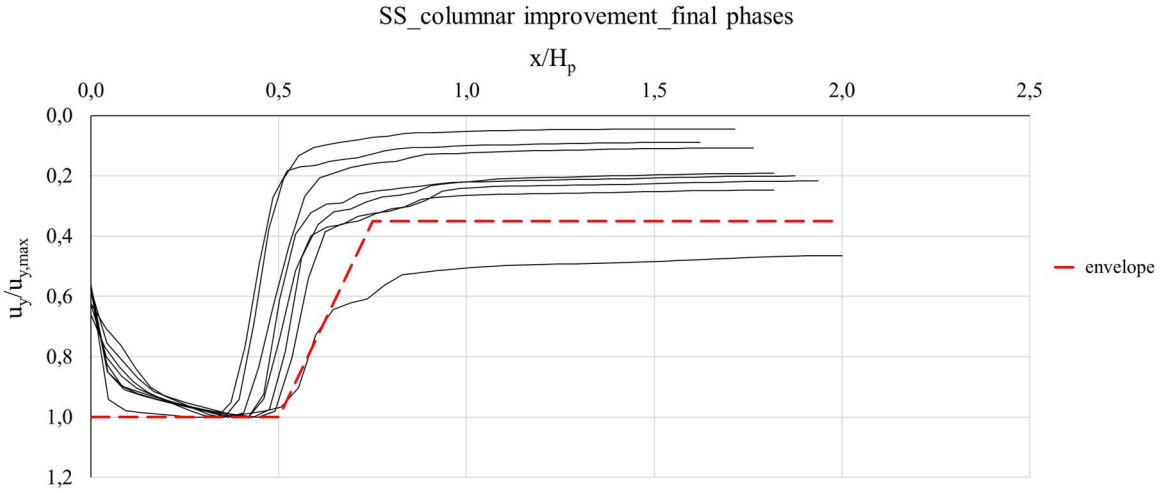

Figure 4.21 Envelope for settlement profile of Soft Soil columnar improvement models at phases close to failure.

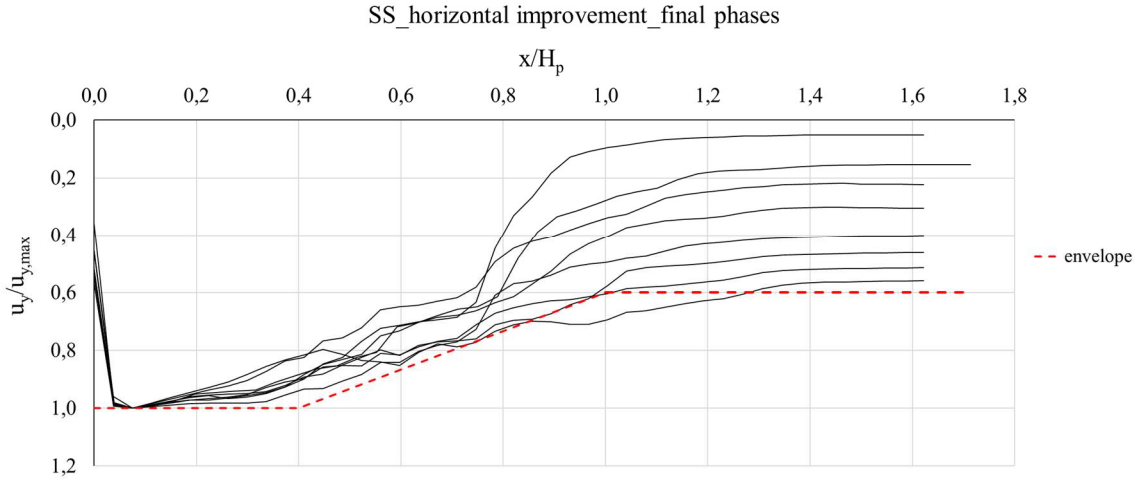

Figure 4.22 Envelope for settlement profile of Soft Soil horizontal improvement models at phases close to failure.

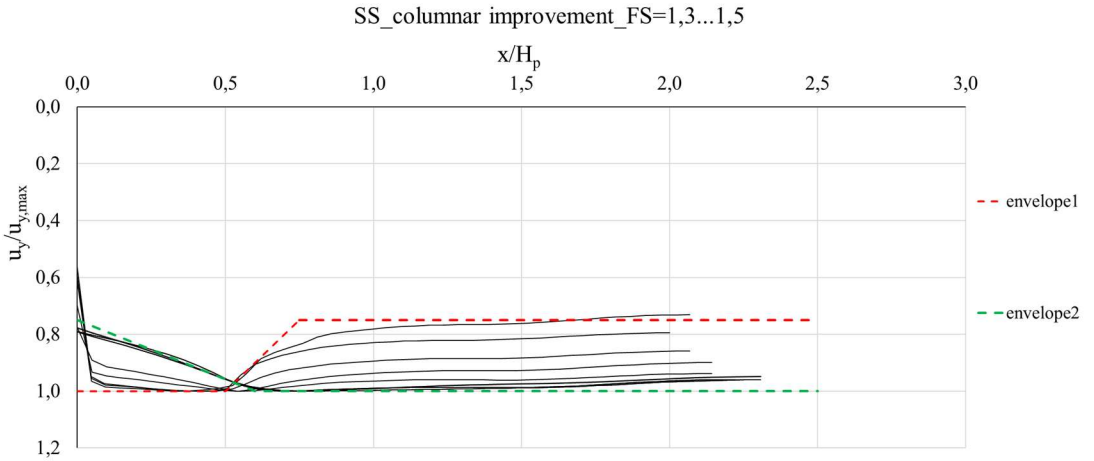

Figure 4.23 Envelopes for settlement profile of Soft Soil columnar improvement models with FS value from 1.3 to 1.5.

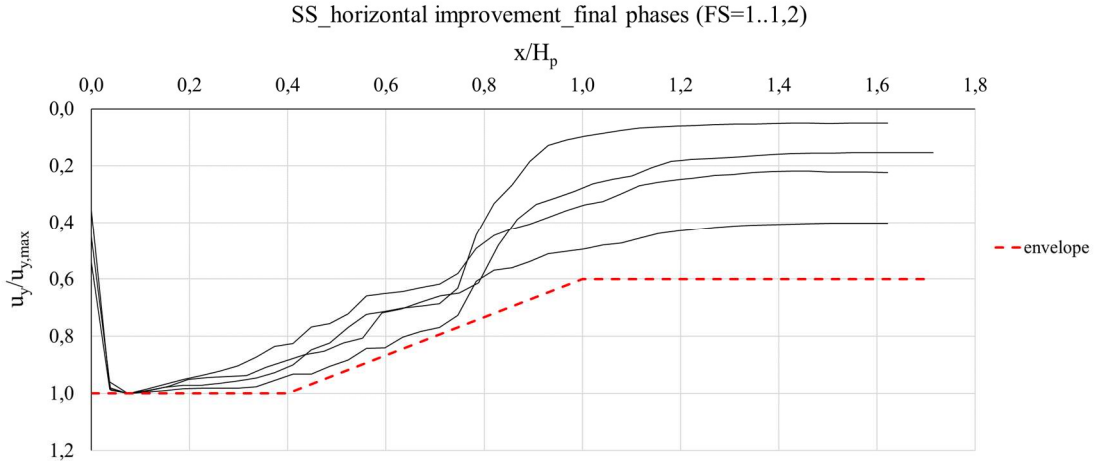

Figure 4.24 Envelope for settlement profile of Soft Soil horizontal improvement models at phases close to failure with FS value from 1 to 1.2.

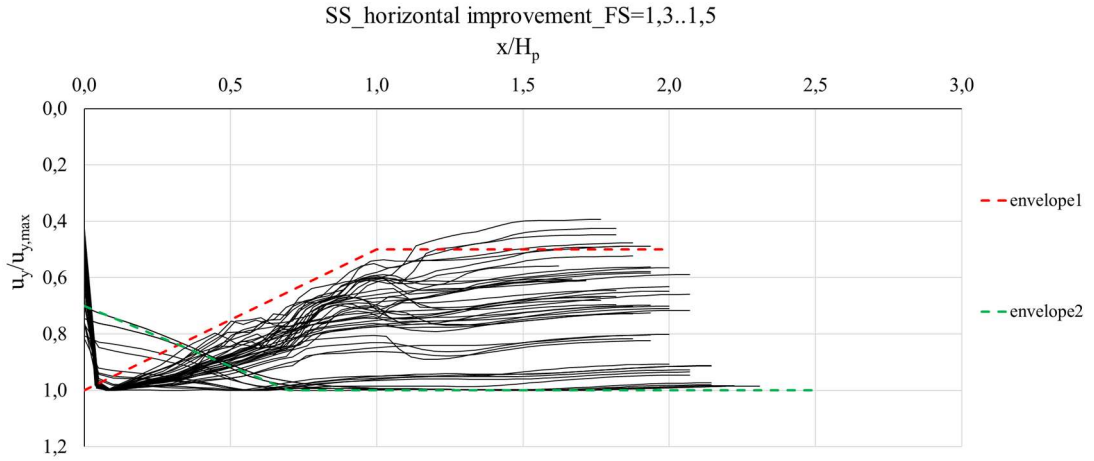

Figure 4.25 Envelopes for settlement profile of Soft Soil horizontal improvement models with FS value from 1.3 to 1.5.

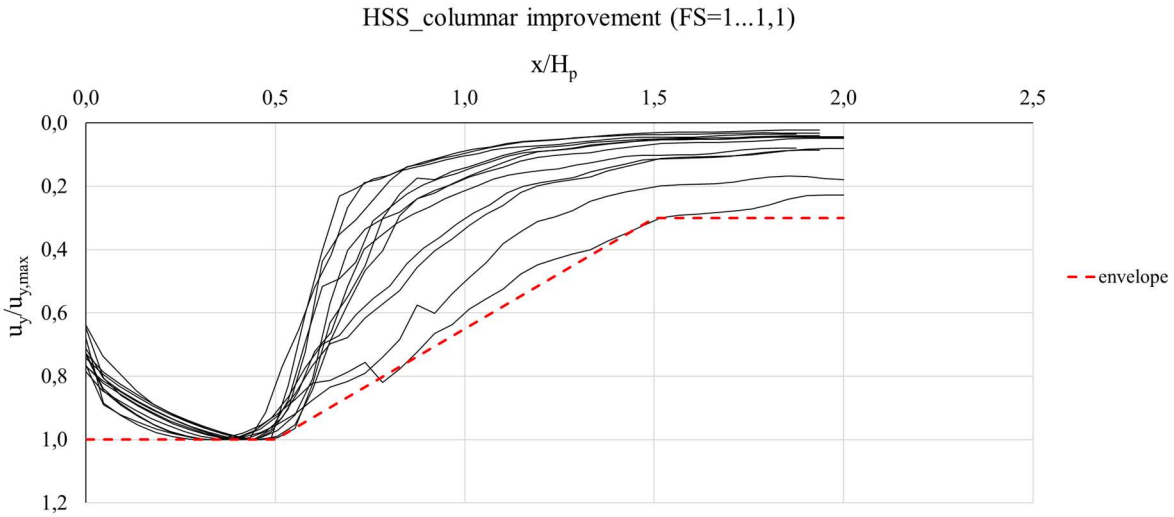

Figure 4.26 Envelope for settlement profile of Hardening Soil Small columnar improvement models with FS value from 1 to 1.1.

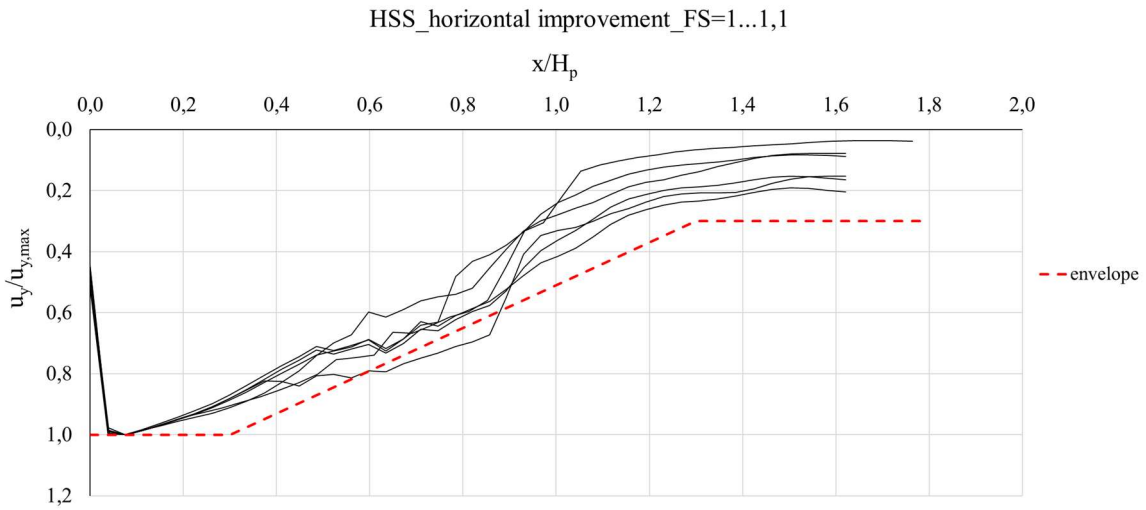

Figure 4.27 Envelope for settlement profile of Hardening Soil Small horizontal improvement models with FS value from 1 to 1.1.

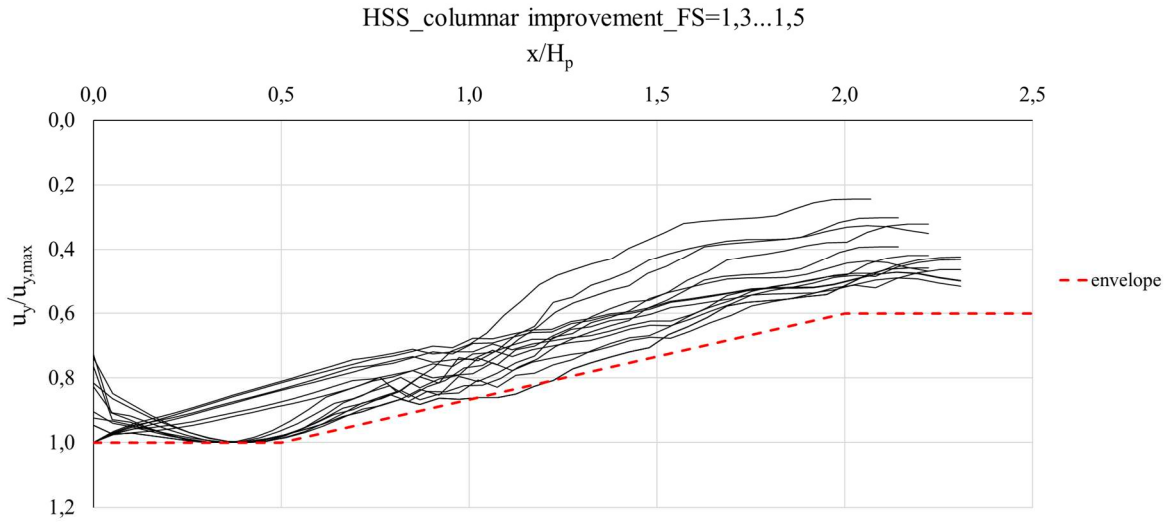

Figure 4.28 Envelope for settlement profile of Hardening Soil Small columnar improvement models with FS value from 1.3 to 1.5.

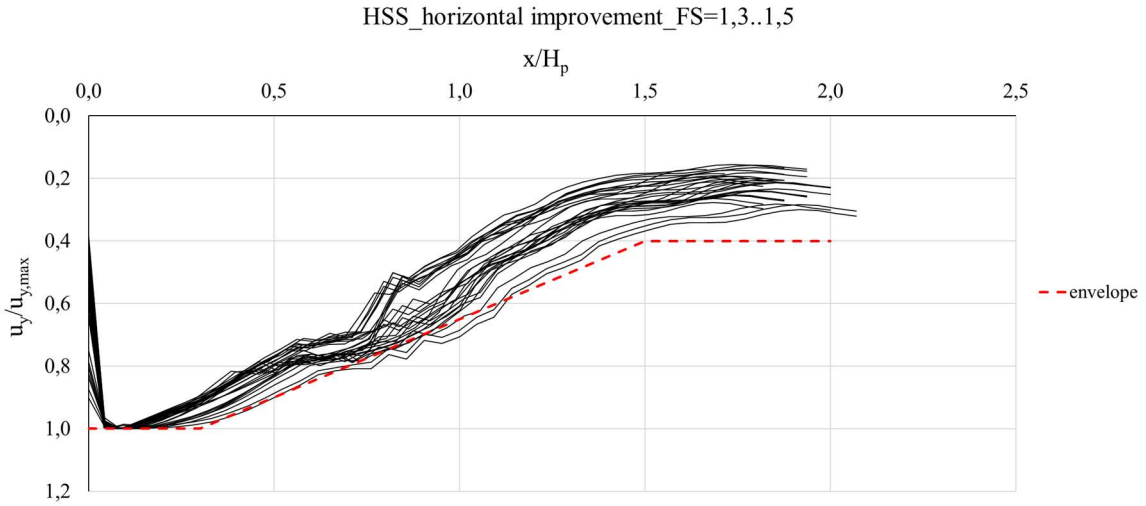

Figure 4.29 Envelope for settlement profile of Hardening Soil Small horizontal improvement models with FS value from 1.3 to 1.5.

By analyzing the following figures from 4.30 to 4.37, in which the normalized settlement profiles are shown, some interesting considerations and results can be drawn. It can be noticed that for safety factor values close to the unit but related to excavation phases not yet close to failure (Figure 4.30), the envelope is similar for horizontal improvement and vertical improvement, while as soon as a near-collapse condition occurs the profile of the envelope is clearly distinguished in both cases (Figure 4.31). In addition, it is noted that for the columnar improvement the localization of the displacements is more evident than for the horizontal improvement, because the deformative mechanism presents a sort of block that tends to slide along a semi-circular surface that passes through the treatment columns (see Figure 4.14).

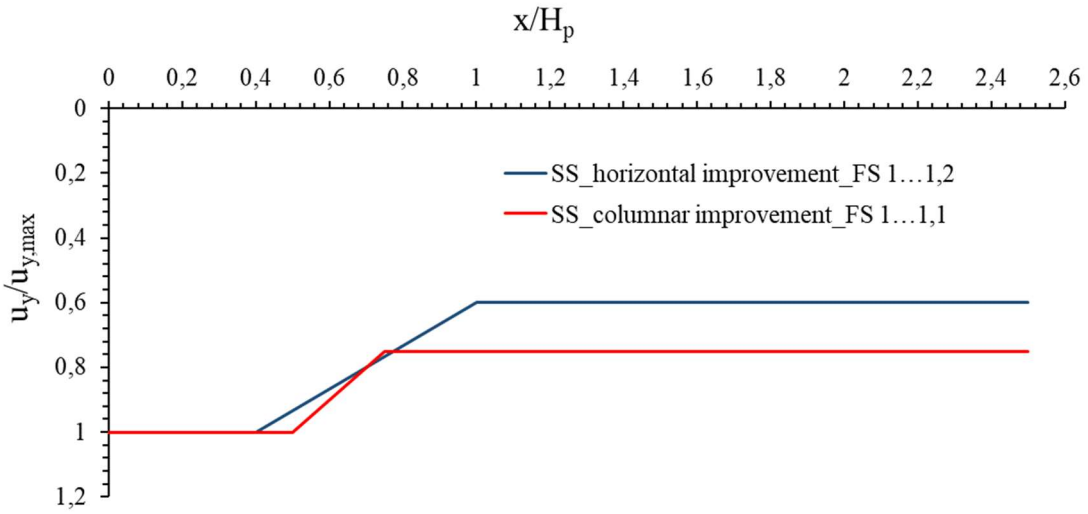

Figure 4.30 Envelope of ground settlement profile on the back of the quay (SS cases)

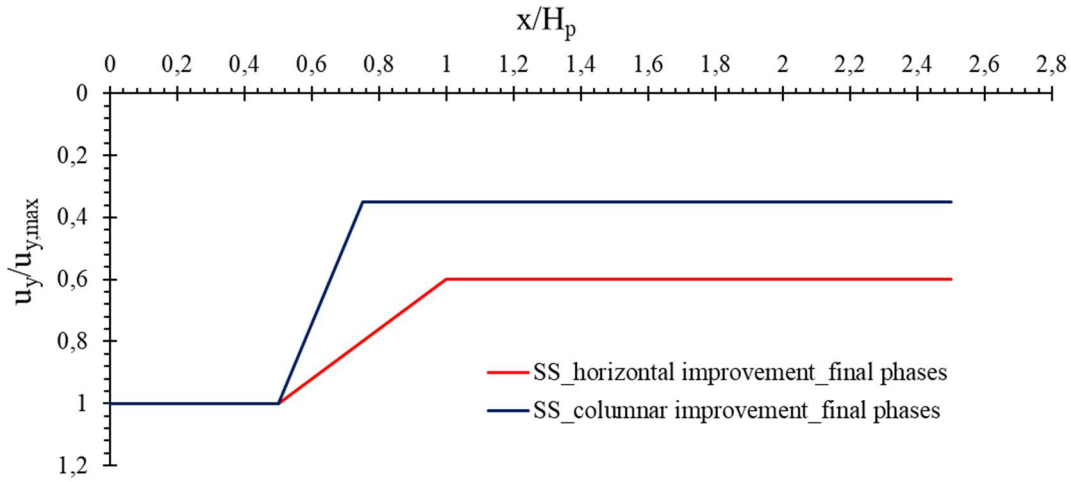

Figure 4.31 Envelope of ground settlement profile on the back of the quay (SS cases)

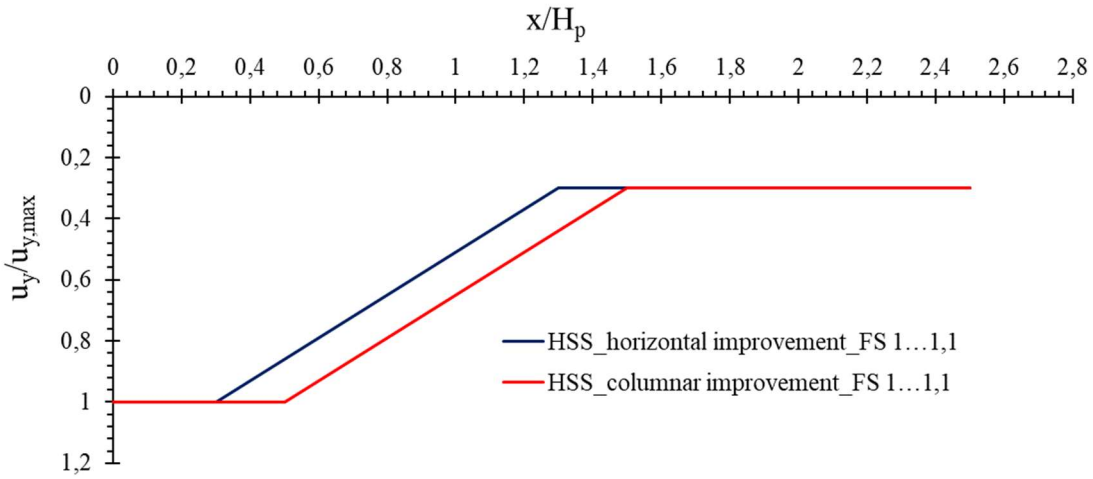

Figure 4.32 Envelope of ground settlement profile on the back of the quay (HSS cases)

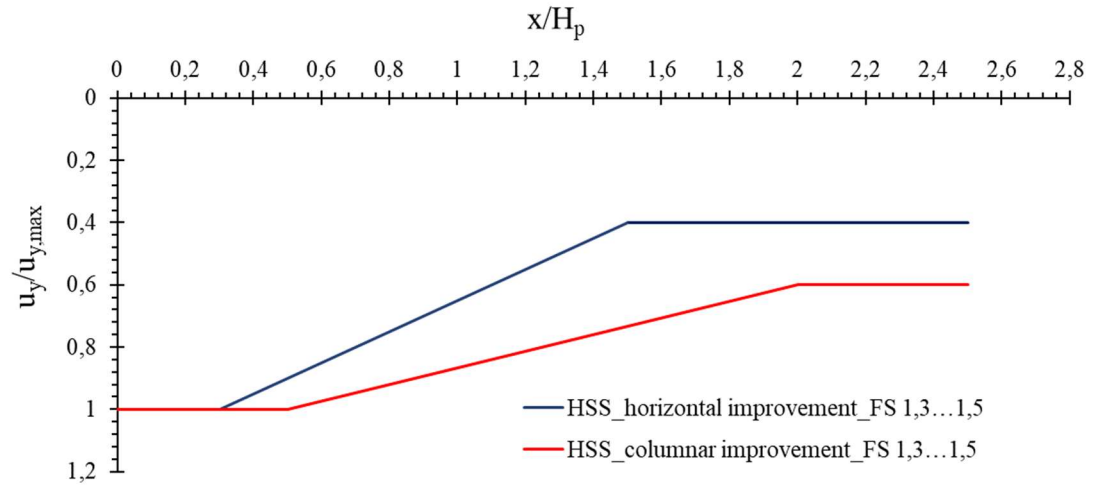

Figure 4.33 Envelope of ground settlement profile on the back of the quay (HSS cases)

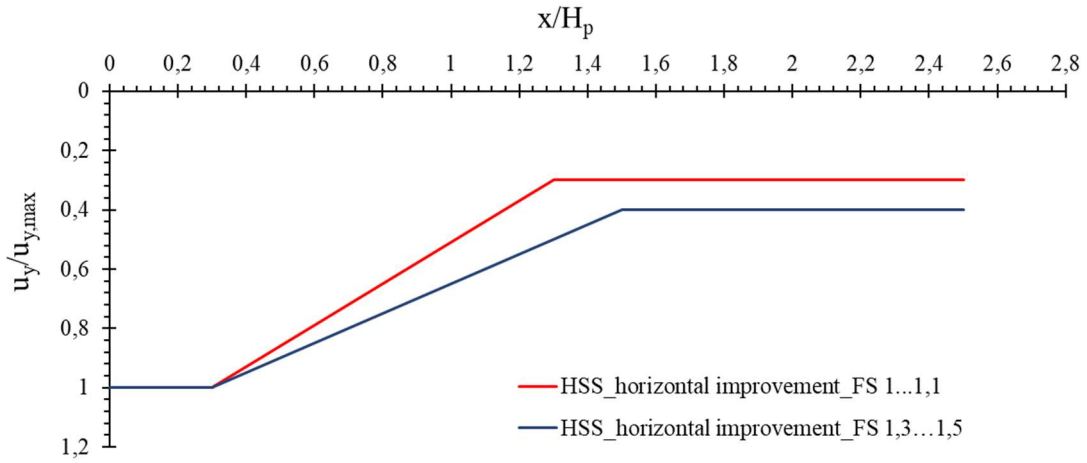

Figure 4.34 Envelope of ground settlement profile on the back of the quay (HSS cases)

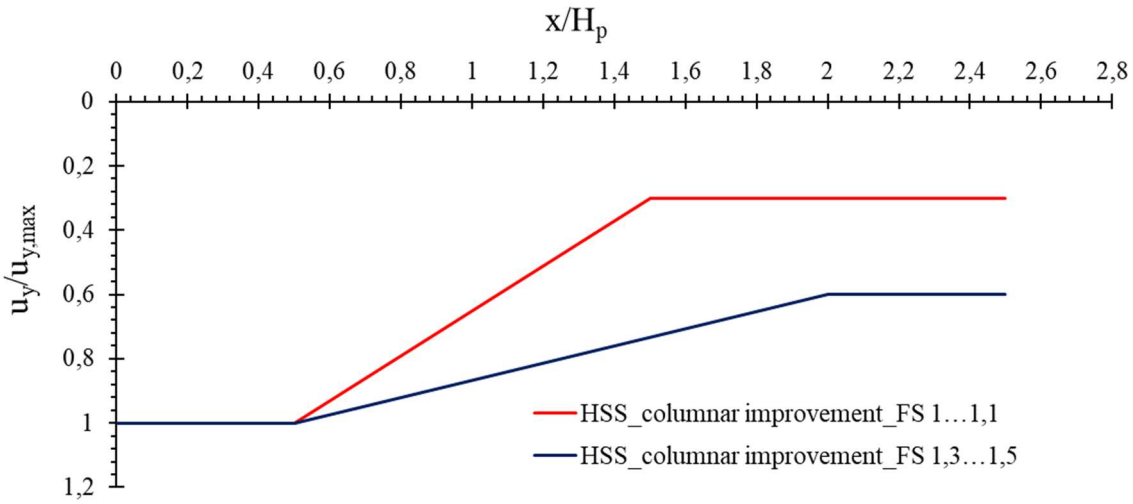

Figure 4.35 Envelope of ground settlement profile on the back of the quay (HSS cases)

In Figures 4.34 and 4.35, with equal ground improvement type it can be observed that as FS increases the envelope tends to smooth over because the displacement decreases and tends to the maximum value. Making a comparison between the soil model (Figures 4.36 and 4.37), the more deformable soil, identified by soft soil model, leads to higher displacements related to the maximum value. In fact, it can be noticed that the value of the ratio $u_y/u_{y,max}$ is overall higher.

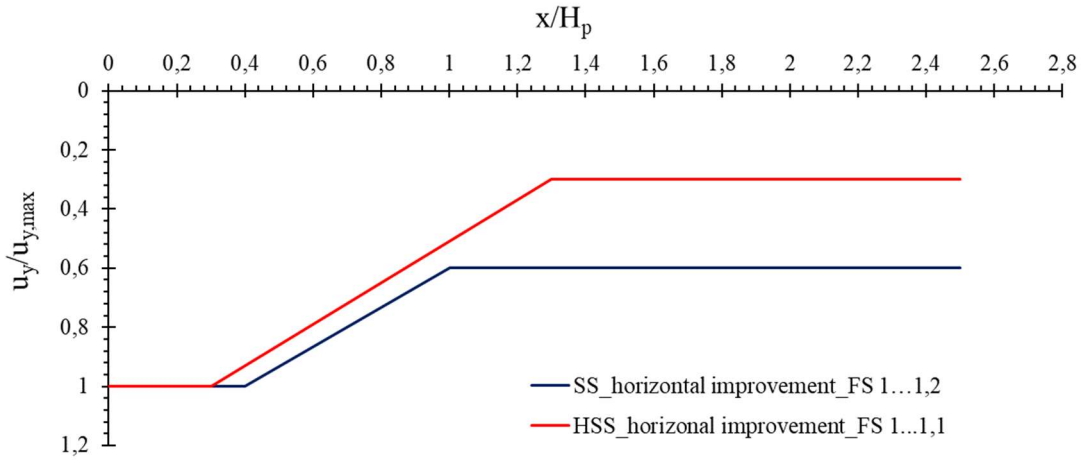

Figure 4.36 Envelope of ground settlement profile on the back of the quay (comparison between SS and HSS cases)

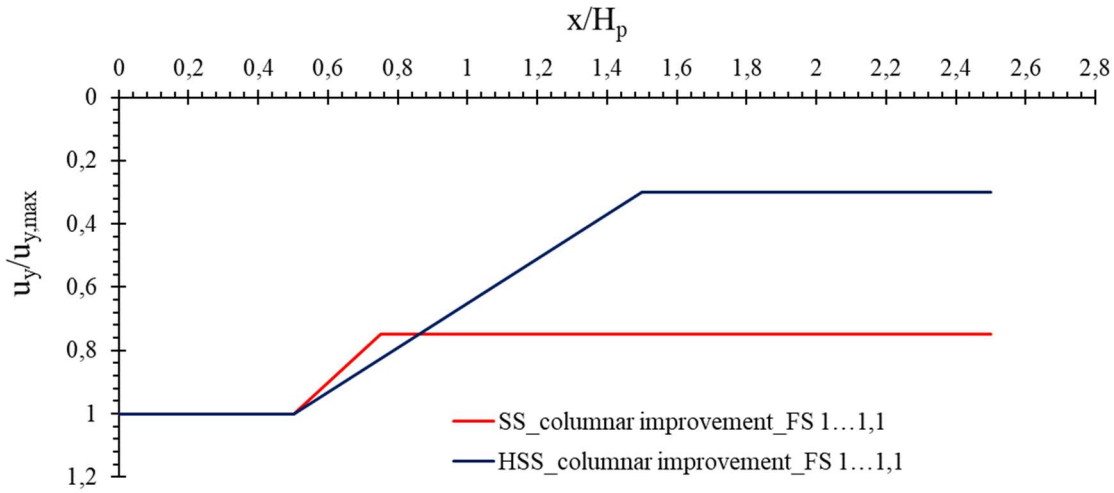

Figure 4.37 Envelope of ground settlement profile on the back of the quay (comparison between SS and HSS cases)

These envelopes can be useful in preliminary design phase of interventions similar to those under study because they provide indications of both the extent of the ground settlement behind the quay and the extent of the area affected by them, depending on the excavation depth and the type of soil improvement.

In addition, for all the models and for each excavation phase, a corresponding safety analysis was carried out and the values of safety factor were obtained. They are dependent not only on the type of soil of the seabed, but also on the current excavation depth and the extent of the improvement intervention. The results are reported in the following graphs.

Figures 4.38 and 4.39 show the trend of the safety factor related to excavation depth for vertical and sloped excavation in cases of columnar improvement (and Soft Soil models).

At the same H_i, FS remains almost equal in either of the cases of vertical and sloped excavation, only the maximum depth of excavation that can be reached changes and it is greater in the case of sloped excavation. So, at equal H_d, FS grows as H_i increases, whatever the excavation modality is.

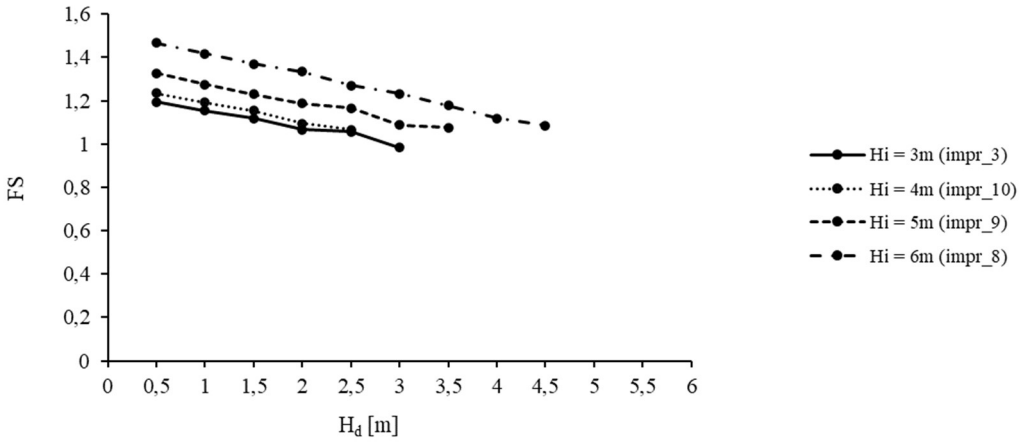

Figure 4.38 Safety factor related to excavation depth for vertical excavation (columnar improvement)

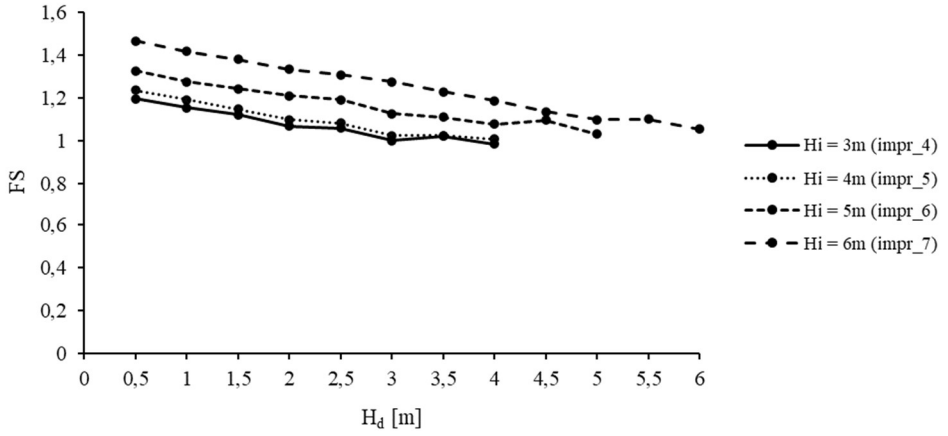

Figure 4.39 Safety factor related to excavation depth for sloped excavation (columnar improvement)

Figures 4.40 and 4.41 shows the trend of the safety factor related to improvement thickness for vertical and sloped excavation in cases of columnar improvement (and Soft Soil models).

As it can be observed, again the trend does not depend on excavation modality and for a fixed H_i, as H_d increases FS decreases. Therefore, it is possible to determine FS value for a thickness of improvement and an excavation depth.

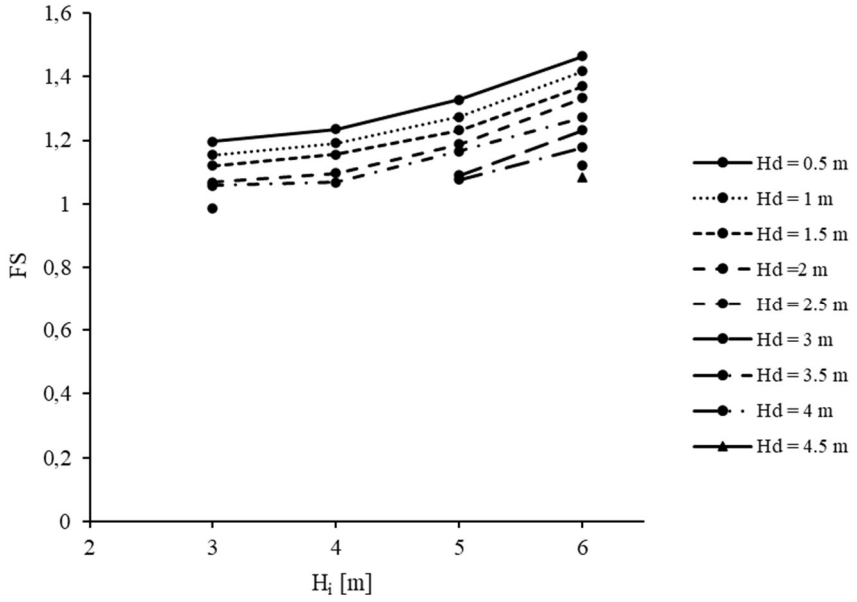

Figure 4.40 Safety factor related to improvement thickness for vertical excavation (columnar improvement)

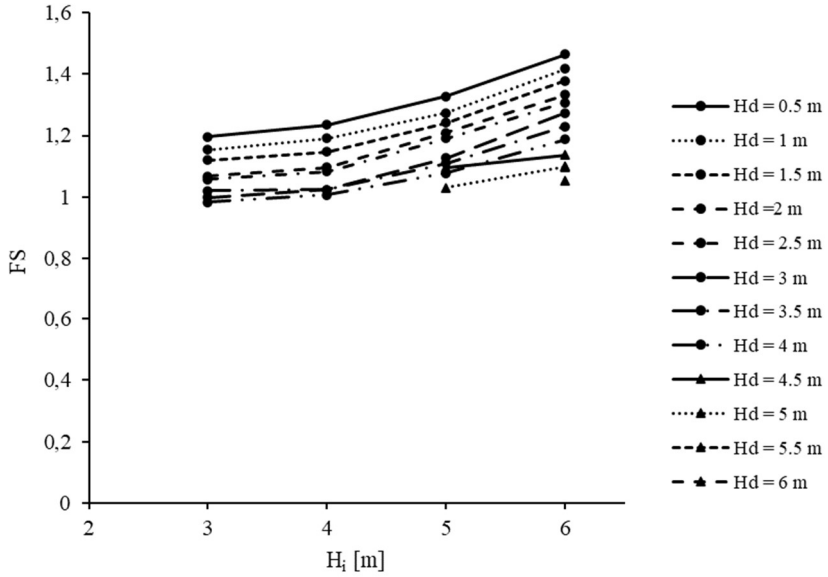

Figure 4.41 Safety factor related to improvement thickness for sloped excavation (columnar improvement)

Figures 4.42 e 4.43 shows the trend of the safety factor related to excavation depth respectively for vertical and sloped excavation in cases of columnar improvement, comparing the results obtained for Soft Soil and Hardening Soil Small models.

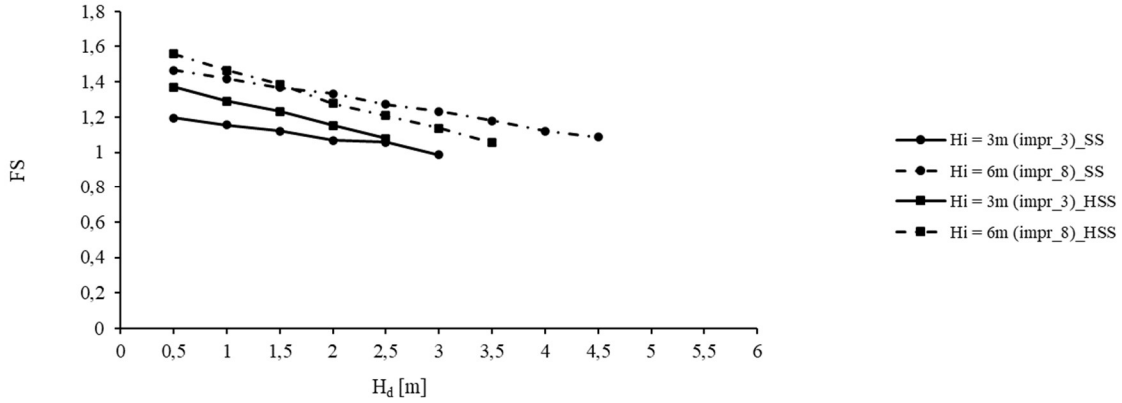

Figure 4.42 Safety factor related to excavation depth for vertical excavation (columnar improvement)

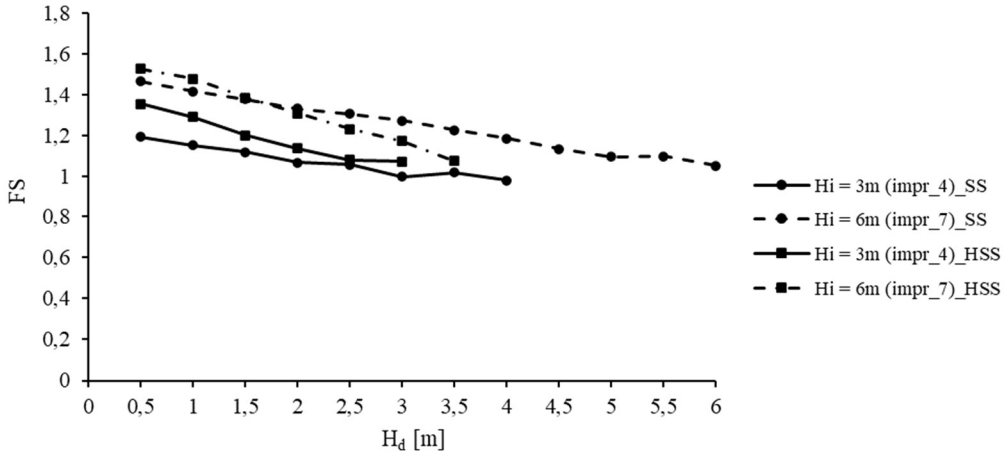

Figure 4.43 Safety factor related to excavation depth for sloped excavation (columnar improvement)

Finally, Figures 4.44, 4.45 and 4.46 show the evolution of the safety factor as a function of the ratio between the current excavation depth H_d and the thickness of the improved soil H_i.

As it can be observed, the safety factor decreases as this relation increases, and its value is globally higher for horizontal improvement, that allows to reach greater depth of excavation with higher safety margin.

Therefore, given a deep of improvement it can be evaluated the value of the safety factor for a determined excavation depth.

These relationships are managed by the power laws listed below:

- for Hardening Soil Small Model and horizontal improvement $FS=1{,}20e^{-0{,}4(H_d/H_i)}$
- for Hardening Soil Small Model and columnar improvement $FS=1{,}48e^{-0{,}46(H_d/H_i)}$
- for Soft Soil Model and horizontal improvement $FS=1{,}62e^{-0{,}22(H_d/H_i)}$
- for Soft Soil Model and columnar improvement $FS=1{,}40e^{-0{,}29(H_d/H_i)}$
- for Hardening Soil Small and Soft Soil Model and horizontal improvement $FS=1{,}76e^{-0{,}30(H_d/H_i)}$

- for Hardening Soil Small and Soft Soil Model and columnar improvement $FS=1{,}40e^{-0{,}34(H_d/H_i)}$

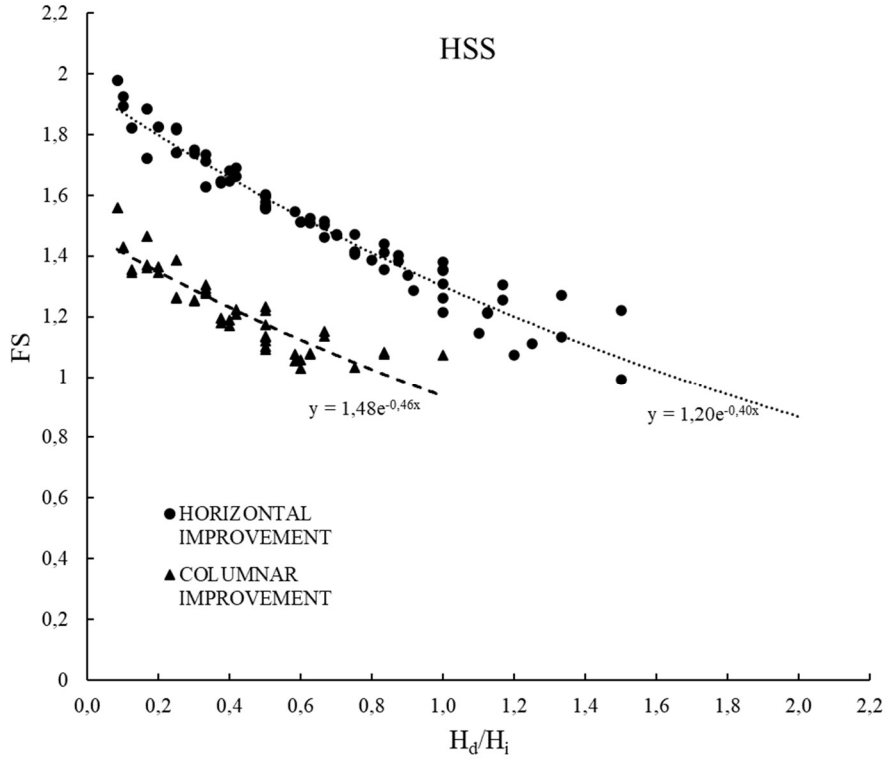

Figure 4.44 Safety factor trend related to the improvement and excavation depth for HSS models

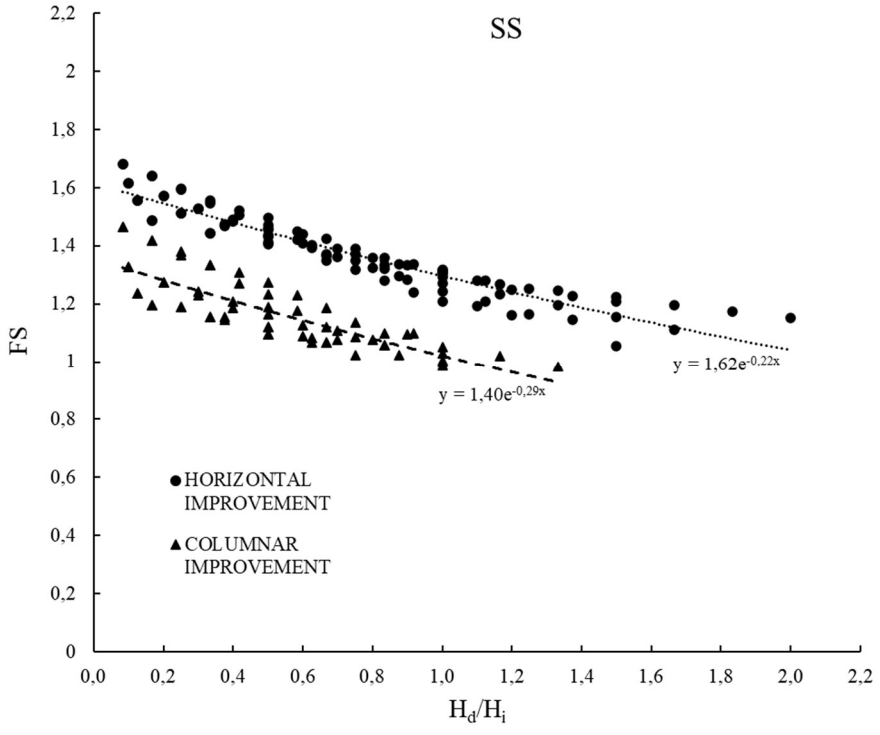

Figure 4.45 Safety factor trend related to the improvement and excavation depth for SS models

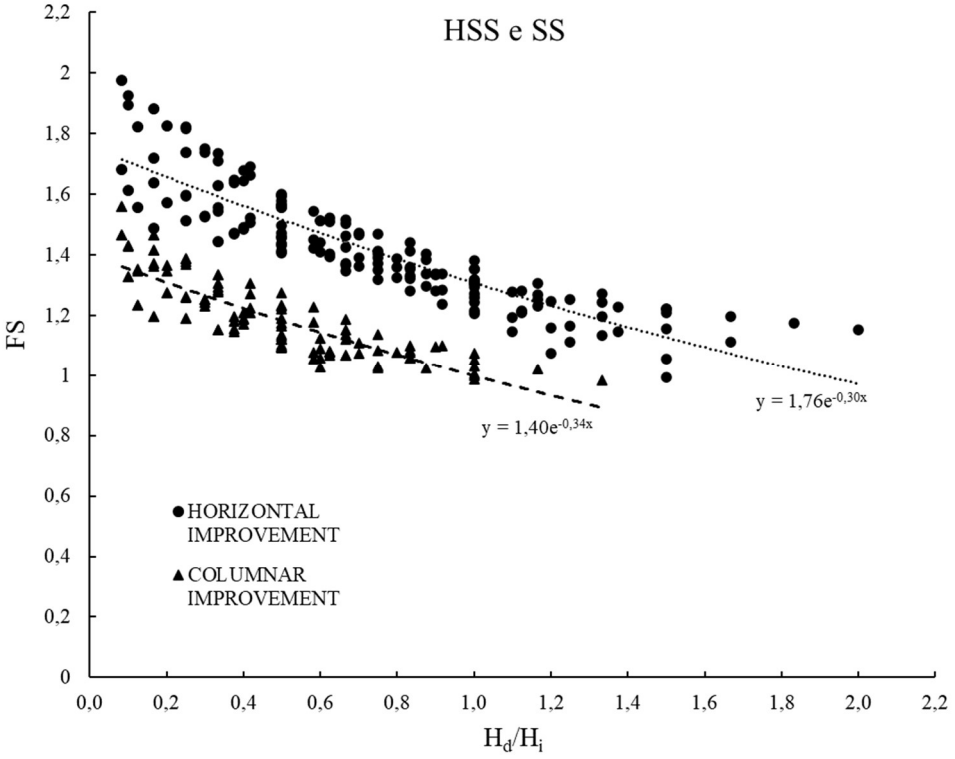

Figure 4.46 Safety factor trend related to the improvement and excavation depth for HSS and SS models

Another interesting result is the relation between the rigid displacement of four control points (Figure 4.47) of the quay wall and the vertical displacement at ground level:

- Control point A: at the top of the quay wall (for horizontal displacement)
- Control point B: at the bottom of the quay wall (for horizontal displacement)
- Control point C: at the foot of the quay wall (for vertical displacement)
- Control point D: at the bottom on the back of the quay wall (for vertical displacement)

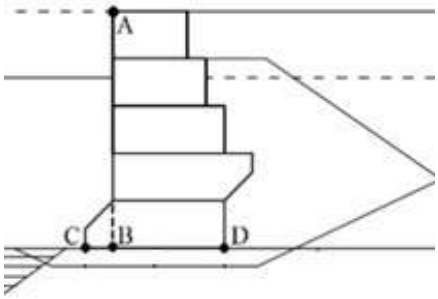

Figure 4.47 Control points of quay wall

In the following graphs are shown the results of the trends of the horizontal displacements of points A and B and the vertical displacements of point C and D, distinguishing Soft Soil and Hardening Soil Small models, related to the maximum vertical settlement at the ground level. (Note that displacements with a

negative sign indicate, for the reference system adopted, outward horizontal displacements and vertical settlements).

In particular, Figure 4.48 shows the trends/tendency lines of the horizontal displacement of control points A and B as a function of the maximum vertical ground settlement, all normalized by the height of the dock H, for Soft Soil models. The results indicate a linear relationship between these displacements, similar to what previously observed for deep excavations (see e.g. Figs. 3.17 and 3.30). Three definite trends are shown for displacements related to point B and for those related to point A, the latter in turn differentiated according to the type of soil treatment.

Comparable results were obtained for Hardening Soil Small models and are shown in Figure 4.49.

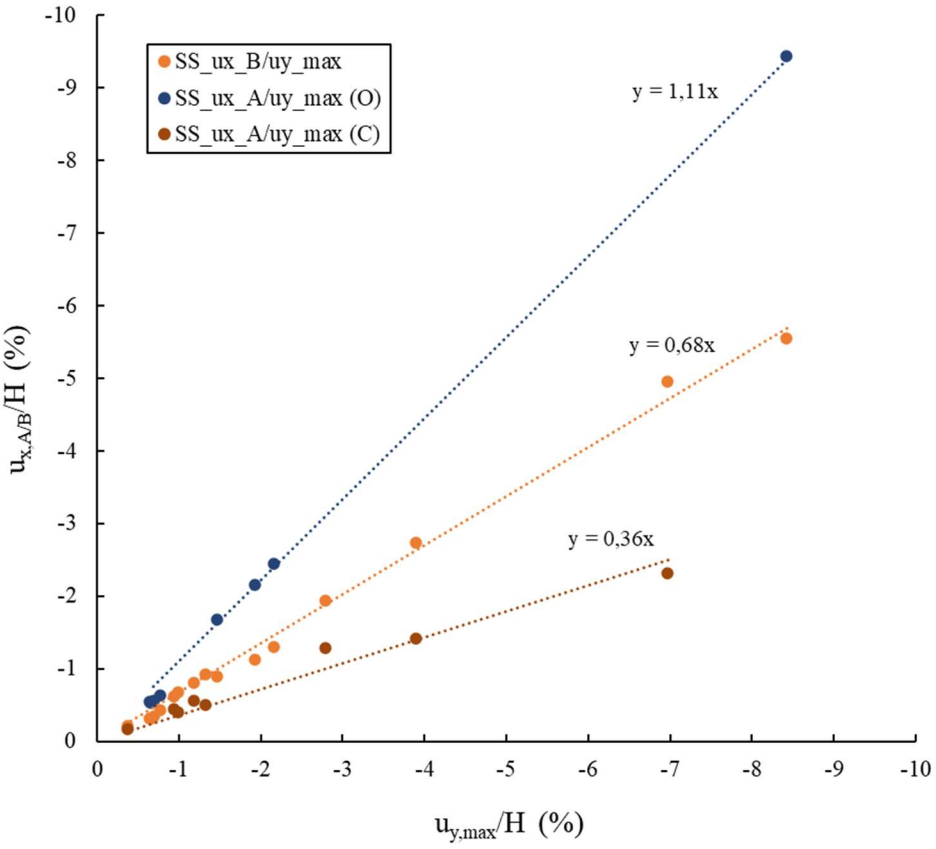

Figure 4.48 Non-dimensional rigid displacements of control point A and B of Soft Soil models (O: horizontal type treatment: C: columnar type treatment)

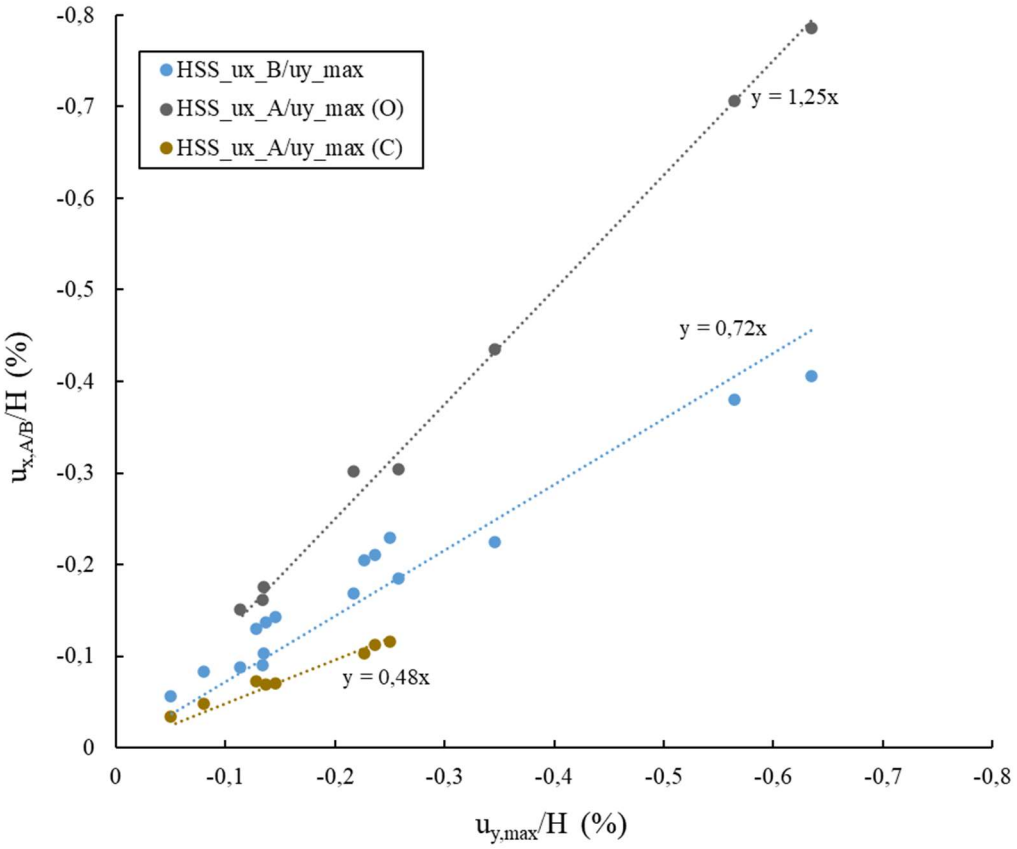

Figure 4.49 Non-dimensional rigid displacements of control point A and B of Hardening Soil Small models (O: horizontal type treatment: C: columnar type treatment)

Figure 4.50 whereas shows the trends of the vertical displacement of control points C and D as a function of the maximum vertical ground settlement, all normalized by the height of the dock H, for Soft Soil models. The results indicate a linear relationship between these displacements and once again three definite tendency are shown for displacements related to point C and for those related to point D, the latter in turn differentiated according to the type of soil treatment.

Comparable results were obtained for Hardening Soil Small models and are shown in Figure 4.51.

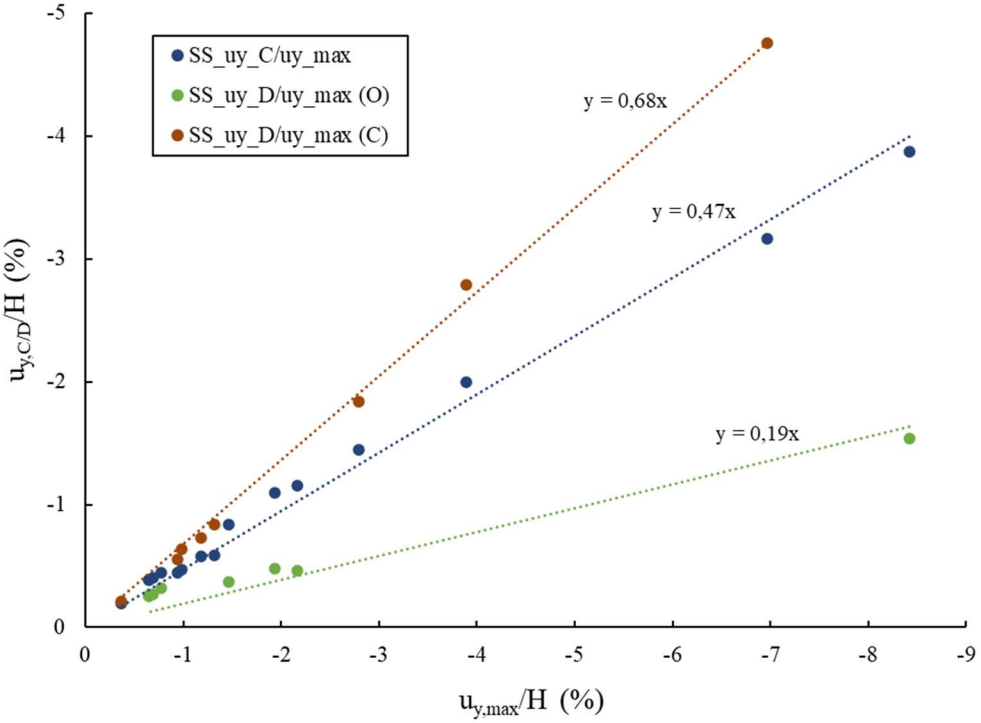

Figure 4.50 Non-dimensional rigid displacements of control point C and D of Soft Soil models (O: horizontal type treatment: C: columnar type treatment)

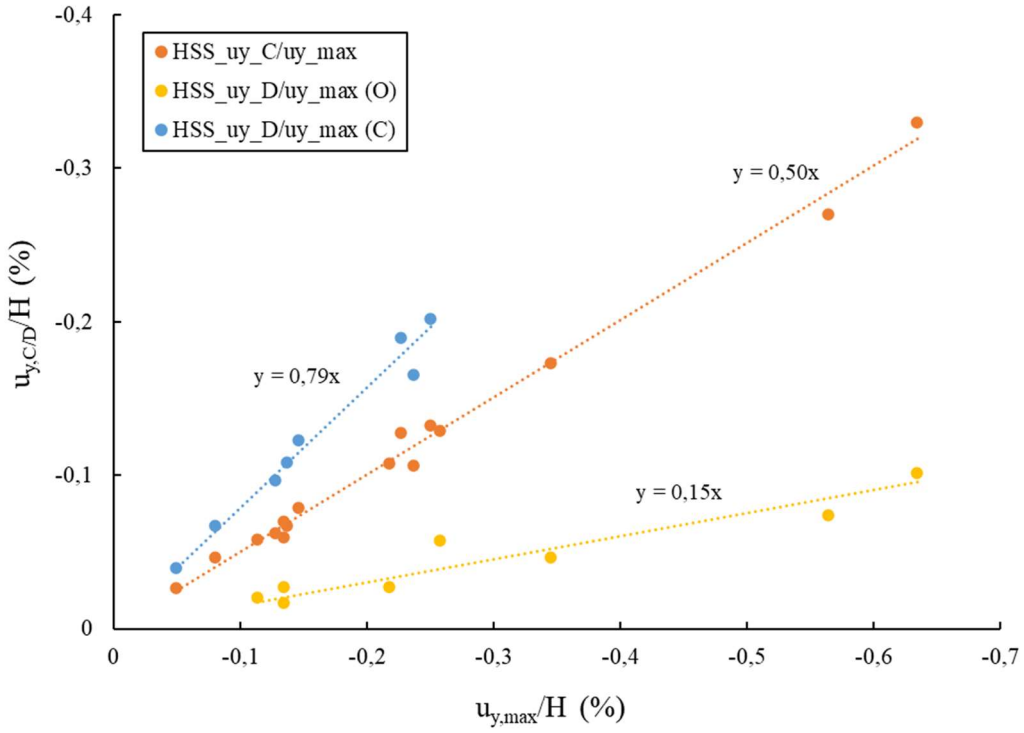

Figure 4.51 Non-dimensional rigid displacements of control point C and D of Hardening Soil Small models (O: horizontal type treatment: C: columnar type treatment)

Table 4.6 Rotation of quay wall - Soft Soil model (Clockwise towards soil backfill)

Model	$u_{x,A}$ (mm)	$u_{x,B}$ (mm)	$\Delta u_{x,AB}$ (mm)	rotation (°)	Direction
Improvement_1	-79.3	-52.7	-26.7	-0.12	↺
Improvement_2	-269.6	-140.8	-128.8	-0.59	↺
Improvement_3	-54.9	-77.2	22.2	0.10	↻
Improvement_4	-50.5	-84.2	33.7	0.15	↻
Improvement_5	-62.1	-114.6	52.6	0.24	↻
Improvement_6	-289	-619.9	330.9	1.52	↻
Improvement_7	-176.3	-342.6	166.3	0.76	↻
Improvement_8	-159.8	-241.8	82	0.38	↻
Improvement_9	-70.3	-100.3	30.	0.14	↻
Improvement_10	-21.2	-25.5	4.4	0.02	↻
Improvement_11	-67.8	-39.1	-28.6	-0.13	↺
Improvement_12	-209.2	-112.1	-97.1	-0.45	↺
Improvement_13	-1179	-693.2	-485.8	-2.23	↺
Improvement_14	-305	-161.8	-143.2	-0.66	↺
Improvement_15	-70.4	-43.5	-26.8	-0.12	↺
Improvement_16	-66.5	-39.4	-27.1	-0.12	↺

Table 4.7 Rotation of quay wall - Hardening Soil Small models (Clockwise towards soil backfill)

Model	$u_{x,A}$ (mm)	$u_{x,B}$ (mm)	$\Delta u_{x,AB}$ (mm)	rotation (°)	Direction
Improvement_1	-38.1	-23.1	-15	-0.07	↺
Improvement_2	-98.2	-50.7	-47.6	-0.22	↺
Improvement_3	-9.1	-16.3	7.1	0.03	↻
Improvement_4	-14.1	-26.3	12.2	0.06	↻
Improvement_5	-4.3	-7.1	2.8	0.01	↻
Improvement_6	-8.7	-17.9	9.2	0.04	↻
Improvement_7	-6.1	-10.4	4.4	0.02	↻
Improvement_8	-12.8	-25.6	12.8	0.06	↻
Improvement_9	-14.4	-28.7	14.3	0.07	↻
Improvement_10	-8.6	-17.1	8.6	0.04	↻
Improvement_11	-20.2	-11.3	-8.9	-0.04	↺
Improvement_12	-37.7	-21	-16.7	-0.08	↺
Improvement_13	-54.3	-28	-26.3	-0.12	↺
Improvement_14	-88.3	-47.5	-40.8	-0.19	↺
Improvement_15	-21.9	-12.9	-9	-0.04	↺
Improvement_16	-18.9	-10.9	-7.9	-0.04	↺

It can be noted that the trend of points B and C is independent from the type of improvement (horizontal or columnar) and strictly linked to the ground vertical displacement, while the trends of points A and D are linked also to the scheme of improvement, and consequently to the direction of rotation of the structure and the failure mechanism.

Tables 4.6 and 4.7 show the values and the direction of rotation of quay wall control points respectively for Soft Soil models and Hardening Soil Small models.

The knowledge of these displacement trends gives a useful tool in the preliminary design phase of an intervention, providing an indication of the order of magnitude of the displacements that can occur by making a given deepening of the dock, as a function of the maximum ground displacement that could occur.

4.4. CONCLUSIONS

In the field of port engineering, there is both the requirement for extensive dredging of seabed and the problems of localized erosion phenomena due to the propulsive action of ships, which can cause loss of stability of parts of existing docks. In this chapter, this issue was addressed by studying the response of a typical quay wall subject to excavation at the foot, with the aim of simulating such potentially dangerous phenomena.

Results obtained performing finite element numerical analyses were proposed, with the purpose of studying the behavior of this typology of structures and the deformation processes occurring in the foundation soil and in the backfill.

In numerical analyses, carried out by Plaxis, typical seabed ground conditions (fine sands and clay-silty soils) were adopted, modelled respectively by a “Hardening Soil Small” model and a “Soft Soil “model.

Also the improvement intervention in the foundation ground is typical, because jet-grouting technique was considered, with geometry of the intervention simulating a possible execution from pontoon and from plan descent, crossing the dock structure. Thus, two different treatment arrangement were defined, namely columnar and horizontal.

In absence of a ground improvement, the quay is subject to instability phenomena when the excavation reaches depths of the order of one meter (a depth about one-tenth the height of the dock): by adopting an improvement of the mechanical characteristics of the foundation soil, simulating a jet-grouting intervention, the excavation depth increases considerably, up to 3-6 meters. As expected, the excavation depth reached up to failure increases as the treatment zone extends.

It has been verified that the failure condition can be achieved even with small excavation increments (between 0.5 and 1 m). In fact, the safety factor associated with a global instability in the calculation phase prior to the failure phase assumes allowable values in any case (FS approximately equal to 1.1).

It has also been observed that the scheme of improvement intervention leads to different global deformation mechanisms of the structure, with different rigid rotation directions for the horizontal and the columnar improvement: the mechanism related to the horizontal treatment is caused by a well-defined wedge in the backfill and an outward rotation of the quay; on the contrary, the mechanism related to the columnar treatment is characterized by a sliding along a semi-circular surface and a backward rotation.

By means of the analysis of progressive displacements in different phases of excavation, extracting the vertical displacement values, it was also possible to define some envelopes of the ground settlement behind the dock. They can be useful in preliminary design phase of interventions because they provide indications on the amount of the ground settlement behind the quay and the extent of the area affected by them, depending on the excavation depth and the geometry of the ground improvement.

In addition, indications were provided on the value of the factor of safety with respect to a global failure mechanism, depending on the type and extent of the intervention and the depth of excavation, obtaining relationships that can be used to assess stability thresholds.

Finally, a study of the rigid displacement of some control point of the quay wall supplied the trends of the horizontal or vertical displacement of the control points as a function of the maximum vertical ground settlement. The results indicate a linear relationship between these displacements, similar to what is known for deep excavations. These results can be useful once again because they provide an indication of the values of the displacement that can occur for a given deepening of the dock, as a function of the maximum ground displacement that is likely to occur.

FINAL REMARKS

As already underlined in the present dissertation, the constant increase in the population of large cities leads to an ever-growing demand for infrastructures, which, given the high density of the built environment, is often only possible through underground construction.

This is the first issue that has been considered in this work, focused on applied research themes.

The execution of an excavation inevitably involves a change in the stress state of the ground and consequently it induces displacements and deformations. In urban environment and, particularly, in presence of a cultural and artistic urban heritage such as that of Italy, it is of crucial importance to minimize such induced displacements. This problem has led over the years, on the one hand, to the development of calculation procedures capable of providing reliable predictions of the effects induced by the execution of deep excavations and, on the other, has encouraged the investigation of construction solutions capable of reducing such displacements.

A second aspect taken into consideration in the present research program, was the exponential growth in the size of commercial and cruise ships and, consequently, the need to make an existing infrastructure within an operating port adequate to ensure the berthing of modern ships.

Solutions must be found for upgrading existing structures to actual requirements. This is particularly true for Italian ports, which were usually constructed in past centuries and are part of very large urban zones, where the possibility of expansion into new areas is minimal.

The upgrading of a quay wall is an actual important issue, but rarely addressed in literature. It needs the consideration of several factors, including the need to deepen the seabed as far as the localized erosion phenomena due to the propulsive action of ships, both of which can induce unacceptable displacements and general stability problems.

It is in this context that the work of the present Phd thesis is to be placed. The objective of the study was to deepen the knowledge on the deformative response of different types of retaining structures, with the aim of providing design guidance in terms of the reliability and applicability of some particular solutions, also to meet current demands in the engineering field.

As far as deep excavations are concerned, the work started from an established knowledge for “typical” solutions for embedded walls; then a series of insights was developed, under conditions different than the usual standards adopted for designing deep excavations and interventions on existing docks.

As discussed extensively in previous chapters, traditional solutions for supporting excavations have limited capability to reduce displacements because they can only be realized after excavation phase, when the displacement rate has already occurred. The research focuses on different reinforcement solutions, particularly buttress walls that can be installed prior to the execution of the excavation and thus counteract a significant portion of the induced displacements.

While, in general, analyses for evaluating the effects induced by excavation assume simple deformation conditions, and in the case of continuous elements this assumption may still be true, considering the area affected by the intervention as homogeneously equivalent, for this type of discontinuous interventions, the three-dimensional character of the problem requires a more in-depth study.

An extensive and rigorous study was conducted based on numerical analyses, supported by experimental evidence, with the aim of highlighting:

- the quantities that govern the deformation response of "unconventional" retaining structures
- the volumes of soil on which to intervene to optimize the structure performance
- the expected displacements and associated deformation profiles
- the degree of safety

From the results produced by numerical analyses on buttress walls, indications are obtained as to the extent of the displacements that may occur and the type of geometric solution to be adopted under similar conditions, thus providing the opportunity to have feedback to verify that the results obtained even from less in-depth analyses have realistic values and to have indications for a preliminary design of this type of structure.

As far as berthing retaining structures are concerned, a typical scheme of an "old" quay wall was considered, with the purpose of studying the problem of excavation at the foot with the aim of obtaining both displacement envelopes, similar to those available in the framework of deep excavation, and indications on the general safety of the structure.

The performed numerical analyses, carried out with typical geometric and geotechnical conditions (for such a harbor infrastructure) have led to displacement envelopes and stability indicator values as a function of the excavation evolution, also to develop effective reinforcement and stabilization criteria.

They can be useful in preliminary design phase of interventions because they provide indications on the amount of the ground settlement behind the quay and the extent of the area affected by them, depending on the excavation depth and the geometry of the ground improvement.

In addition, indications were provided on the value of the factor of safety with respect to a global failure mechanism, depending on the type and extent of the intervention and the depth of excavation, indications that can be used to assess stability thresholds.

Finally, results have supplied relationships between horizontal and vertical displacements, similar to those for deep excavations. Assuming a maximum ground displacement that is likely to occur, for a given deepening of the dock, these results could help in serviceability limit state analyses, especially when the the functionality of quay equipments is of concern.

To summarize, for both the engineering problems that have been analyzed, both relating to the behavior of structures interacting with excavations, some original aspects concern the provision of indications and quantitative guidelines (through design abacuses and the study of deformation mechanisms) useful for the

preliminary design of interventions and for the eventual verification of results that can be assessed with simplified numerical analyses and analytical evaluations.

As a final remark, it is worth noting that the topics covered in this thesis, and thus the results obtained, may require further research efforts to obtain more general conclusions.

The situations examined are representative of typical conditions, but it would be advantageous to extend the case study from a geometric point of view, by varying geometric features (e.g. excavation depth, buttress spacing and length, wall embedment, etc..) and, from a geotechnical point of view, by using other soil types and more complex stratigraphy, as well as the effects of pore pressures due to excavation under water table.

Moreover, it would be interesting not only to analyze the general displacement patterns, but also to consider more specific stress paths.

As a further step, coupled analyses could be carried out in the presence of structures and superstructures (e.g. buildings, large cranes) at ground level (so far not analyzed because free-field conditions have been considered), in order to assess possible damage levels induced by differential settlements, the latter of which have been well identified by the analyses carried out.

Finally, with regard to the quayside earth retaining structures, the study would merit further investigation by means of a three-dimensional numerical analysis to study the possible edge effects if, instead of simulating a generic deepening of the seabed, localized erosion were recreated.

REFERENCES

Atkinson, J. H., 2000, "Non-linear soil stiffness in routine design." Géotechnique 50.5 ,487-508.

Bauduin, c., Mengeot, P., Ganne, P., 2017, “Design and construction issues for deepening and strengthening of existing quay walls”. In: Proc. of the 19th Int. Conf. on Soil Mechanics and Geotechnical Engineering, Seoul.

Berardi, R., 2021, Fondamenti di geotecnica. 4a Ed. Città Studi edizioni.

Brinkgreve, R.B.J. et al., 2019, “PLAXIS User’s manual 2019”. Plaxis bv, Bentley Systems Inc.

Bustamante, M., & Doix, B.,1985, “Une méthode pour le calcul des tirants et des micropieux injectés.” Bull Liaison Lab Ponts Chauss, (140).

Callisto L., 2011 “Inclusioni strutturali per la riduzione degli spostamenti indotti da scavi profondi”, Atti XXIV Convegno Nazionale di Geotecnica “Innovazione tecnologica nell’ingegneria geotecnica”, AGI, Napoli, Vol. 1., 51-62.

Callisto, L., 2011, “Diaframmi a sostegno di scavi profondi in terreni a grana fine.”, Opere di sostegno e di stabilizzazione dei pendii. Vol. 1. ITA.

Clayton, Chris RI, et al., 2013, “Earth pressure and earth-retaining structures.” CRC press.

Clough, G.W.; Smith, E.M. & Sweeney, B.P., 1989, “Movement control of excavation support systems by iterative design.” Proc. ASCE Conf. on Foundation Engineering: Current Principles and Practices, v. 2, pp. 869-884.

Clough, G.W., O'Rourke, T.D., 1990, "Construction induced movements on insitu walls", ASCE GSP25: Design and performance of earth retaining structures, 439-470.

Clough, G. W., and J. M. Duncan, 1991, “Earth pressures.” Foundation engineering handbook. Boston, MA: Springer US. 223-235.

Eurocode EC7: Geotechnical design - Part 1: general rules, EN 1997-1, CEN European Committee for standardization, Bruxelles, Belgium.

Hacegaba, N., 2014. “Big Ships, Big Challenges – the Impact of Mega Container Vessels on U.S.” Port Authorities. Long Beach, CA, USA.

Herold, Andreas; Wolffersdorff, P., 2009, “The use of hardening soil model with small-strain stiffness for serviceability limit state analyses of GRE structures”. Proceedings of GeoAfrica, 22.10, 1-5.

Hsieh P.G., Ou C.Y., 1998 “Shape of ground surface settlement profiles caused by excavation”, Canadian Geotecnical Journal 35, 1004-1017.

Janbu, N. (1985). Soil models in offshore engineering (25th Rankine lecture). Géotechnique, 35, 241–280.

Long, M., 2001, “Database for retaining wall and ground movements due to deep excavations”, J. of Geotech. and Geoenviron. Engng 127(3): 203-224.

Mana A.I., Clough G.W., 1981, “Prediction of movement for braced cuts in clay”, Journal of the Geotechnical Division, ASCE, 759-777.

Matos Fernandes, M. ,2007, An overview on induced movements by deep excavations in soft ground and eight golden rules for their control. Proc. XIVth ECSMGE, Madrid, Vol. 5, 379-384.

Matos Fernandes, M., 2015, New developments in the control and prediction of the movements induced by deep excavations in soft soils. Soils and Rocks, 38(3), 191-215.

Ou, C.Y., Hsieh, P.G., and Chiou, D.C., 1993, “Characteristics of ground surface settlement during excavation.” Canadian Geotechnical Journal, 30(5):758–767.

Ou C.Y., Lin Y.L., Hsieh P.G.,2006, “Case Record of an Excavation with Cross Walls and Buttress Walls” Journal of GeoEngineering, Vol. 1, n.2,79–86.

Ou C.Y., Hsieh P.G., 2011, “A simplified method for predicting ground settlement profiles induced by excavation in soft clay”, Computers and Geotechnics 38 (2011) 987-997.

Pane, V., Tamagnini, C., 1997, “Problemi generali dell'analisi delle opere di sostegno.” Gruppo nazionale CNR-IV Convegno Nazionale dei Ricercatori Universitari. Vol. 2. Hevelius Edizioni srl

Peck, R. B., 1969, “Deep excavations and tunneling in soft ground.” Proc. VIIth ICSMFE, Mexico City, General Report, State-of-the-Art Volume, pp. 225-290.

Potts, D., Axelsson, K., Grande L., Schweiger, H., Long, M., “Guidelines for the Use of Advanced Numerical Analysis”, Thomas Telford Publishing, 2002.

Raccomandazioni sugli Ancoraggi nei Terreni e nelle Rocce AGI - AICAP, 2012

Rampello S., 2017, “Scavi profondi nelle grandi città: una convivenza possibile”, XXVI Convegno Nazionale di Geotecnica “La Geotecnica nella Conservazione e Tutela del patrimonio costruito”, AGI, 3-54.

Ruggeri P., Fruzzetti V., Vita A., Segato D., Scarpelli G., 2014, “Stiffness of wall-type grouting under transversal loading” Ground Improvement, 167, Issue GI4, 301-310.

Ruggeri, P., Fruzzetti, V. M. E., & Scarpelli, G., 2019, “Renovation of quay walls to meet more demanding requirements: Italian experiences.” Coastal Engineering, 147, 25-33.

Sauvageon D., 2021, “Risposta deformativa e meccanismo di collasso per banchine a gravità soggette a scavi al piede”, X Incontro Annuale dei Giovani Ingegneri Geotecnici. Atti del Convegno Roma, AGI, ISBN 978-88-97517-16-0

Sauvageon D., Berardi R., 2021, “Infrastrutture portuali: modellazione della risposta di banchine a gravità soggette ad erosione localizzata”, IARG 2021, Atti dell'Incontro Annuale dei Ricercatori di Geotecnica, 2021, AGI, ISBN 978-88-97517-15-3

Scarpelli, G., Fruzzetti, V.M.E., Ruggeri, P., Sakellariadi, E., Segato, D., 2011. “The Link between EC7 and EC8 in the Seismic Design of an Anchored Sheet Pile Wall. Evaluation of Geotechnical Aspects of EC8”, Patron Ed. Athina, 11 September 2011, Greece.

Scarpelli, G., Ruggeri, P., Fruzzetti, V.M.E., Segato, D., Vita, A., 2012, “Performance based design of earth retaining structures and building codes. In: Proceedings of Second International Conference on performance-Based Design in Earthquake Geotechnical Engineering, Patron ed. pp. 579‑594 28-30 May 2012, Taormina, Italy.

Scarpelli G., Fruzzetti V., Ruggeri P. 2017, “Interventi di adeguamento delle banchine portuali alle crescenti esigenze dei traffici commerciali”, XXVI Convegno Nazionale di Geotecnica “La Geotecnica nella Conservazione e Tutela del patrimonio costruito”, AGI, 335-357.

Schanz, T., Vermeer, P.A., Bonnier, P.G., 1999. “The hardening soil model: formulation and verification”. Proc. Beyond 2000 in Computational Geotechnics-10 Years of Plaxis, Balkema, Rotterdam, 281-290.

Thoresen, C.A., 2003. Port Designer's Handbook: Recommendations and Guidelines. Thomas Telford, London.

Tsinker, G.P., 1997, “Handbook of Port and Harbor Engineering”, Chapman & Hall